Università di Genova

SCUOLA DI SCIENZE MATEMATICHE FISICHE E NATURALI

Doctorate in Physics and Nanosiences
Curriculum: Physics

Ph.D Thesis

Towards the resummation of high-energy next-to-leading logarithms in QCD

Supervisors:

Prof. Simone Marzani
Prof. Giovanni Ridolfi

Candidate:
Anna Rinaudo

XXXV Ph.D cycle

Abstract

During the past few years, with the ongoing Run 3 of the LHC and its upcoming High-Luminosity upgrade, the need to study observables that can be both experimentally measured and theoretically predicted with high precision has grown. In particular, on the theory side, improvements of fixed-order perturbative predictions, resummation of logarithmic enhancements, and accurate determination of proton structure have become mandatory.

With this thesis, we want to contribute to this effort. We aim to improve the present accuracy in the resummation of the logarithmic enhancements that arise in the coefficient function for partonic scattering, in the high-energy limit. At present, we know how to resum the Leading Logarithmic (LL) contributions to coefficient functions. We aim to extend this resummation to achieve the resummation for the Next-to-Leading Logarithmic (NLL) contributions and this thesis takes a first step in this direction.

High-energy (or small-x) resummation of LL terms in the coefficient function is based on the so-called k_t-factorization theorem, which allows us to separate the coefficient function into two parts. The first one is the so-called off-shell coefficient function, which is similar to the usual coefficient function but is computed with the incoming gluon off-shell. If this coefficient function is computed in a physical gauge, it is free from small-x logarithms. The second is the evolution factor, $\mathcal{U}$, which resums the logarithmic contributions in the coefficient function. To extend this procedure to resum NLL contribution we have to work on these two elements.

In this thesis, we take a first step in the direction of this resummation by presenting the light-cone gauge calculation for the off-shell coefficient function for a specific process, the Higgs-induced Deep-Inelastic Scattering (HDIS). Thanks to the work described in this thesis, we have been able to clarify several technical and conceptual aspects of calculations in the light-cone gauge, which because of its complexity, is not commonly used. In particular, we present two prescriptions to regularise the spurious infra-red singularities due to the gauge choice and a general method to compute non-covariant loop integrals. We also discuss in detail the renormalization procedure in this gauge, which is highly nontrivial due to the non-covariant nature of the gauge choice. Our approach and presentation differ from what can be found in the literature because our focus is always on computing off-shell scattering amplitudes.

Acknowledgements

Contents

1 Introduction **1**

2 Small-x resummation **5**
2.1 Perturbative QCD 6
2.1.1 QCD running coupling 7
2.1.2 Logarithms in the perturbative coefficients 8
2.2 Small-x resummation 9
2.2.1 Small-x resummation of the parton distribution functions 10
2.2.2 Small-x resummation of the coefficient function 12

3 Small-x resummation from LL to NLL **15**
3.1 High-energy factorisation 15
3.1.1 The soft emission chain and unintegrated gluon distribution . . 20
3.2 Leading-Log small-x resummation for the Higgs induced DIS 23
3.3 From LL to NLL resummation 27
3.3.1 Dominant contribution at high-energy 27
3.3.2 Factorisation of the logarithmic contributions 28
3.3.3 Off-shell coefficient function in light-cone gauge 29

4 Light-cone gauge **31**
4.1 Light-cone gauge and small-x resummation 31
4.1.1 Principal value prescription 33
4.1.2 Mandelstam-Leibbrandt prescription 35
4.2 Renormalisation in light-cone gauge 37
4.2.1 Counterterms with PV prescription 38
4.2.2 Counterterms with ML prescription 39

5 Higgs-induced DIS **41**
5.1 Higgs-induced DIS: kinematic and definitions 42
5.2 Next-to-leading order on-shell coefficient function 44
5.2.1 Real emission 45
5.2.2 Virtual corrections 47
5.2.3 Charge renormalisation 51
5.2.4 Complete NLO correction 52
5.3 Renormalisation in light-cone gauge 52
5.3.1 Counterterm for the gluon self-energy 52

5.3.2 Renormalization of the effective vertex 54
5.4 Next-to-leading order off-shell virtual contribution to the coefficient function 60
5.4.1 Diagram A 61
5.4.2 Diagram B 64
5.4.3 Diagram C 66
5.4.4 Diagram D 67
5.4.5 Ultraviolet singularities cancellation 68
5.4.6 One-loop virtual contribution to Higgs induced DIS 68
5.5 Outlook 69

6 Conclusions **71**

A Integrals in light-cone gauge **73**
A.1 Non-covariant one loop integrals with Mandelstam Leibbrandt prescription 73
A.1.1 One covariant denominator: ML prescription 77
A.1.2 Two covariant denominators: ML prescription 78
A.1.3 Three covariant denominators: ML prescription 79
A.2 Non-covariant one loop integrals with principal value prescription . . . 86
A.2.1 One covariant denominator: PV prescription 87
A.2.2 Two covariant denominators: PV prescription 88
A.2.3 Three covariant denominators: mass-less case 90
A.2.4 Three covariant denominators: massive case 91

B Counterterms computed with PV prescription **95**
B.1 Counterterm for the gluon self-energy 95
B.2 Counterterm for the effective vertex 96
B.2.1 Diagram with a bubble on the incoming (outgoing) leg 96
B.2.2 Triangle diagram 98
B.3 Total contribution to the effective vertex counterterm 100

C One-loop virtual correction to the HDIS computed with PV prescription **103**
C.1 Diagram A 103
C.2 Diagram B 104
C.3 Diagram C 105
C.4 Renormalised result 106

D Coefficients of the contribution from the diagram B to the off-shell virtual amplitude **109**

E Coefficients of the one-loop off-shell virtual correction to the HDIS **113**

Bibliography **115**

Chapter 1

Introduction

Since its first run of measurements, the Large Hadron Collider (LHC) aimed to verify the validity of the predictions of the Standard Model. This ambitious program led to many successes, first of all, the discovery, in 2012, of the Higgs Boson.

Nowadays, many things have changed. The Standard Model (SM) has received many confirmations and it is considered the theory that better describes the interactions among the constituents of the matter. However, this is not the end of the story. There are phenomena that involve energy scales that are different from the ones explored by the colliders and that are still to be understood. These can be, for example, the matter-antimatter asymmetry, the lack of CP violation in strong interactions, the origin and pattern of flavor mixing and neutrino masses, and the presence of dark matter. All these phenomena are not explained by the Standard Model and suggest that some kind of physics Beyond the Standard Model (BSM) should manifest itself at higher energy scales, with respect to those explored by the LHC.

The research program of the LHC has therefore evolved and entered into a precision era. The purpose is to make ever more precise measurements of different observables, searching for hints of non-standard physics in some discrepancy between the measured observable and the theoretical prediction. The ongoing Run 3 of the LHC, together with its High-Luminosity upgrade, will produce a large amount of new experimental data. The LHC is a proton-poroton collider, and protons are strongly interacting particles; further strongly-interacting particles are abundantly produced in every such collision. These interactions are described by Quantum-Chromo Dynamics (QCD). The possibility of making discoveries relies on our ability to separate new and rare phenomena from an overwhelming background, which is often several orders of magnitude larger than the signal. This background consists of Standard Model processes and its dominant component comes from strong interactions. It follows that improving the precision of QCD predictions is mandatory for the analysis of LHC data. This thesis looks in this direction.

Various inputs are required to improve the predictions for control QCD effects that dominate the physics investigated by hadron colliders like the LHC. During the past few years, there have been many steps forward in this sense. First of all, fixed-order calculations have significantly progressed. Many observables are now known up to next-to-next-leading order (NNLO) and there have been many promising developments in

the determination of third-order correction (N^3LO).

High-order perturbative calculations, however, is not always enough because we need an accurate understanding of physics in the presence of disparate energy scales, which range from the unprecedentedly large colliding energy, through the electroweak scale, all the way down to hadron masses. The appearance of multiple scales renders perturbative QCD calculations unreliable at any finite order in some specific cases.

This happens because logarithms of the scales that are involved in the process appear in the perturbative coefficients. In some regions of the phase space, these logarithmic contributions become large and spoil the convergence of the perturbative series. To solve this problem, we can take into account these large contributions to all perturbative orders, using a technique called resummation. During the last few years, great efforts have been made to improve the resummation techniques to reduce the theoretical uncertainties on the observables. This is important for the precise study of LHC phenomenology, but will become ever more relevant at the energies that future lepton-proton or proton-proton colliders will explore.

This thesis concentrates on the logarithmic contributions that become relevant in the high-energy part of the phase space, namely where the collider energy is large. These terms can be written as

$$\ln \frac{Q^2}{S} = \ln x, \tag{1.1}$$

where Q^2 is some hard scale of the process and S is the collider energy. When $S \gg Q^2$, $x \to 0$ for this reason, this resummation is called small-x resummation.

Thus far, the intricate structure of small-x resummation has prevented the community from reaching the precision frontier. High-energy logarithms appear both in partonic cross-sections and in the DGLAP anomalous dimensions, which govern the evolution of the parton densities.

The resummation of the logarithmic contributions in the parton densities is based on the BFKL equation [1–6]. However, it turns out that the correct inclusion of LL and NLL corrections is far from trivial. This problem received great attention in 1990s, by more than one group, see, for instance, Refs. [7–10] and Refs. [11–16], which resulted in resummed anomalous dimensions for PDF evolution.

Small-x resummation of partonic cross-sections is based on the so-called high-energy factorization or k_t-factorization theorem [17–24]. Over the past twenty years, this formalism has been extended to processes that are relevant for LHC phenomenology, including differential distributions [24–31] and implemented in a numerical framework called `HELL` (High-Energy Large Logarithms) that allows performing small-x phenomenology [32–34]. In particular, fits of parton distribution functions that include small-x resummation have been performed [35, 36]. Despite this success, these studies also show the limitations of the current state-of-the-art. In particular, the resummation of partonic coefficient function at small x is only known to the first non-trivial logarithmic order.

The puropose of this thesis is to explore the possibility of extending the small-x resummation for the coefficient functions to the Next-to-Leading Logarithmic (NLL) accuracy.

We start our discussion in Chapter 2 by introducing some useful definitions and

showing how the small-x logarithmic contributions become relevant in the coefficients of the perturbative expansion. We also discuss the factorization properties on which the small-x resummation is based and the general strategy to achieve it. One of these factorization properties is the *Collinear Factorization Theorem*, which allows us to separate a hadronic cross-section in a process-dependent part, the *coefficient function*, that can be computed in perturbation theory, and a universal part the *Parton Distribution Function* (PDF) that is universal and that takes in account the non-perturbative nature of the hadrons. Since we are interested in resumming small-x logarithms in the coefficient function, we will also present the *High-Energy Factorization Theorem*. This theorem is the one we will use to perform the resummation.

In Chapter 3, we give more details on small-x resummation for the coefficient function. We show the factorization between a *Off-Shell Coefficient function*, a quantity similar to the usual coefficient function but computed with an off-shell incoming gluon, and a *Unitegrated Parton Distribution Function* that relates the evolution of the momentum of the off-shell gluon and the PDFs. If we compute the off-shell coefficient function in a physical gauge, we find out that it is free from divergent logarithmic contribution, all of them are factorized in the unintegrated PDF. This fact is crucial for the small-x resummation and it has been proved at LL. In the last part of this chapter, we present our program to extend the LL small-x resummation for the coefficient function to NLL. We give a series of strong motivations for the necessity of calculating the off-shell coefficient function for a specific process in a physical gauge.

In Chapter 4, we present a discussion on the light-cone gauge. This is the physical gauge we chose to compute the off-shell coefficient function. Since this gauge is not commonly used in perturbative calculation, we find it useful to dedicate a chapter describing its properties and the strategies we used to perform the calculations. In particular, we concentrate on the treatment of some spurious singularities that arise due to this gauge choice. These singularities must be regularized and, in this chapter, we present two prescriptions to do so. We compare these two prescriptions showing what is the correct one to use and why. Another problem linked to the gauge-dependent singularities is the presence in this calculation of non-covariant loop integrals. The development of general a method to compute these integrals required a great amount of work since the light-cone gauge is not much used and there were few examples in the literature. We report this method in Appendix A only for readability proposes. In this chapter, we also present the problem of the resummation in light-cone gauge and the necessity of defining some gauge-dependent counterterms.

We perform the explicit calculation of the off-shell coefficient function in light-cone gauge for a specific process in Chapter 5. The process we chose is the Higgs-induced Deep Inelastic Scattering (HDIS). This process is similar to the usual DIS but has a Higgs Boson instead of the photon in the initial state. The first result presented in this chapter is the on-shell coefficient function for this process computed in the light-cone gauge. This preliminary calculation helped us to set the basis for the off-shell calculation, teaching us to overcome some first difficulties due to the gauge choice. Some of these difficulties are the growing number of terms that contribute to the amplitude in this gauge and the calculation of non-covariant loop integrals. The on-shell calculation, moreover, is an example where the Principal Value (PV) prescription

for the spurious gauge singularities works well. Then we move on to the off-shell coefficient function. This calculation is quite more complicated than the previous one and it required a great deal of work. In particular, in this chapter, we focus on the virtual correction and the non-covariant loop integrals. We see that in this case PV fails in regularising the gauge-dependent singularities and we must resort to a more refined prescription, the Mandelstam Leibbrandt (ML) prescription. While this prescription is well-defined from the theoretical point of view it is also more complicated to implement in the calculations. We present the final result for the NLO off-shell virtual amplitude of this process and we present the next step to reach a final definition for the NLO off-shell coefficient function.

Some Appendices follow the main body of this thesis. Appendix A, which has already been mentioned above, contains an important part of this work. In this appendix, we present a method we developed to compute a large class of non-covariant loop integrals. In Appendix B and Appendix C we reported some calculations done with the PV prescription, in order to compare these results with the ones obtained with ML prescription. Finally, in Appendix D and Appendix E are reported some results too long to be inserted in the main part of this work.

Chapter 2

Small-x resummation

We start our discussion by introducing the theoretical framework in which we will work in this thesis. This thesis aims to investigate the possibility of extending the known techniques of resummation in the high-energy regime of perturbative Quantum Chromo-Dynamics (QCD) in order to get more precise theoretical predictions. The goal of this chapter is, then, to give an overview of the main tools used to study QCD observables in this regime.

We are not interested in giving a complete description of QCD: it is a very broad topic and an exhaustive discussion can be found in [37–40]. We will also use the technology of Quantum Field Theory (QFT), we refer to [41–43] for an introduction to this subject.

Before addressing the main theme of resummation, let us give some general definitions to set the notation. First of all, the dynamics we are interested in is described by the QCD Lagrangian,

$$\mathcal{L}_{YM} = -\frac{1}{2} Tr\left\{F^{\mu\nu}F_{\mu\nu}\right\} + \sum_{j=1}^{n_f} \overline{q}_j \left(\mathrm{i}\not{D} - m_j\right) q_j, \tag{2.1a}$$

$$D_\mu = \partial_\mu + \mathrm{i} g_s A^a_\mu t_a, \tag{2.1b}$$

$$F_{\mu\nu} = \left(\partial_\mu A^a_\nu - \partial_\nu A^a_\mu - g_s f_{a\,b\,c} A^b_\mu A^c_\nu\right) t_a, \tag{2.1c}$$

where g_s is the gauge coupling, A^a_μ are the gluon fields in the adjoint representation of the Lie Algebra of $SU(3)$, and q_j are the fermionic fields in the fundamental representation of $SU(3)$, with masses m_j and n_f different flavors. Moreover, t_a are the generators of the Lie algebra of $SU(3)$ which satisfy the relations

$$\begin{aligned} \left[t^a, t^b\right] &= \mathrm{i} f^{a\,b\,c} t_c, \\ Tr\left(t^a t^b\right) &= \frac{1}{2}\delta^{a\,b}, \end{aligned} \tag{2.2}$$

where $f^{a\,b\,c}$ are the real structure constants of the algebra, and a, b, and c are the color indices that run from 1 to 8.

Having set our notations, we continue our discussion, taking some inspiration from [44–46]. In this chapter, we start in Section 2.1 with a brief introduction on the study of the QCD perturbatively. This is useful to set some notation and give some

fundamental definition. Then, we address the problem of the resummation of the large logarithmic contributions in the high-energy limit. In Section 2.2, we introduce the topic and describe a method to resum these logarithmic contributions based on some factorization properties of the observables, which will be detailed in the following chapter.

2.1 Perturbative QCD

To study a theory perturbatively means to assume that observables can be expanded in powers of some parameter:

$$O = \sum_{n=0}^{\infty} c_n \, \lambda^n, \tag{2.3}$$

where λ is the parameter of the expansion and c_n are the perturbative coefficients. In a renormalizable field theory, the perturbative coefficients are finite and computable (at least in principle) to any finite order. When truncated at some finite order, this expansion provides reliable predictions only if each term in the sum is smaller compared to the following. This means that the expansion parameter must be $\lambda \ll 1$, but, on the other hand, the coefficients c_n of the expansion must grow too fast with n. Under these assumptions, we have that

$$c_{i+1}\lambda^{i+1} < c_i\lambda^i \ll 1, \tag{2.4}$$

and this assures that we can trust fixed-order perturbative calculations, at least in the sense of asymptotic series.

There are however some difficulties with the practical implementation of perturbation theory. First of all, the equality in Eq.(2.3) does not hold in QCD (and in field theories in general), because the perturbative series are not convergent in the usual sense of Cauchy. This is because of the presence in the coefficients of the expansion of some terms (renormalons are an example) that grow as $n!$. The solution to this problem is to treat the expansion as an asymptotic series. We do not want to describe here this solution, it is not the aim of this work and it would require at least a whole chapter since it is an interesting and ongoing field of research. [47] For the purposes of this work, it is sufficient to know that we can truncate the perturbative expansion of a QCD observable at some order and get a good approximation of the exact value.

From now on, we will consider a generic cross-section and we will write Eq.(2.3) more precisely as

$$\sigma(Q^2) \simeq \sum_n c_n(Q^2) \, \alpha_s^n(Q^2), \tag{2.5}$$

where Q is the energy scale characteristic of the process, and we have defined

$$\alpha_s = \frac{g_s^2}{4\,\pi}, \tag{2.6}$$

in analogy with QED. In order to trust the perturbative expansion, the coupling constant of QCD must be sufficiently small and so must be the coefficients of the expansion.

In the following sections, we will address both points: we will show that the expansion parameter can be chosen to be small enough, provided Q is sufficiently larger than the typical hadronic scale, and that the perturbative coefficients can grow large in certain kinematic regimes.

2.1.1 QCD running coupling

We start by summarising well-known results about the dependence of the QCD coupling constant on the scale of the process.

In principle, as long as quarks are considered massless, QCD would be scale invariant. However, this does not hold when we take into account higher-order (loop) corrections. In this case, the renormalized Lagrangian parameters get a logarithmic dependence on a renormalization scale μ, that is governed by Renormalisation Group Equations (RGEs)

$$\begin{aligned} \mu^2 \frac{d\alpha_s(\mu^2)}{\mu^2} &= \beta\left(\alpha_s(\mu^2)\right), \\ \beta\left(\alpha_s(\mu^2)\right) &= -\alpha_s(\mu^2)\left(\beta_0 + \beta_1\,\alpha_s(\mu^2) + \beta_2\,\alpha_s^2(\mu^2) + \ldots\right), \end{aligned} \tag{2.7}$$

where $\beta\left(\alpha_s(\mu^2)\right)$ is the QCD β-function and its coefficients, β_i, can be computed in perturbation theory. At the current state of the art, the β-function is known up to five loops [48, 49]. The Eq.(2.7) can be solved by iteration and at the lowest order the solution is

$$\alpha_s(\mu^2) = \frac{\alpha_s(\mu_0^2)}{1 + \beta_0 \alpha_s(\mu_0^2) \ln\left(\frac{\mu^2}{\mu_0^2}\right)}, \tag{2.8}$$

where μ_0 is a scale where the coupling is known or measured.

The β-function governs how the coupling constant α_s varies as the renormalization scale, μ^2 increases. In particular, the positive sign of its initial term,

$$\beta_0 = \frac{11 C_A - 2 n_f}{12\pi}, \tag{2.9}$$

ensures that the coupling diminishes at larger scales. This characteristic, known as asymptotic freedom, is unique to local non-Abelian gauge theories among renormalizable field theories in four-dimensional spacetime [50].

On the other hand, the coupling grows large for small μ^2, and perturbative methods can no longer be trusted. The demarcation between these two domains is conventionally associated with the Landau pole, determined by the equation

$$\frac{1}{\alpha_s(\Lambda_{\mathrm{QCD}})} = 0 \tag{2.10}$$

At this scale, which is of the order of a few hundred MeV, QCD enters a strong-coupling regime, where perturbation theory is of no use. In this regime, strong interactions are characterized by the confinement phenomenon: quarks and gluons are not directly observable, and physical states carry zero color charge.

Thanks to the property of the asymptotic freedom, we can always find a region of the phase space where the QCD coupling is small. This, however, is not enough to ensure reliable perturbative predictions. In fact in some regions of the phase space, the coefficients c_n can become quite large, making

$$c_i \, \alpha_s^i \to 1, \tag{2.11}$$

and spoiling the convergence of the series. This means that we cannot trust anymore the predictions we get with perturbation theory. In the following, we will analyze in detail why these coefficients are large and what we can do to solve this problem and restore the predictivity of the series.

2.1.2 Logarithms in the perturbative coefficients

As we discussed in the previous section, perturbation theory in QCD can be employed for processes characterized by an energy scale which is much larger than Λ_{QCD}. The typical example is the production process of some heavy system, such as a weak vector or scalar boson or a Drell-Yan pair at hadron colliders, accompanied by undetected radiation. In such cases, the role of the hard scale Q is played by the invariant mass M of the produced system.

In the general case, however, more energy scales can be relevant for a given process; it is useful to choose one scale Q^2 as the hard scale of the process, and form a collection of dimensionless ratios

$$x_i = \frac{Q_i^2}{Q^2} \tag{2.12}$$

on which the perturbative coefficients may depend. In the example quoted above, choosing the hard scale as the mass of the heavy system in the final state, $Q^2 = M^2$, there is at least one relevant ratio of quadratic invariants, namely

$$x = \frac{Q^2}{s}; \qquad 0 \leq x \leq 1, \tag{2.13}$$

where s is the squared center-of-mass energy of the initial state. The fraction x is related to the energy of the undetected radiation: when x is close to one, the available energy is barely sufficient to produce the observed heavy system, and correspondingly the extra radiation is soft. This is usually referred to as the threshold limit. We will be mainly interested in the opposite end-point, $x \to 0$, where the available energy is much larger than M; this is called the large-energy, or small-x, regime.

It turns out that the order n perturbative coefficient displays a polynomial dependence on logarithms of both x and $1 - x$, with the degree of the polynomial linear in n. As a consequence, a truncated perturbative expansion is only reliable for values of x not too close to the end-points.

At the two boundaries these logarithmic contributions spoil the convergence of the series and the predictivity of the perturbative expansion is lost. Restoring the validity of the perturbative expansion can be achieved if we group together large terms by the power of the logarithms, write them as a series, and sum it. This procedure is called resummation. Of course, there are many different resummation techniques depending

on which contribution is dominant in the region of the phase space we are interested in. In this work, we will focus on the high-energy region of the phase space, focusing on the techniques to resum small-x logarithms.

First of all, we can take a closer look at the structure of the small-x logarithm to better understand what it means to resume a series. The structure of radiative corrections will generate logarithmic terms recursively. Each coefficient c_n will contain up to one extra power of the logarithm for each extra order in the coupling constant α_s. This pattern is called a single-logarithmic enhancement and schematically we can write it as

$$\begin{aligned}\sigma(Q^2, S, \ldots, \alpha_s) = \sigma_0(Q^2, S, \ldots, \alpha_s)\,(1+ \\ \alpha_s\left[a_1 \ln(x) + b_1\right] + \\ \alpha_s^2\left[a_2 \ln^2(x) + b_2 \ln(x) + c_2\right] + \\ \ldots \\ \alpha_s^n\left[a_n \ln^n(x) + b_n \ln^{n-1}(x) + \ldots\right] + \ldots\big)\,,\end{aligned} \tag{2.14}$$

where to write the cross-section in the most general way, we assumed that it depends on a certain number of scales (Q^2, S, and more). When $x \to 0$, the product $\alpha_s \ln(x) \to 1$ and so we can say that all terms in the first column of Eq.(2.14) will be of the same order. In these kinematic conditions, if we truncate the series at any n, we generate errors as large as the truncated series itself. To make reliable predictions and restore the validity of the perturbative expansion, the first step is to gather together the large terms by the power of the logarithms. We can formally write

$$\begin{aligned}\sigma(Q^2, S, \ldots, \alpha_s) = \sigma_0(Q^2, S, \ldots, \alpha_s) \\ \times \left[\sum_{k=0}^{\infty} a_k \left(\alpha_s \ln(x)\right)^k + \alpha_s \sum_{k=0}^{\infty} b_k \left(\alpha_s \ln(x)\right)^k + \ldots + \text{non log}\right],\end{aligned} \tag{2.15}$$

where we have reconstructed a series, in which each successive term is suppressed by an extra power of α_s as compared to the previous and all logarithmic contributions are confined in the coefficients of each order. We call each term of the series leading logarithms (LL), next-to-leading logarithms (NLL) and so on. Once we wrote the perturbative expansion in this way, in order to restore the validity of perturbation theory, we need to identify a strategy to capture all terms inside each logarithmic expansion in order to write

$$\sigma(Q^2, S, \ldots, \alpha_s) \sim \sigma_0(Q^2, S, \ldots, \alpha_s)\left[g_0(\text{LL}) + g_1(\text{NLL}) + \ldots + \text{non log}\right]. \tag{2.16}$$

This procedure is called resummation. This was only a general introduction to explain why it it so important the resummation procedure. In the following sections, we will describe the resummation procedure in the high-energy region, the small-x resummation.

2.2 Small-x resummation

In this thesis, we are interested in studying the resummation of the logarithmic contributions arising in the high-energy limit. As mentioned in the previous section, since

in the high energy limit, the ratio between the scale of the energy of the process and any other scale goes to zero, this is also called the small-x limit.

Since every resummation always relies on some factorization properties, we need to find these properties in the observable we are interested in, namely the cross-section.

The first factorization we can use is the standard *collinear factorization theorem*, which is the conceptual basis for the calculation of QCD corrections to parton model predictions. This theorem allows us to factorize the contribution to any QCD cross-section in two parts. The first is the *parton distribution function* (PDF) that describes the dynamics of the partons inside a proton. This object cannot be determined from first principles, since it receives contributions from the non-perturbative regime of strong interactions. It is, however, process-independent since essentially describes dynamics that pertain to the proton wavefunction. The second term is the *coefficient function*. This object is process-dependent and describes the interaction of the free partons, quarks and gluons, with the hard probe. This can be computed perturbatively at the desired order and then convoluted with the parton distribution function to get the cross-section. This can be written as

$$\sigma(x,Q^2) = \sum_i \int_x^1 \frac{dz}{z} C_i\left(\frac{x}{z}, Q^2, \alpha_s(Q^2)\right) f_i(z,Q^2), \tag{2.17}$$

where x is the ratio between the hard scale of the process Q^2 and the centre-of-mass energy S. The first term in this expression, $C_i\left(\frac{x}{z}, Q^2, \alpha_s(Q^2)\right)$ is the process-dependent coefficient function, while $f_i(z,Q^2)$ is the parton distribution function. The sum runs over all the parton, namely the quarks and the gluons. To write Eq.(2.17), considered the case shown in Fig.(2.1), where a hadron interacts with a lepton. This is a simplified situation because, since we have only one hadron, we need only one PDF and one coefficient function. If we have two hadrons interacting, like in the case of LHC, Eq.(2.17) must be modified and becomes

$$\sigma(x,Q^2) = \sum_{i,j} \int_x^1 \frac{dz_1}{z_1} \int_x^1 \frac{dz_2}{z_2} C_{i,j}\left(\frac{x}{z_1\, z_2}, Q^2, \alpha_s(\mu^2)\right) f_i(z_1,\mu^2) f_j(z_2,\mu^2). \tag{2.18}$$

This formula has been proven to all orders in perturbation theory [51, 52], for a wide set of processes.

Unfortunately, collinear factorization is not enough to resum small-x logarithms. These logarithms are present both in the coefficient function and in the parton distribution function and must be resummed separately. In this thesis, we are mostly interested in studying the resummation for the logarithmic contribution of the coefficient function. In the following, after having briefly summarised the techniques to achieve the resummation in the PDFs, we discuss the strategy to perform the small-x resummation in the coefficient function.

2.2.1 Small-x resummation of the parton distribution functions

First of all, we point out how small-x logarithms arise in parton distribution functions (PDFs). Since to factorize the collinear singularities we need to introduce an arbitrary

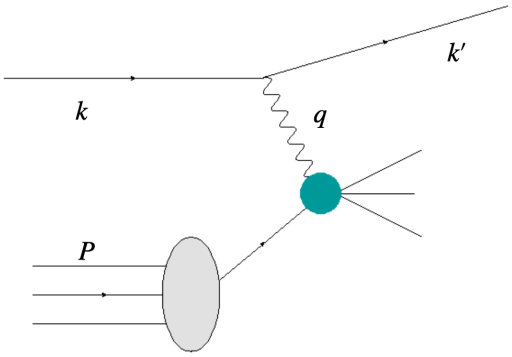

Figure 2.1: Interaction of a hadron with a lepton. In this case, we have only one coefficient function and one parton distribution function because we have only one hadron in the initial state.

energy scale μ^2, the parton densities must satisfy the equation

$$\mu^2 \frac{\partial f_q(x,\mu^2)}{\partial \mu^2} = -\frac{\alpha_s}{2\,\pi} \int_x^1 \frac{dz}{z} \left[P_{qq}\left(\frac{x}{z}\right) f_q(z,\mu^2) + P_{qg}\left(\frac{x}{z}\right) f_g(z,\mu^2) \right]. \tag{2.19}$$

This is the Dokshitzer-Gribov-Lipatov-Altarelli-Parisi (DGLAP) equation [53–55] that enables one to compute the scale dependence of the PDFs. Thanks to DGLAP evolution, PDFs can be fitted from the data collected in a given experiment at some energy scale and used as a phenomenological input for a different experiment at a different energy scale. Indeed, while PDFs are non-perturbative objects, their evolution kernels P_{ij} can be computed in perturbation theory,

$$P_{ij}\left(\alpha_s(s), z\right) = \sum_{n=0}^{\infty} \left(\frac{\alpha_s}{2\pi}\right)^n P_{ij}^{(n)}(z). \tag{2.20}$$

Of course Eq.(2.19) describes only the evolution of the distribution function of a quark. We can write an analogous equation for the gluon and the antiquark. The leading-order splitting functions are

$$\begin{aligned}
P_{qq}^{(0)}(z) &= C_F \left[\frac{1+z^2}{(1-z)_+} + \frac{3}{2}\delta(1-z) \right], \\
P_{qg}^{(0)}(z) &= T_R \left[z^2 + (1-z)^2 \right], \\
P_{gq}^{(0)}(z) &= 2C_A \left[\frac{1+(1-z)^2}{z} \right], \\
P_{gg}^{(0)} &= 2C_A \left[\frac{z}{(1-z)_+} + \frac{1-z}{z} + z(1-z) \right] + \delta(1-z)\frac{12C_A - 4n_f T_R}{12\pi},
\end{aligned} \tag{2.21}$$

where the plus distribution is defined according to

$$\int_0^1 dz \left[f(z)\right]_+ g(z) = \int_0^1 f(z) \left[g(z) - g(1)\right]. \tag{2.22}$$

In Eq.(2.21) we see that in the limit $z \to 0$, that corresponds to the high energy limit, P_{gq} and P_{gg} diverge, in this sense the PDFs contain small-x singularities. The divergent contribution form P_{qq} and P_{qg} appears only at higher orders and, therefore, it is subleading.

We summarise here how we can resum the small-x singularities in the splitting functions. This resummation relies on the Balitsky-Fadin-Kuraev-Lipatov (BFKL) equation [5, 6, 56–59]. This is an evolution equation that governs the dependence of the PDFs on the variable x in the small x region, similarly to what DGLAP equation does with the scale. This evolution equation is obtained by studying the high energy limit of physical amplitudes in the context of the so-called *Regge theory* (see [60] for an exhaustive introduction of this formalism).

In the BFKL equation, we can identify a counterpart of the DGLAP splitting function, the BFKL kernel. Requiring that PDFs satisfy both BFKL and DGLAP evolution equations leads to a consistency relation between the splitting functions and the BFKL kernel. This consistency relation is called *duality* and allows one to resum the small-x singularities in the splitting functions given the knowledge of the BFKL kernel at fixed order.

However, there are still some issues in this procedure. The BFKL evolution kernel, in fact, is perturbatively unstable. If we use it to directly resum the small-x singularities we get a perturbatively unstable resummed result. This means, for example, that the NLL is a larger correction than the LL. Stabilizing the BFKL kernel and the resummation required a great deal of work that has been carried out over fifteen years by more than one group [7, 8, 10–16, 61–65]. The idea is to stabilize the BFKL kernel, and thus the resummation, using the duality in reverse to resum the collinear part of the unstable contributions to BFKL using DGLAP at fixed order. At this point, one can exploit a symmetry property of the BFKL kernel to resum the other anti-collinear part too. Moreover, it has also been realized that to remove a further source of instability, it is necessary to consider the resummation of a class of contributions originating from the running of the strong coupling, despite being formally sub-leading.

More recently, around a decade after the last publication on small-x resummation of splitting functions, the results of the Altarelli-Ball-Forte (ABF) [11–16] group have been further developed and improved. Moreover, they have been made publicly available through the numerical code `HELL` (High-Energy Large Logarithms) [32, 33, 66].

2.2.2 Small-x resummation of the coefficient function

We now move on to consider the resummation for the coefficient function. First of all, we review the state of the art for this kind of resummation, then we summarise the strategy we will follow in this thesis.

The coefficient function resummation, at present, is consistently known only to relative Leading Logarithmic (LL) accuracy. The logarithmic accuracy has already been improved in some other resummation schemes. For example, in the hybrid factorization framework, the effects of resummation in Mueller–Navelet jets [67] were subject to extensive study, as well as the exclusive electroproduction of light vector mesons [68, 69]. A partial NLL treatment was achieved for multi-jet detection [70–72], and for final

states where a J/ψ [73], a Drell–Yan pair [74], or a heavy-flavored jet [75] is inclusively emitted in association with a light-flavoured jet, provided that the two objects are well separated in rapidity. Similar analyses on inclusive heavy quark pair obtained by photo-production and hadro-production were respectively proposed in Refs. [76, 77]. More recently, Ref. [78] featured a full computation of the next-to-leading order correction to the impact factor for the production of a forward Higgs boson, obtained in the infinite top-mass limit. This was a missing ingredient for the next-to-leading (NLL) description of the inclusive hadro-production of a forward Higgs at small-x in the language of the BFKL equation.

In this thesis, we want to investigate the extension of the LL resummation for the coefficient function, in the context of `HELL` formalism [32,33,66], to NLL accuracy. This resummation formalism is on the high-energy factorization theorem, also known as k_t-factorization. This theorem reflects the properties of the amplitudes in the high-energy limit, for an exhaustive treatment on this subject see [60]. In the high-energy limit, we can write the coefficient function as [18, 19, 22, 79]

$$\sigma(x,Q^2) = \int dk_\perp^2 \int_x^1 \frac{dz}{z} \mathcal{C}\left(\frac{x}{z}, k_\perp^2, Q^2\right) \mathcal{F}_g\left(z, k_\perp^2, Q^2\right), \tag{2.23}$$

where the first term in the convolution, $\mathcal{C}\left(\frac{x}{z}, k_\perp^2, Q^2\right)$, is the so-called off-shell coefficient function while the second term, $\mathcal{F}_g\left(z, k_\perp^2, Q^2\right)$, is called unintegrated PDF. The first term is process-dependent and it is different from the usual coefficient function because the incoming parton is taken off its mass shell. The unintegrated PDF is related to the ordinary PDF by means of an evolution operator,

$$\mathcal{F}_g\left(z, k_\perp^2, Q^2\right) = \mathcal{U}\left(z, \frac{k_\perp}{Q^2}\right) f_g(z, Q^2). \tag{2.24}$$

Comparing Eq.(2.17) and Eq.(2.23) we can immediately see that

$$C(x,Q^2) = \int dk_\perp^2 \int_x^1 \frac{dz}{z} \mathcal{C}\left(\frac{x}{z}, k_\perp^2, Q^2\right) \mathcal{U}\left(z, \frac{k_\perp}{Q^2}\right). \tag{2.25}$$

This is the formula that allows us to resum small-x logarithms in the coefficient function. If we work in a physical gauge, the off-shell coefficient function does not contain any term that is logarithmically enhanced at small x. All the small-x enhancements are resummed by the evolutor $\mathcal{U}$. We will discuss this procedure more in details in Chapter 3, computing $\mathcal{U}$ in a simple case and showing that it contains the all-order leading logarithmic terms.

Note that in Eq.(2.23) and in Eq.(2.24) only the gluon PDF appears. This is because, in the high-energy regime, the main contribution to the amplitude comes from the evolution of the gluon [60]. The Eq.(2.25) has proved to work at leading logarithmic accuracy [32]. This means that the off-shell coefficient function must be computed at leading order, while the evolution operator must be computed at LL. In Fig.(2.2) we report a schematic representation of the meaning of Eq.(2.25).

We aim to investigate the possibility of extending this formula to NLL. To do so, we need to compute the off-shell coefficient function at NLO and the evolution operator

at NLL. In particular, in this thesis, we concentrate on the computation of the off-shell coefficient function. Indeed, the first test of Eq.(2.25) is to prove that at one loop $\mathcal{C}\left(\frac{x}{z}, k_\perp^2, Q^2\right)$, computed in a physical gauge, is free from small-x logarithms.

In the following, we will give a detailed description of the collinear and the high-energy factorizations, that have been introduced in this section to explain small-x resummation.

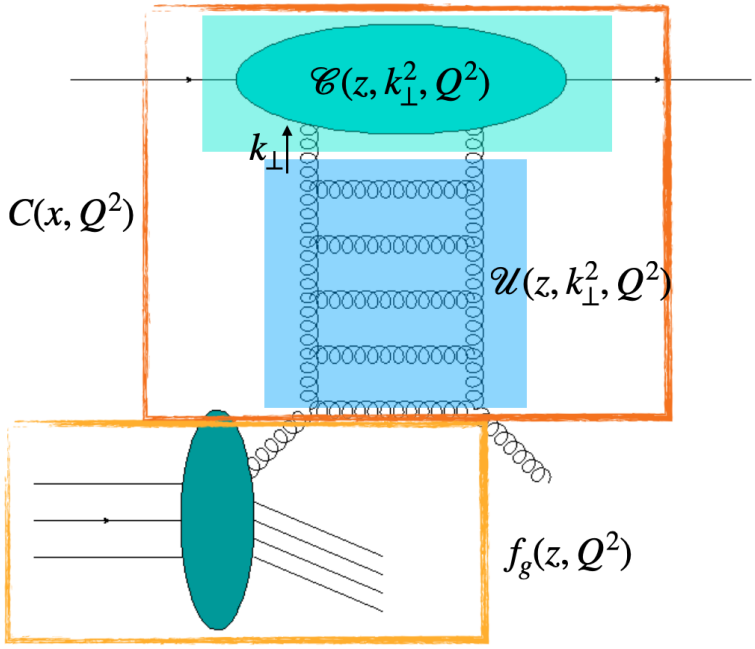

Figure 2.2: Schematic representation of the result in Eq.(2.25). In the case of a proton, the green ball at the bottom, interacting with a lepton, we highlighted the factorization between the coefficient function, the orange box, and the PDF, the yellow box. In the coefficient function, we highlighted with the light-blue box the off-shell coefficient function and with the blue box the evolution operator. We also labeled with the name $k_\perp$ the momentum of the last gluon in the ladder that is the off-shell gluon entering in the off-shell coefficient function.

Chapter 3

Small-x resummation from LL to NLL

After having presented in Chapter 2 the general strategy we follow to resum the small-x logarithms, in this chapter we discuss the extension of the formalism to the next term in the logarithmic expansion, namely Next-to-Leading Logarithmic (NLL) accuracy.

We start in Section 3.1 by giving some details about the high-energy factorization theorem. We will give a definition of the off-shell coefficient function and of the un-integrated parton distribution function. In Section 3.2, we give an example of the LL small-x resumation procedure, by applying it to the coefficient function of the Higgs-induced deep-inelastic scattering. Finally, in section 3.2, we will establish the basis for the next-to-leading logarithm resummation for the coefficient function.

3.1 High-energy factorisation

We start by deriving the high-energy factorization theorem we introduced in Chapter 2. This theorem is the foundation of the resummation formula in Eq.(2.25). To extend this formula to the NLL we have to understand where it comes from. This will allow us to identify the key ingredients that will be useful to extend Eq.(2.25) to the NLL. In this presentation, we closely follow Refs. [18,22,79]. We start by considering the photo-production of a heavy-quark pair. We can exploit the collinear factorization theorem, discussed in Chapter 2, to write the cross section for this process as the convolution of a PDF and a partonic coefficient function. Since we are interested in the small-x regime we can focus on the gluon-initiated process:

$$\gamma^*(p_1) + g(p_2) \to Q(p_3) + \bar{Q}(p_4) + X, \tag{3.1}$$

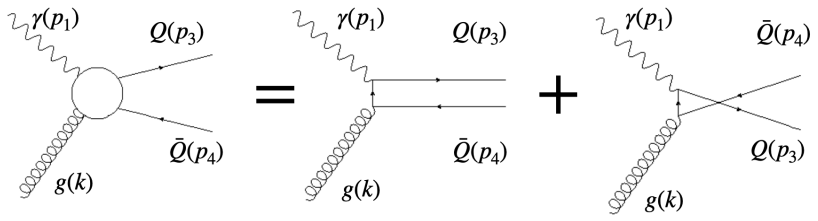

Figure 3.1: Born level for the photo-production of a $Q\bar{Q}$ pair.

where we can take $p_{1,2} = \frac{\sqrt{S}}{2}(1,0,0,\pm 1)$ and S is the center of mass energy. In Fig.(3.1) we reported the tree level of this process. The mass of the heavy quarks is $p_3^2 = p_4^2 = M^2$ and, in high energy limit, we have

$$S = 2(p_1 \cdot p_2) \gg 4M^2, \tag{3.2}$$

that corresponds to consider

$$x = \frac{4M^2}{S} \to 0. \tag{3.3}$$

At Born-level the coefficient function of this process does not contain logarithmic enhancements, but when we consider the leading order gluon corrections, namely the NLO coefficient function for the scattering in Eq.(3.1), we see that $\ln\left(\frac{1}{x}\right)$ are present. These logarithmic contributions spoil the perturbativity of the coefficient function and so, as we discussed in Chapter 2, we have to resum them. In this section, we want to prove at LL the high-energy factorization formula,

$$\sigma(x,Q^2) = \int dk_\perp^2 \int_x^1 \frac{dz}{z} \mathcal{C}\left(\frac{x}{z}, k_\perp^2, Q^2\right) \mathcal{F}_g\left(z, k_\perp^2, Q^2\right). \tag{3.4}$$

This proof relies heavily on the proprieties of the amplitude in the high-energy regime, the so-called Regge behavior [5,56–59] and also on the related particle production [80]. For a complete discussion on this subject see [60]. According to this analysis, many-gluon exchanges in the s-channel, shown in Fig.(3.2), are sub-leading in a physical gauge by at least one power of α_s. In the following, we will use the light-cone gauge, where the gauge vector is taken to be massless, $n^2 = 0$. The diagrams providing leading logarithms are the ones with multiple gluon exchanges in the t-channel that define what is called a generalized ladder. In Fig.(3.3) we show an example of multi-gluon exchange in the t-channel, from this picture, it is also clear why this exchange is called ladder of gluons.

We can separate the last rung of the ladder in Fig.(3.3) from the others. This corresponds to the exchange of a single off-shell gluon of momentum k while we can embody all the remaining gluons in the function $\mathcal{F}$. We choose to parametrize the momentum of this gluon with the Sudakov parameterization,

$$k^\mu = z p_2^\mu + k_\perp^\mu + \beta p_1, \tag{3.5}$$

where the momentum $k_\perp$ is defined to be transverse to p_1^μ and p_2^μ. One can show that the dominant region of the integration in the momentum of this gluon is the one of fixed $k_\perp^\mu$, small z, and where $k^2 \simeq -\mathbf{k}_\perp^2$.

To prove Eq.(3.4), we need to give a precise definition for the off-shell coefficient function and for $\mathcal{F}$. To do so we need to show that a single gluon polarization contributes to the diagram in Fig.(3.4). We name $A^{\mu\nu}$ the lowest order $Q\,\bar{Q}$ contribution to the $\gamma\, g \to \gamma g$ process, while we name $G_{\mu\nu}$ the full $g\, g \to g\, g$ part of the process, including the gluon propagator, computed in light-cone gauge with $n = p_1$. The coefficient function in Fig.(3.4) can therefore be written as

$$C(x,Q^2) = \frac{1}{2S} \int \frac{d^4k}{(2\pi)^4} A^{\mu\rho}(p_1,k) d_\mu^\sigma(k,n) d_\rho^\nu(k,n) G_{\sigma\nu}(p_2,k), \tag{3.6}$$

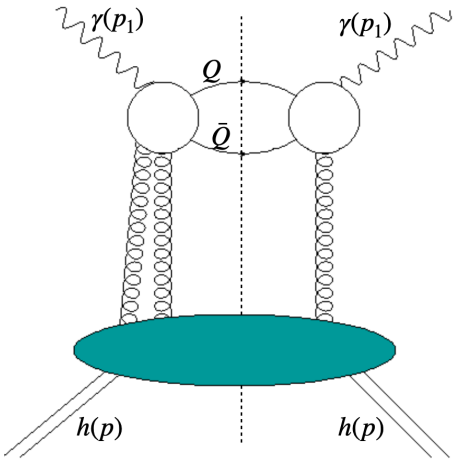

Figure 3.2: Feynman diagram for the multi-gluon exchange in the s-channel for the photo-production of $Q\bar{Q}$ pair.

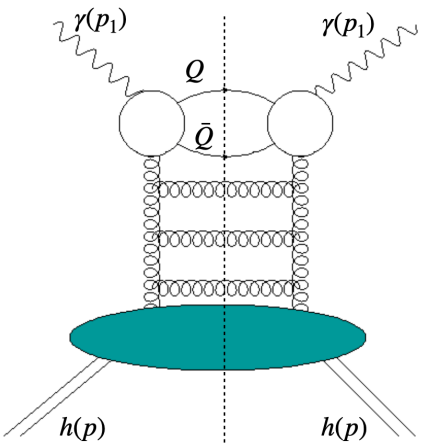

Figure 3.3: Feynman diagram for the multi-gluon exchange in the s-channel for the photo-production of $Q\bar{Q}$ pair.

where $d^{\sigma}_{\mu}(k,n)$, is the numerator of the propagator of the gluon of momentum k. This propagator is computed in light-cone gauge, the corresponding denominators are hidden inside G. At this point, we note that the $A^{\mu\nu}$ part of the coefficient function can be decomposed as

$$\begin{aligned} A^{\mu\nu}(p_1,k) =& A_1\left(\frac{x}{z},\frac{k^2}{zS}\right)\left(-g^{\mu\nu}+\frac{k^{\nu}}{k^2}\right) \\ &-\frac{1}{k^2}A_2\left(\frac{x}{z},\frac{k^2}{zS}\right)\left(\frac{k^2}{p_1\cdot k}p_1^{\mu}-k^{\mu}\right)\left(\frac{k^2}{p_1\cdot k}p_1^{\nu}-k^{\nu}\right), \end{aligned} \tag{3.7}$$

where A_1 and A_2 can be explicitly computed in perturbation theory. It is important to note that we could decompose this tensor in this way because at this order $A^{\mu\nu}$ does not depend on the gauge vector n. If we want to extend this factorization to the following order in perturbation theory, computing $A^{\mu\nu}$ at NLO, the tensor will, in general, depend on n and so in Eq.(3.7) we should add a dependence on the gauge vector.

It can be proved that in the high energy limit, A_1 and A_2 are small and of the same order [18]. We will see a practical example of this in Section 3.2 where we compute the LL resummed coefficient function for the Higgs-induced Deep-Inelastic-Scattering.

This scaling means that the dominant behavior of Eq.(3.7) is determined by the polarisation factor in front of the two coefficients A_1 and A_2. In particular, the tensorial structure that multiplies A_2 can be written as

$$-\frac{1}{k^2}\left(\frac{x}{z},\frac{k^2}{zS}\right)\left(\frac{k^2}{p_1\cdot k}p_1^{\mu}-k^{\mu}\right)\left(\frac{k^2}{p_1\cdot k}p_1^{\nu}-k^{\nu}\right)\sim\frac{4\mathbf{k}_{\perp}^2}{zS}\frac{p_1^{\mu}p_1^{\nu}}{S}\frac{1}{z}, \tag{3.8}$$

that gives a net $\frac{1}{z}$ enhancement (in the high energy limit if $x\to 0$ also $z\to 0$). This means that in the high energy limit, the contribution from A_2 is dominant. We can

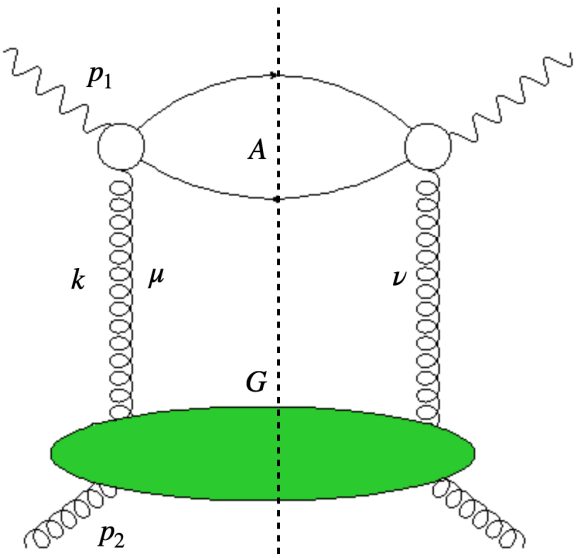

Figure 3.4: Factorized structure for the coefficient function in the high-energy limit.

write Eq.(3.6) as

$$\begin{aligned} C(x,Q^2) &\simeq \frac{1}{2S}\int \frac{d^4k}{(2\pi)^4}\left(\frac{4\mathbf{k}_\perp^2}{zS}\frac{p_1^\mu p_1^\nu}{S}\frac{A_2}{z}\right) d_\mu^\sigma(k,n) d_\rho^\nu(k,n) G_{\sigma\nu}(p_2,k) \\ &\simeq \frac{1}{2S}\int \frac{dz dk^2}{zS}\int \frac{d^2k_\perp}{(2\pi)^4}\frac{4\mathbf{k}_\perp^2}{zS} A_2 p_1^\mu p_1^\rho\, d_\mu^\sigma(k,n) d_\rho^\nu(k,n) G_{\sigma\nu}(p_2,k) \\ &\simeq \int \frac{dz}{z}\int dk_\perp^2 \left(\frac{x}{z}A_2\right)\left[\int \frac{d^2k}{(2\pi)^4}\frac{\mathbf{k}_\perp^2}{zS^2} p_1^\mu p_1^\rho G_{\sigma\nu}(p_2,k)\right] \\ &= \int dk_\perp^2 \int_x^1 \frac{dz}{z}\mathcal{C}\left(\frac{x}{z},k_\perp^2,Q^2\right)\mathcal{F}_g\left(z,k_\perp^2,Q^2\right), \end{aligned} \tag{3.9}$$

where we defined

$$\mathcal{C}\left(\frac{x}{z},k_\perp^2,Q^2\right) = \frac{x}{z}A_2\left(\frac{x}{z},\frac{k^2}{zS}\right) \tag{3.10}$$

and

$$\mathcal{F}_g\left(z,k_\perp^2,Q^2\right) = \int \frac{dk^2}{(2\pi)^4}\frac{\mathbf{k}_\perp^2}{zS^2} p_1^\mu p_1^\rho G_{\sigma\nu}(p_2,k). \tag{3.11}$$

In this way, we proved the factorization formula in Eq.(3.4) when the off-shell coefficient function is computed at Born level. Moreover, we gave a method to compute both the off-shell coefficient function and the unintegrated PDF. In particular, from Eq.(3.10), we find out that the easiest way to extract the A_2 coefficient is to couple eikonal vertices to the tensor

$$d^{\mu\nu}(k) = \frac{k_\perp^\mu k_\perp^\nu}{\mathbf{k}_\perp^2}. \tag{3.12}$$

In this way, we can write

$$\begin{aligned}\mathcal{C}\left(\frac{x}{z},k_\perp^2,Q^2\right)=\frac{x}{z}A_2&=A^{\mu\nu}(k,p_1)d_{\mu\sigma}(k,n)d_{\nu,\rho}(k,n)\left(\frac{z^2}{\mathbf{k}_\perp^2}p_2^\rho p_2^\sigma\right)\\&=A^{\mu\nu}(k,p_1)\frac{k_\perp^\mu k_\perp^\nu}{\mathbf{k}_\perp^2}.\end{aligned}\tag{3.13}$$

In this way, we find a prescription to compute the off-shell coefficient function $\mathcal{C}$ by finding a definition for the off-shell counterpart of the polarisation tensor of a gluon. We will discuss better the definition of this tensor in the following section since this is a crucial point to define the off-shell coefficient function. In this section, working in dimensional regularisation, we will use

$$d_{CH}^{\mu\nu}=(d-2)\,\frac{k_\perp^\mu k_\perp^\nu}{\mathbf{k}_\perp^2}\tag{3.14}$$

to contract the off-shell amplitude. As we just saw, this tensor selects the dominant part of the amplitude in the high-energy limit. Moreover, it is easy to see that this tensor reduces to the usual polarisation tensor of a gluon if we take the on-shell limit.

It is important to note that this derivation is only proved when the off-shell coefficient function is computed at leading order. If we compute the NLO off-shell coefficient function then the tensor $A^{\mu\nu}$ acquires a dependence on the gauge vector n and the decomposition in Eq.(3.7) will not be valid anymore. Moreover, in general, also the scaling of the coefficients A_1 and A_2 could be different. This becomes relevant if we want to use the factorization formula Eq.(3.4) to resum the NNL terms in the coefficient function with Eq.(2.25). In this case, in fact, we have to compute the NLO off-shell coefficient function and we have to verify that the factorization in Eq.(3.4) still holds. To do so, we will have to explicitly compute the NLO off-shell coefficient function for at least one process to verify if the scaling in Eq.(3.7) still holds and if not to give a different definition tensor in Eq.(3.14).

The use of the light-cone gauge is important in this context because allows us to separate the diagrams contributing to the off-shell coefficient function from the ones contributing to the unintegrated PDF. To do so, we have to define the *two gluon reducible* (2GR) diagrams and the *two gluon irreducible* (2GI) diagrams. We say that a diagram is 2GR if it can be separated into two independent diagrams by cutting two gluon lines in the t-channel. We say that it is 2GI otherwise. In Fig.(3.5) you can see an example of a one-loop two-gluon reducible diagram for the Higgs-induced DIS, while in Fig.(3.6) you can see an example of a 2GI one-loop diagram for the same process. It has been proved that 2GR diagrams contribute to the unintegrated PDF forming the gluon ladder, while the 2GI diagrams contribute to the off-shell coefficient function. Moreover, if we compute these diagrams in light-cone gauge we find out that the 2GI diagrams do not contain any logarithmic enhancement. They are all collected by the 2GR terms that can be computed to all order by computing $\mathcal{F}$ [18, 22]. This means that in Eq.(2.25) all the logarithmic enhancements can be encoded in the evolutor $\mathcal{U}$ that is linked to the unintegrated PDF as we saw in Eq.(2.24). This provides a proof for the small-x resummation. All this machinery has proved to work well at LL.

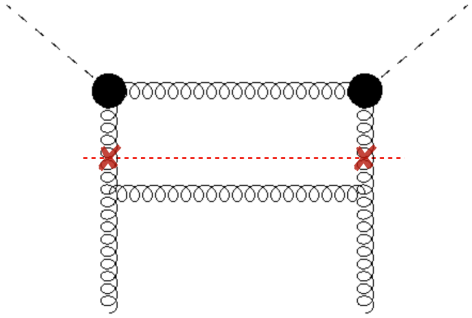

Figure 3.5: One loop two gluon reducible diagram for the HDIS process.

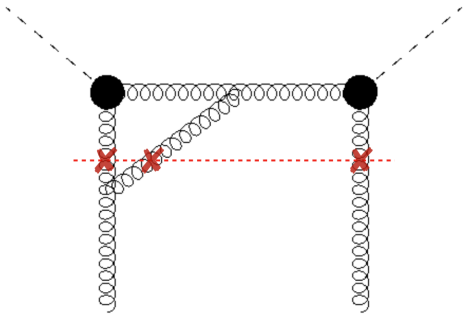

Figure 3.6: One loop two gluon irreducible diagram for the HDIS process.

We will discuss what we need to extend this resummation to NLL in Section 3.3. Here we want to underline the fact that, from the derivation we did in this section, we see that it is important to compute the NLO off-shell coefficient function for a test process. We think that is it important to do this calculation in a physical gauge in order to verify that the high-energy factorization theorem, Eq.(3.4), holds also beyond LO.

While in the following chapters we will focus on the first term in Eq.(2.25), in the following section we show how we can compute the unintegrated PDF and the evolutor $\mathcal{U}$.

3.1.1 The soft emission chain and unintegrated gluon distribution

In this section, we want to compute the unintegrate gluon distribution $\mathcal{F}$ in Eq.(3.4). As we saw in the previous section, this can be written as Eq.(3.11). A formal proof of this relation is complicated and beyond the scope of this discussion. More detail can be found in Ref. [22]. Here we will use a simpler argument under the assumptions of fixed coupling, following the discussion in Ref. [24].

We begin by comparing Eq.(3.9) to its counterpart in collinear factorization. If we consider only a single extra emission from the collinear initial state, we can write the collinear coefficient function as

$$C_{1\,\mathrm{bare}}\left(x,\frac{\mu_F^2}{Q^2},\alpha_s,\epsilon\right)=\int_x^1\frac{dz}{z}\int\frac{d\xi}{\xi^{1+\epsilon}}\mathcal{C}\left(\frac{x}{z},\xi,\alpha_s,\epsilon\right)K_1\left(z,\frac{\mu_F^2}{\xi Q^2},\alpha_s,\epsilon\right), \tag{3.15}$$

where K_1 is the amplitude for a single gluon emission contracted with the expression in square brackets in Eq.(3.9) and the polarisation tensor of the initial collinear gluon. We also used the definition

$$\xi=\frac{\mathbf{k}_\perp^2}{Q^2}, \tag{3.16}$$

in order to have dimensionless integration variables.

Since there are some IR singularities, we used dimensional regularisation with $d=4-2\epsilon$ and $\epsilon<0$. The dimensional regularisation also introduces the addition factor

$\xi^{-\epsilon}$ that in Eq.(3.15) is factorized for convenience. To reduce this convolution to a product we can take the Mellin transform over the variable x, defined as

$$g(N,Q^2)=\int_0^1 dx x^{N-1} g(x,Q^2). \tag{3.17}$$

We get

$$C_{1\,\text{bare}}\left(N,\frac{\mu_F^2}{Q^2},\alpha_s,\epsilon\right)=\int_0^\infty \frac{d\xi}{\xi^{1+\epsilon}}\mathcal{C}\left(N,\xi,\alpha_s,\epsilon\right)K_1\left(N,\left(\frac{\mu_F^2}{\xi Q^2}\right)^\epsilon,\alpha_s,\epsilon\right). \tag{3.18}$$

At this point, we can identify the IR singularities by expanding the integrated in ϵ parameter using

$$\frac{1}{\xi^{\epsilon+1}}=-\frac{\delta(\xi)}{\epsilon}+\sum_{k=0}^{\infty}\left[\frac{\ln^k\xi}{\xi}\right]_+\frac{(-\epsilon)^k}{k!}. \tag{3.19}$$

We get

$$C_{1\,\text{bare}}\left(N,\frac{\mu_F^2}{Q^2},\alpha_s,\epsilon\right)=-\frac{1}{\epsilon}\mathcal{C}\left(N,0,\alpha_s,\epsilon\right)\times K_1\left(N,\alpha_s\right)+\mathcal{O}\left(\epsilon^0\right), \tag{3.20}$$

where, at this point, we can identify this singular contribution as the leading N pole of the gluon anomalous dimension

$$K_1(N,\alpha_s)=\frac{\alpha_s C_A}{\pi(N-1)}=\alpha_s\gamma_0(N). \tag{3.21}$$

We can now consider repeating this process n times, each with one more gluon emission from the collinear initial state, we get

$$\begin{aligned}C_{n\,\text{bare}}\left(N,\frac{\mu_F^2}{Q^2},\alpha_s,\epsilon\right)=&\left[\alpha_s\left(\frac{\mu_F^2}{Q^2}\right)^\epsilon\gamma_0(N)\right]\int_0^\infty\frac{d\xi_n}{\xi_n^{1+\epsilon}}\mathcal{C}\left(N,\xi_n,\alpha_s,\epsilon\right)\times\\&\int_0^{\xi_n}\left[\alpha_s\left(\frac{\mu_F^2}{Q^2}\right)^\epsilon\gamma_0(N)\right]\frac{d\xi_{n-1}}{\xi_{n-1}^{1+\epsilon}}\times\ldots\times\int_0^{\xi_2}\left[\alpha_s\left(\frac{\mu_F^2}{Q^2}\right)^\epsilon\gamma_0(N)\right]\frac{d\xi_1}{\xi_1^{1+\epsilon}}.\end{aligned} \tag{3.22}$$

We can remove the collinear singularities by subtracting the collinear pole before each integration with the same tools of normal collinear factorization in the language of Ref. [81],

$$\begin{aligned}\int_0^{\xi_2}\left[\alpha_s\left(\frac{\mu_F^2}{Q^2}\right)^\epsilon\gamma_0(N)\right]\frac{d\xi_1}{\xi_1^{1+\epsilon}}\to&(1-\mathcal{P}_{\overline{\text{MS}}})\int_0^{\xi_2}\left[\alpha_s\left(\frac{\mu_F^2}{Q^2}\right)^\epsilon\gamma_0(N)\right]\\&=\alpha_s\gamma_0(N)\left(-\frac{1}{\epsilon}\frac{(4\pi)^\epsilon}{\Gamma(1-\epsilon)}\left(\frac{\mu_F^2}{\xi_2 Q^2}\right)^\epsilon+\frac{S_\epsilon}{\epsilon}\right).\end{aligned} \tag{3.23}$$

Here we choose to do this subtraction in the $\overline{\text{MS}}$-scheme. The result will also depend on the scheme of subtraction one chooses. In our case we have

$$\mathcal{P}_{\overline{\text{MS}}}f(\epsilon)=\sum_{k>0}\lim_{\epsilon\to0}\left[\epsilon^k(\epsilon)\right]\frac{S_\epsilon^k}{\epsilon^k}, \tag{3.24}$$

where

$$S_\epsilon = \left(\frac{e^{-\gamma_E}}{4\pi}\right)^\epsilon. \tag{3.25}$$

We can recursively carry out this operation to factorize the collinear singularities out of the coefficient function and into the PDFs to all orders in α_s.

We can write the insertion of $n-1$ iterative subtractions as

$$C_n\left(N, \frac{\mu_F^2}{Q^2}, \alpha_s, \epsilon\right) = \left[\alpha_s \left(\frac{\mu_F^2}{Q^2}\right)^\epsilon \gamma_0(N)\right] \int_0^\infty \frac{d\xi_n}{\xi_n^{1+\epsilon}} \mathcal{C}\left(N, \xi_n, \alpha_s, \epsilon\right)(1-\mathcal{P}) \times$$
$$(1-\mathcal{P}) \int_0^{\xi_n} \left[\alpha_s \left(\frac{\mu_F^2}{Q^2}\right)^\epsilon \gamma_0(N)\right] \frac{d\xi_{n-1}}{\xi_{n-1}^{1+\epsilon}} \times \ldots \times (1-\mathcal{P}) \int_0^{\xi_2} \left[\alpha_s \left(\frac{\mu_F^2}{Q^2}\right)^\epsilon \gamma_0(N)\right] \frac{d\xi_1}{\xi_1^{1+\epsilon}}. \tag{3.26}$$

At this point, we can compute the first $n-1$ integrals obtaining

$$\begin{aligned} C_n\left(N, \frac{\mu_F^2}{Q^2}, \alpha_s, \epsilon\right) &= \left[\alpha_s \left(\frac{\mu_F^2}{Q^2}\right)^\epsilon \gamma_0(N)\right] \\ &\times \int_0^\infty \frac{d\xi_n}{\xi_n^{1+\epsilon}} \mathcal{C}\left(N, \xi_n, \alpha_s, \epsilon\right) \frac{1}{(n-1)!} \frac{1}{\epsilon^{n-1}} \left[\alpha_s \gamma_0(N) \left(1 - \left(\frac{\mu_F^2}{\xi_n Q^2}\right)^\epsilon\right)\right]^{n-1}. \end{aligned} \tag{3.27}$$

The next step is to sum over the number of gluon emissions n. We get

$$\begin{aligned} C\left(N, \frac{\mu_F^2}{Q^2}, \alpha_s, \epsilon\right) &= \sum_{n=0}^\infty C_n\left(N, \frac{\mu_F^2}{Q^2}, \alpha_s, \epsilon\right) \\ &= \left[\alpha_s \left(\frac{\mu_F^2}{Q^2}\right)^\epsilon \gamma_0(N)\right] \int_0^\infty \frac{d\xi}{\xi^{1+\epsilon}} \mathcal{C}(\alpha_s, \xi, N, \epsilon) \exp\left[\frac{\alpha_s \gamma_0(N)}{\epsilon}\left(1 - \left(\frac{\mu_F^2}{Q^2 \xi}\right)^\epsilon\right)\right]. \end{aligned} \tag{3.28}$$

This gives us the result for the resumed coefficient function in Mellin space:

$$C\left(N, \frac{\mu_F^2}{Q^2}, \alpha_s, \epsilon\right) = \int_0^\infty d\xi\, \mathcal{C}(\alpha_s, \xi, N, \epsilon) \left[\alpha_s \gamma_0(N) \xi^{\alpha_s \gamma_0(N) - 1}\right], \tag{3.29}$$

where we took the limit $\epsilon \to 0$ and we chose $\mu_F^2 = Q^2$. Comparing Eq.(3.29) with Eq.(2.25), we can derive an expression for the evolution operator that resums the LL terms:

$$\mathcal{U}(N, \xi) = \alpha_s \gamma_0(N) \xi^{\alpha_s \gamma_0(N) - 1} = \frac{d}{\xi}\left[\xi^{\alpha_s \gamma_0(N)}\right]. \tag{3.30}$$

Now, if we multiply the coefficient function with the PDF of the gluon in Mellin space we get

$$C\left(N, \frac{\mu_F^2}{Q^2}, \alpha_s, \epsilon\right) f_g(N, Q^2) = \int_0^\infty \mathcal{C}(\alpha_s, \xi, N, \epsilon) \left[\mathcal{U}(N, \xi) f_g(N, Q^2)\right], \tag{3.31}$$

that provides a definition for the unintegrated gluon PDF,

$$\mathcal{F} = \mathcal{U}(N, \xi) f_g(N, Q^2). \tag{3.32}$$

This definition is the same as the one we gave in Eq.(3.11), the only difference is that Eq.(3.32) is in Mellin space. In this way, we show how to compute the evolutor $\mathcal{U}$ in

a simple case where we considered fixed coupling and only one hadron in the initial state.

This formula to resum the LL terms in the coefficient function can be extended taking into account the running coupling and more complicated initial states. Moreover, in general, $\mathcal{U}$ depends on the renormalization scheme. The general expression of this term can be written as [32, 33, 66]

$$\begin{aligned}\mathcal{U}\left(N,\frac{k_t^2}{Q^2}\right) = \int_0^\infty \frac{dq_2^2}{q_2^2}\overline{\mathcal{R}}\left(\frac{q_2^2}{k_t^2}\right)\exp\left[\int_{k_t^2}^{q_2^2}\frac{dq_1^2}{q_1^2}\gamma_+\left(N,\alpha_s(q_1^2)\right)\right] \\ \times\frac{d}{dk_t^2}\exp\left[\int_{Q^2}^{k_t^2}\frac{dq_1^2}{q_1^2}\gamma_+\left(N,\alpha_s(q_1^2)\right)\right],\end{aligned} \tag{3.33}$$

where $\overline{\mathcal{R}}$ is the renormalization scheme dependent factor, while γ_+ is the resummed anomalous dimension. This expression is quite complicated but it can be simplified if we choose the $Q^0\overline{MS}$ renormalization scheme. In this scheme, in fact, the evolutor becomes

$$\mathcal{U}\left(N,\frac{k_t^2}{Q^2}\right) = \frac{d}{dk_t^2}\exp\left[\int_{Q^2}^{k_t^2}\frac{dq_1^2}{q_1^2}\gamma_+\left(N,\alpha_s(q_1^2)\right)\right], \tag{3.34}$$

More details can be found in Refs. [32, 33, 66].

The resummation formula in Eq.(2.25) has an analog in the Mellin space. For completeness, we spend some words discussing it because in some cases can be useful. In Eq.(3.29) we recognize the structure of a Mellin transform over the variable ξ. Using this we can define the so-called impact factor

$$h(N,M) = M\int_0^\infty \xi^{M-1}\frac{d}{d\,\xi}\mathcal{C}(N,Q^2,\xi,\alpha_s), \tag{3.35}$$

that resum all the leading logarithmic contributions when evaluated in $M = \alpha_s\gamma_0(N)$. This technique is very elegant but to obtain physical predictions for phenomenology the Mellin transform in N must be undone. This is often impossible to do analytically and quite complicated to perform numerically. For this reason, it is usually convenient to compute both the off-shell coefficient function and the evolution operator directly in the ξ (or $k_\perp$) space [32, 33].

3.2 Leading-Log small-x resummation for the Higgs induced DIS

In this section, we apply the procedure explained in Section 3.1 to a specific process, the deep-inelastic scattering (DIS) induced by a Higgs boson. This process is suitable for studying small-x resummation because it involves only gluons, so the leading logarithmic terms appear already at leading order. This is useful to understand how the resummation formula of Eq.(2.25) works and where the small-x logarithms come from. A more detailed definition of this process is given in Chapter 5, which is dedicated to the computation of the one-loop off-shell coefficient function of this process. Here we

only define the parametrization for the incoming off-shell gluon and some kinematics to make the following calculations clear.

We parametrize the incoming gluon momentum following [18] as

$$k_1^\mu = zk^\mu + k_t^\mu, \tag{3.36}$$

where

$$\begin{aligned} &k^2 = n^2 = 0; \\ &k \cdot k_t = n \cdot k_t = 0; \\ &k_1^2 = -\mathbf{k}_t^2, \end{aligned} \tag{3.37}$$

The first ingredient of Eq.(2.25) is the tree-level off-shell coefficient function for the process. We start by computing the leading order off-shell amplitude. To do so we have to compute the squared matrix element of the Born level diagram shown in Fig.(5.3). We perform this calculation leaving free the two Lorentz indices of the off-shell gluon. In this way, we can point out the scaling of the tensorial structures in Eq.(3.7) and so we can identify the tensorial structures that give the main contribution in the small-x limit. As we saw in Section 2.2, these structures are the ones selected by the projector proposed by Catani, Ciafaloni, and Hautmann in [18],

$$d^{\mu\rho}_{\mathrm{CH}}(k_1) = (d-2)\frac{k_\perp^\mu k_\perp^\rho}{\mathbf{k}_\perp^2}. \tag{3.38}$$

This way of doing the calculation will also be useful when we will address the one-loop off-shell calculation. Since the one-loop off-shell coefficient function is involved in the next-to-leading logarithmic resummation, we do not know a priori what tensorial structure gives the dominant contribution. Making no assumptions on the polarisation tensor of the off-shell gluon allows us to look at the coefficients of the different tensorial structures and see what are the dominant ones in the small-x region.

The object we want to compute is, then,

$$\mathcal{A}^{\mu\rho}_{0\,a,c} = \int \frac{d^d\,k_2}{(2\pi)^{d-1}} M^{\mu\nu}_{a,b}(k_1,k_2) M^{*\rho\sigma}_{c\,d}(k_1,k_2) d^{b,d}_{\nu\sigma}(k_2)\delta^d(k_1+q-k_2)\delta^+(k_2^2), \tag{3.39}$$

where $d^{\nu\sigma}(k_2)$ is the usual polarisation tensor for a gluon in light-cone gauge,

$$d^{\nu\sigma}_{b,d}(k_2) = \delta_{bd}\left(-g^{\nu\sigma} + \frac{k_2^\nu n^\sigma + k_2^\sigma n^\nu}{k_2\cdot n}\right), \tag{3.40}$$

and $M^{\mu\nu}_{a,b}(k_1,k_2)$ is the tree-level Higgs-gluon effective vertex we defined as

$$M^{\mu\nu}_{ab}(k_1,k_2) = \mathrm{i}\,c\,(k_1^\nu k_2^\mu - g^{\mu\nu}k_1\cdot k_2)\,\delta_{ab}. \tag{3.41}$$

Since the tree-level vertex is transverse with respect to the gluon momentum k_2, this calculation can be simplified. In Eq.(3.40) only the first term in the brackets survives and the dependence on the gauge vector vanishes. Moreover, the integration can be easily made using the momentum conservation Dirac-delta that sets

$$k_2 = k_1 + q. \tag{3.42}$$

We get

$$\begin{aligned}\mathcal{A}_0^{\mu\nu} =& c^2\left(k_1^2+(k_1\cdot q)^2\right)\delta\left[(k_1+q)^2\right]\left\{-g^{\mu\nu}+\frac{Q^2}{\left(k_1^+(k\cdot q)^2\right)}k_1^\mu k_1^\nu-\frac{k_1^2}{\left(k_1^+(k\cdot q)^2\right)}q^\mu q^\nu\right.\\ &\left.+\frac{k\cdot q}{\left(k_1^+(k\cdot q)^2\right)}\left(k_1^\mu q^\nu+k_1^\nu q^\mu\right)\right\}\\ &=\delta\left[z-x(1+\xi)\right]c^2Q^2x\left\{-q^{\mu\nu}Q^2k_1^\mu k_1^\nu+\xi q^\mu q^\nu+x(1+\xi)\left(k_1^\mu q^\nu+k_1^\nu q^\mu\right),\right\}\end{aligned} \tag{3.43}$$

where we used the definitions

$$\begin{aligned}\xi &= \frac{\mathbf{k}_\perp^2}{Q^2}\\ x &= \frac{Q^2}{2k\cdot n}.\end{aligned} \tag{3.44}$$

The expression in Eq.(3.43) can be expanded for small-x and rearranged to get

$$\begin{aligned}\mathcal{A}_0^{\mu\nu} = \frac{\pi c^2Q^4}{2}\delta\left[z-x(1+\xi)\right]\left\{-\frac{(z-2\xi x)^2}{x^2}\left[-g^\mu\nu+\frac{k_1^\mu k_1^\nu}{k_1^2}\right]\right.\\ \left.-\frac{z^2}{x^2k_1^2}\left[\frac{k_1^2}{k_1\cdot q}q^\mu-k_1^\mu\right]\left[\frac{k_1^2}{k_1\cdot q}q^\nu-k_1^\nu\right]\right\}.\end{aligned} \tag{3.45}$$

This expression obeys the scaling properties behind Eq.(3.7). In particular, we can identify

$$\begin{aligned}A_1 &= -\frac{(z-2\xi x)^2}{x^2}\\ A_2 &= -\frac{z^2}{x^2k_1^2}.\end{aligned} \tag{3.46}$$

We explicitly see that these have the same small-x limit. This means that the second term in the brackets is dominant because the tensorial structure provides a net $\frac{1}{x}$ enhancement. This is a simple verification of the universality of k_t-factorisation. This also means that the tensor in Eq.(3.38) selects precisely the dominant part of Eq.(3.45) in the small-x limit.

From this expression, we can compute the Leading-Order off-shell coefficient function for the process. To do so, we contract Eq.(3.45) with the tensor in Eq.(3.38) and we normalize over the initial state flux and spin. We get

$$\mathcal{C}_0\left(\frac{x}{z},\xi\right)=\frac{\pi c^2Q^2z^2}{4\,x^2}\delta\left(-\frac{x}{z}+\xi+1\right) \tag{3.47}$$

This expression can be used to extract the logarithmic structure of this process. To do so, we use the impact factor approach to resummation of Refs. [44, 82]. First of all, we

compute the impact factor as explained in Section 3.1, we get

$$\begin{aligned} h(N,M) &= M\int_0^\infty d\xi\,\xi^{M-1}\int_0^\infty d\tau\tau^{N-1}\mathcal{C}_0(\tau,\xi) \\ &= \frac{\pi c^2Q^2z^2}{4}M\int_0^\infty d\xi\,\xi^{M-1}\left(\frac{1}{1+\xi}\right)^{N-1} \\ &= \frac{\pi c^2Q^2z^2}{4}\frac{\Gamma(M+1)\Gamma(N-1-M)}{\Gamma(N-1)}, \end{aligned} \tag{3.48}$$

where the convergence constraints are $0 < Re(M) < Re(N) - 1$. Since in Mellin space the high energy logarithms, $\frac{\ln^k x}{x}$ are mapped in poles $\left(\frac{1}{N-1}\right)^k$, we can reconstruct the leading-logarithms terms by expanding this expression around $M = 0$. We get

$$h(N,M) \simeq \frac{\pi c^2Q^2z^2}{4}\left[1+\frac{M}{N-1}+\left(\frac{M}{N-1}\right)^2+\dots\right]. \tag{3.49}$$

At this point, we can set $M = \gamma(\alpha_s, N)$, where we use the NLL expansion for the anomalous dimension,

$$\gamma(\alpha_s,N) = \alpha_s\left[\frac{C_A}{\pi(N-1)} - \frac{11C_A+2n_f\left(1-2\frac{C_F}{C_A}\right)}{12\pi}\right] + \alpha_s^2\frac{n_f(26C_F-23C_A}{36\pi^2(N-1)} + \mathcal{O}(N^0,\alpha_s^3) \tag{3.50}$$

taken form [66]. The resumed impact factor takes, then, the form

$$\begin{aligned} h(N,\gamma(\alpha_s,N)) = \frac{\pi c^2Q^2z^2}{4}\Bigg\{1+\frac{\alpha_s}{4\pi}\left[\frac{4C_A}{(N-1)^2}-\frac{11C_A}{3(N-1)}\right] \\ +\left(\frac{\alpha_s}{4\pi}\right)^2\left[\left(\frac{4C_A}{(N-1)^2}\right)^2-\frac{88C_A^2}{3(N-1)^3}\right]+\mathcal{O}\left(\left(\frac{\alpha_s}{N-1}\right)^2,\alpha_s^3\right)\Bigg\}. \end{aligned} \tag{3.51}$$

This result can be compared with the high-energy expansion of the impact factor obtained by Mellin transformation of the NNLO coefficient function from [83],

$$\begin{aligned} h_{\rm FO}(\alpha_s,N) = \frac{\pi c^2Q^2z^2}{4}\Bigg\{1+\frac{\alpha_s}{4\pi}\left[\frac{4C_A}{(N-1)^2}-\frac{11C_A}{3(N-1)}\right] \\ +\left(\frac{\alpha_s}{4\pi}\right)^2\left[\left(\frac{4C_A}{(N-1)^2}\right)^2-\frac{220C_A^2}{3(N-1)^3}\right]+\mathcal{O}\left(\alpha_s^3\right)\Bigg\}. \end{aligned} \tag{3.52}$$

First of all, we can observe the presence of a double-logarithmic enhancement. In Mellin space, this emerges with two extra powers of the term $\frac{1}{N-1}$ at each new order in α_s while, as we saw in Chapter 2, we will expect only one power (single logarithm). This difference is generated by the simplified $2 \to 1$ kinematics of the Higgs-induced DIS and by the fact that Eq.(3.47) does not vanish in the high-energy limit [24, 84]. Since Eq.(3.51) shows that the extra $\frac{1}{N-1}$ power is generated systematically at all orders, we could hope that the NLL information from the anomalous dimension could intercept both LL and NLL terms. As shown by the comparison between Eq.(3.51) and Eq.(3.52), this information is insufficient to predict the NLL contributions beyond NLO.

3.3 From LL to NLL resummation

In this section, we want to explain our program to extend the LL resummation method for the coefficient function to NLL. In particular, we want to list all the ingredients we need and comment on the ones that are still missing. We want to extend the small-x resummation of the coefficient function using the method presented in [32, 33, 66] that we discussed in Chapter 2. The formula we use to resum the small-x logarithms is

$$C(x,Q^2) = \int dk_\perp^2 \int_x^1 \frac{dz}{z} \mathcal{C}\left(\frac{x}{z}, k_\perp^2, Q^2\right) \mathcal{U}\left(z, \frac{k_\perp}{Q^2}\right), \tag{3.53}$$

where, as we discussed in Chapter 2, the first term is the off-shell coefficient function of the process computed at leading order, and the second term is the evolutor that resums the leading logarithmic contributions.

If we want to use Eq.(3.53) to resum NLL terms in the coefficient function first of all we have to compute the evolutor,

$$\mathcal{U}\left(N, \frac{k_t^2}{Q^2}\right) = \frac{d}{dk_t^2} \exp\left[\int_{Q^2}^{k_t^2} \frac{dq_1^2}{q_1^2} \gamma_+\left(N, \alpha_s(q_1^2)\right)\right], \tag{3.54}$$

at NLL. This is possible if we take the NLL resummed expression for the anomalous dimension, γ_+. This is well-known and can be found, in [66]. This, however, is not enough to get the correct expression for the NLL resummed coefficient function, as we saw in Section 3.2. This means that we have to compute the off-shell coefficient function in Eq.(3.53) at NLO.

Computing the off-shell coefficient function at NLO opens some questions that must be answered before applying this procedure to resum NLL terms in the coefficient function. First of all, Eq.(3.53) relies on the k_t-factorisation theorem that has been proved considering the LO off-shel coefficient function, as we discussed in Section 3.1. This means that if we want to use Eq.(3.53) we have to prove that the factorization in Eq.(3.4) still holds when the off-shell coefficient function is computed at NLO. Moreover, the factorization in Eq.(3.4) has been proved in a physical gauge, when the contribution from the multiple gluon exchange in the t channel is dominant.

In the following sections, we will give some details on what are the many things we will learn by computing the NLO off-shell coefficient function in a physical gauge and for a specific process and how this will help us to establish the NLL resummation.

3.3.1 Dominant contribution at high-energy

As we said before, the factorization formula in Eq.(3.4) has been proven to work when the coefficient function is computed at LO. In this gauge, in fact, as we discussed in Section 3.1, $\mathcal{C}$ does not depend on the gauge vector n and we decompose as we saw in Eq.(3.7). In this decomposition, we can easily identify the dominant contribution in the high-energy region and we can define a projector that selects the dominant part of the off-shell amplitude.

This projector, as we saw in Section 3.1, is

$$d^{\mu\nu}(k) = (d-2)\frac{k_\perp^\mu k_\perp^\mu}{\mathbf{k}_\perp^2}, \tag{3.55}$$

where d are the dimensions of the space-time. If we take the on-shell limit of this projector, mediated over the azimuthal angle, we get

$$\lim_{\bar{k}_\perp^2 \to 0} \langle d^{\mu\nu} \rangle_\phi = g_\perp^{\mu\nu}, \tag{3.56}$$

that is the usual sum over polarizations of an on-shell gluon. This means that this object can be viewed as the off-shell counterpart of the sum over polarisation of an on-shell gluon. This property is fundamental because it allows us to define the off-shell coefficient function so that if we take its on-shell limit we get the usual definition of the coefficient function of a process.

The question is if this form for the projector is still valid if we are interested in resumming the NLL terms in the coefficient function and, eventually, how to modify it. If we compute the amplitude at NLO, in fact, it will depend on the gauge vector n and the decomposition in Eq.(3.7) will not be valid. We have to define another decomposition and, moreover, it is not guaranteed that the coefficients of the new decomposition will have the same scaling properties of the A_1 and A_2 function that we discussed in Section 3.1. For this reason, it is important to compute the NLO off-shell coefficient function for a specific process. In this way, we can verify if the scaling we have to find out the scaling of the coefficients of various tensorial structures that contribute to the amplitude is the same as the LO case. If it is different, we will be able to modify Eq.(3.56) in order to take into account all the dominant terms in the high-energy limit and to get the correct on-shell limit.

3.3.2 Factorisation of the logarithmic contributions

To resum the LL logarithms using Eq.(3.53), it is crucial that the off-shell coefficient function, $\mathcal{C}$ does not contain any logarithmic contributions so that they can be all taken into account by the evolution operator $\mathcal{U}$. This is true, as we discussed in Section 3.1, if we compute the off-shell amplitude in a physical gauge like the light-cone gauge. In this gauge, in fact, the contributions from multiple exchanges in the t channel are the ones that generate the small-x logarithms. They can be identified with the 2GR diagrams and separated from the 2GI diagrams. The former ones contribute to the evolution operator, while the latter ones contribute to the off-shell coefficient function. This has proved to work with LL logarithms and with the off-shell coefficient function computed at LO.

Extending this procedure to NLL resummation is nontrivial. First of all, as we saw in Section 3.3.1, the off-shell coefficient function must be computed at NLO. The factorization of the small-x logarithms between 2GI and 2GR diagram has been proved only with the LO off-shell coefficient function [16, 32, 33, 66] so the first question we must answer is if this remains true when considering the NLO amplitude. In order to verify this property, we have decided to compute the NLO off-shell coefficient function

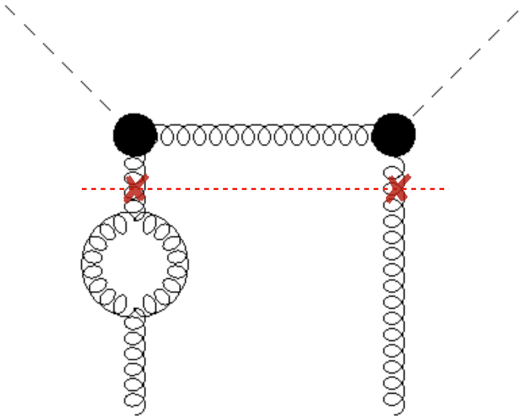

Figure 3.7: Diagram with a bubble on the incoming gluon. This diagram is formally 2GR because by cutting the gluon propagators as shown in this picture we get two separate diagrams.

for a specific process and explicitly see if the separation of the logarithmic contributions still holds.

Another issue we aim to clarify by performing an explicit calculation concerns the treatment of some of the virtual contributions. If we consider the diagram in Fig.(3.7), we see that this diagram is 2GR because we can cut the gluon propagators over the bubble and get two separate diagrams. However, this diagram is not part of the gluon ladder we defined in Section 3.1. In principle, this kind of correction should be taken into account by the running of the QCD coupling constant that enters in the definition of the evolution operator $\mathcal{U}$ in Eq.(3.54), leaving the definition of the 2GI amplitude unchanged. However, the only way we have to verify this is to actually perform the calculation of the off-shell coefficient function in a physical gauge for a specific process.

3.3.3 Off-shell coefficient function in light-cone gauge

In the previous sections, we discussed why the key ingredient that is still missing for the extension of the resummation formula for the coefficient function,

$$C(x,Q^2) = \int dk_\perp^2 \int_x^1 \frac{dz}{z} \mathcal{C}\left(\frac{x}{z}, k_\perp^2, Q^2\right) \mathcal{U}\left(z, \frac{k_\perp}{Q^2}\right), \tag{3.57}$$

form LL to NLL is the off-shell coefficient function for a specific process computed in a physical gauge. In this thesis, we then focus on the calculation of this quantity for the Higgs-induced DIS process. Among all the possible physical gauges, we choose to work in the light-cone gauge because it simplifies the calculations.

The choice to use the light-cone gauge turned out to be quite complicated, especially for the presence of non-covariant loop integrals and spurious gauge singularities. Acquiring a deep understanding of these problems has required a long work that is discussed throughout Chapter 4 and Appendix A. These calculations have somewhat shifted the focus of the thesis from phenomenology to more fundamental issues about perturbative field theory in non-covariant gauges. We think we made some significant

progress in the understanding of how to treat calculations involving a gauge that, due to its complication, is not commonly used.

Chapter 4

Light-cone gauge

In Chapter 3, we pointed out that, in order to obtain the correct NLL resummed result for the coefficient function for a given process, we need to compute the off-shell coefficient function in an axial gauge. For simplicity, we choose to work in light-cone gauge, where $n^2 = 0$.

In this chapter, we will discuss the main challenges that one has to face when working in this gauge. In fact, the structure of the propagator of the gluon is more complicated and so the number of terms in the amplitude increases considerably. Moreover, as we will discuss in Section 4.1, there are some non-physical singularities that must be regularised with the right prescription. We will present two different prescriptions to regularise these singularities the *Principal Value* (PV) prescription and the *Mandelstam Leibbrandt* (ML)prescription. We will see why the ML is the one to prefer in light-cone gauge calculations. In Section 4.2, then, we will face the problem of the renormalization in a physical gauge.

4.1 Light-cone gauge and small-x resummation

As we saw in Chapter 2, working in a physical gauge is crucial to achieving the LL small-x resummation of the coefficient function. In this gauge, in fact, the off-shell coefficient function does not contain logarithmic contributions. When we write the coefficient function as

$$C(x,Q^2) = \int dk_\perp^2 \int_x^1 \frac{dz}{z} \mathcal{C}\left(\frac{x}{z}, k_\perp^2, Q^2\right) \mathcal{U}\left(z, \frac{k_\perp}{Q^2}\right). \tag{4.1}$$

all the logarithmic contributions are resumed by the evolutor $\mathcal{U}$ that has a process-independent all-order definition.

Since we want to investigate small-x resummation beyond leading order, we need to prove that Eq.(4.1) works also when we take into account NLL terms. To resum the NLL terms using Eq.(4.1), we need to compute the off-shell coefficient function, $\mathcal{C}$, at next-to-leading order and we have to compute $\mathcal{U}$ resumed at NLL. In particular, while the computation of the resummed evolutor can be derived from the LL calculation, as we discussed in Chapter 3, we must pay attention to the calculation of the off-shell coefficient function. We have to verify that working in a physical gauge $\mathcal{C}$ is free from

logarithmic contribution. To do so, we choose a particular process, the Higgs-induced DIS, and we compute its off-shell coefficient function in an axial gauge.

Before presenting the calculation in Chapter 5, we spend some words explaining how calculations in axial gauges work.

In axial gauges the manifest Lorentz-invariance of the theory is broken by introducing a privileged direction in the Minkowski space-time, the gauge vector n^μ. This vector is introduced by adding to the Lagrangian density a gauge fixing term

$$\mathcal{L}_{\text{GF}} = -\frac{1}{2}\left(n \cdot A\right)^2, \tag{4.2}$$

where A_a^μ are the gauge potentials. This results in the gauge-fixing condition

$$n \cdot A = 0. \tag{4.3}$$

Depending on the sign of the square of the gauge vector n^μ, we can classify the axial gauges into three categories: temporal gauges ($n^2 > 0$), spatial gauges ($n^2 < 0$) and light-cone gauge ($n^2 = 0$). In particular, from now on, we concentrate on the light-cone gauge, because in this gauge the calculations are simpler since we do not have to worry about the scale of the gauge vector.

In light-cone gauge, the propagator of the gluon takes the form

$$\Pi_{a,b}^{\mu\nu}(k,n) = \frac{\mathrm{i}\delta_{a,b}}{k^2}\left[-g^{\mu\nu} + \frac{k^\mu n^\nu + k^\nu n^\mu}{k \cdot n}\right]. \tag{4.4}$$

From this expression, we see some of the complications that the choice of this gauge implies. First of all, calculations become more involved due to the presence of more than one term in the gluon propagator which means that we will have a growing number of loop integrals to compute. We can also observe that the second term in the bracket of Eq.(4.4) breaks manifest Lorentz invariance and also gives rise to infrared singularities at $k \cdot n = 0$. Because these singularities originate from the gauge choice, they are not physical and must not be present in the gauge-invariant final result. A third difficulty is that, since the light-cone gauge breaks Lorentz invariance, also the ultraviolet counterterms are not constrained anymore by it and so cannot be derived from the Lorentz-invariant Lagrangian terms. On the other hand, the use of a physical gauge like the light-cone gauge constrains the polarizations of the gluon to be physical. This means that we do not have to worry about the ghost fields when computing higher-order contributions.

In this section, we particularly concentrate on the non-physical gauge singularities and how they are cured. The problem of the definition of the counterterms and the renormalization is faced in Section 5.3, while we refer to Chapter 5 to the technicalities of the calculations of non-covariant loop integrals.

Two prescriptions are typically adopted in the literature to regularise the infrared singularities due to the gauge choice. One is the *Principal Value* (PV) prescription [81, 85], while the other is the *Mandelstam-Leibbrandt* (ML) prescription [86, 87].

In literature, both the PV and the ML are used to perform calculations in light-cone gauge, but as we will show in detail in the following, the correct choice will be the ML prescription. This is because, unlike the PV, ML prescription does not modify the

Wick rotation procedure. This procedure is fundamental to avoid the usual mass-shell physical singularities and must still be used with non-covariant integrals. Even though ML is quite complicated, it is the only correct option to regularise the gauge-dependent singularities [88].

We think, however, that presenting in some detail also how PV prescription works is still useful. In fact, there are some cases in which it gives the correct results and it has been used in literature [81]. Moreover, in these simplified situations one could prefer to use it because calculations in ML prescription become quickly quite involved.

In the following, we will present these two prescriptions in some detail.

4.1.1 Principal value prescription

We start with the simpler, the PV prescription consists of replacing

$$\frac{1}{k\cdot n} \to \frac{1}{2}\left(\frac{1}{k\cdot n + i\,\delta\, p\cdot n} + \frac{1}{k\cdot n - i\,\delta\, p\cdot n}\right) = \frac{k\cdot n}{(k\cdot n)^2 + \delta^2 (p\cdot n)^2}, \tag{4.5}$$

where the scalar product $p{\cdot}n$ preserves the homogeneity in n, and p is a fixed momentum of an incoming parton. Here, the IR spurious singularities regulator is the parameter δ. The limit $\delta \to 0$ must be taken at the end of the calculation.

Since prescription is not too complicated, it is the first that has been used, for example by Curci, Furmansky, and Petronzio in [81]. Following the work of Pritchard and Stirling in [89], they use this prescription to regularise the gauge-dependent singularities for their light-cone gauge calculations.

In this work emerges the main problem of the PV prescription when applied to the light-cone gauge. When we compute loop integrals like

$$\int \frac{d^d k}{(2\pi)^2} \frac{1}{k^2 (k-l)^2} \frac{1}{k\cdot n}, \tag{4.6}$$

we will expect from power counting the result to be finite in the ultraviolet. If we do the calculation regularising the gauge singularities with the principal value prescription, instead, we find that this integral is UV divergent and it still depends on the regularisation parameter δ.

Curci, Furmansky, and Petronzio in [81] solve this problem by observing that integrals like the one in Eq.(4.6) are finite until we keep $n^2 \neq 0$. Moreover, the result when $n^2 \neq 0$ contains terms proportional to

$$\ln^2\left(\frac{n^2 l^2}{(l\cdot n)^2}\right) \tag{4.7}$$

that diverges when we take the limit $n^2 \to 0$. On the other hand, if we take the limit $n^2 \to 0$ from the beginning the power counting breaks down and we get UV poles. For this reason, they can argue that these spurious poles are counterparts of the logarithmic terms when $n^2 = 0$. When we compute a gauge-invariant quantity the spurious poles, since are gauge-dependent, must cancel out. As pointed out in [88], however, the failure of the power counting is due to the fact that, with the PV prescription, we

cannot perform correctly the Wick rotation. This is manifest in the dependence on the regularisation parameter δ of the integrals. Although Curci Furmansky and Petronzio show in [81] that in their calculation not only the spurious UV singularities but also the δ-dependence disappears once we compute gauge-invariant quantities, we showed that when facing more complicated calculation the δ dependence can be an issue.

In the following, we will point out where the Wick rotation fails and how we can solve this problem.

The computation of loop integrals with the PV prescription exploits the identity [89]:

$$\begin{aligned} S &= \int \frac{d^d k}{(2\pi)^d} \frac{1}{(k^2 - 2P\cdot k + M^2 + \mathrm{i}\eta)^\alpha} \frac{1}{(k\cdot n)^\beta} \\ &= \frac{\mathrm{i}(-1)^\alpha}{(4\pi)^{\frac{d}{2}}} \frac{\Gamma\left(\alpha - \frac{d}{2}\right)}{\Gamma(\alpha)} \frac{1}{(P^2 - M^2)^{\alpha - \frac{d}{2}} (P\cdot n)^\beta}, \end{aligned} \tag{4.8}$$

where α and β are natural numbers, η is the usual regulator of the singularities in the propagators, and we also assumed $n^2 = 0$, for the light-cone gauge.

This result relies on the fact that one can perform the Wick rotation because the non-covariant term does not have an imaginary part. If we want to use the PV prescription from the start, this would not be true anymore. In particular, by using Eq.(4.5) we will get

$$S = \int \frac{d^d k}{(2\pi)^d} \frac{1}{(k^2 - 2P\cdot k + M^2 + \mathrm{i}\eta)^\alpha} \frac{1}{(k\cdot n + \mathrm{i}\delta p\cdot n)^\beta (k\cdot n - \mathrm{i}\delta p\cdot n)^\beta}, \tag{4.9}$$

where we get an extra imaginary part. One can show that, if we perform the Wick rotation with this extra contribution, we end up getting a pinch between the Feynman and the spurious poles in the complex k_0 plane. From Eq.(4.9), in fact, we see that the imaginary part of the non-covariant denominators appears with both a positive and a negative sign. This means that we will always have an imaginary contribution that has a sign that is different from the one of the $+\mathrm{i}\eta$ Feynman prescription. This is the point where the PV prescription fails to give a good description of the singular structure of these integrals.

Curci Furmansky and Petronzio in [81] bypass this problem by applying the PV prescription after doing the Wick rotation. In this sense, they use this prescription not to regularise a singularity of the propagator of the gluon but to regularise an extra infrared singularity that appears in loop integrals. In this framework, if the PV prescription is used in the virtual contribution to the amplitude the δ-dependence must disappear at the level of the virtual amplitude. This works until the amplitudes are not too complicated, like in the case analyzed by Curci Furmansky and Petronzio, or the on-shell amplitude for the Higgs-induce DIS that we present in Chapter 5. However, when the calculations become more complicated and we need an explicit cancellation of the gauge singularities between the real and the virtual part, this mechanism does not work anymore. We will see explicit proof of this when we address the calculation of the off-shell Higgs-induced DIS amplitude in Chapter 5.

4.1.2 Mandelstam-Leibbrandt prescription

After analyzing how PV works and its strengths and weaknesses, we now address the Mandelstam-Leibbrandt prescription. This prescription consists of modifying the light-cone gauge part of the gluon propagator with the substitution

$$\frac{1}{k\cdot n}\to\frac{k\cdot\bar{n}}{(k\cdot n)\,(k\cdot\bar{n})+i\delta}, \tag{4.10}$$

where the IR spurious singularities regulator is the parameter δ. This prescription forces the introduction of another gauge vector, $\bar{n}$, with a further violation of the Lorenz covariance. This vector, if $n^\mu=(n_0,\overrightarrow{n})$, is defined as $\bar{n}=(n_0,-\overrightarrow{n})$, it is, then, the conjugate vector of n.

The presence of this vector makes the calculations more involved. On the other hand, this prescription has the important feature that places the spurious poles within the same pattern of the covariant poles in the complex k_0 plane. This means that, with this prescription, we can perform the Wick rotation without the problems we encounter with PV prescription. For this reason, we can use this prescription from the beginning modifying the non-covariant part of the propagator of the gluon. In this sense, the regulator δ plays the same role as the $+\mathrm{i}\eta$ prescription in Feynman gauge. After the Wick rotation, we can take the limit $\delta\to 0$ and our result will not depend on δ anymore.

This is an important difference between this prescription and the PV prescription. This is also the reason because, even if in some particular cases PV prescription proves to work, the ML prescription is the correct one to use in the context of light-cone gauge. ML prescription also restores the power counting criterion, so we do not have spurious UV singularities anymore.

The detailed description of how this prescription modifies the integrals together with the derivation of some general results for non-covariant integrals can be found in Appendix A. In the following, we will concentrate on the Wick rotation, showing how it can be performed exactly as in the usual Feynman gauge.

The general one-loop integral in ML prescription can be written as

$$I_{ML}=\int\frac{d^dk}{(2\pi)^d}\frac{1}{(k^2-2P\cdot k+M^2+\mathrm{i}\eta)^\alpha}\frac{k\cdot\bar{n}}{(k\cdot n)(k\cdot\bar{n})+\mathrm{i}\delta}, \tag{4.11}$$

where δ is the regulator for the gauge spurious IR singularities while $+\mathrm{i}\eta$ is the usual Feynman prescription for the regularisation of the singularities of the gluon propagators.

To identify the singularities in the complex plane k_0 we choose a spefific direction for the gauge vector:

$$\begin{aligned} n^\mu&=(n_0,\overrightarrow{0},n_0)\\ \bar{n}^\mu&=(n_0,\overrightarrow{0},-n_0)\end{aligned} \tag{4.12}$$

where also used the fact that in the light-cone gauge $n^2=0$. We use Feynman parametrization to write this integral with only one denominator and make a shift

in the integration variable k_0. We get

$$I_{ML} = \frac{\Gamma(1+\alpha)}{\alpha}\frac{1}{n_0}\int_0^1 dx\, x^{\alpha-1}\int \frac{d^{d-1}k}{(2\,\pi)^d}\int_{-\infty}^{+\infty} dk_0\, \frac{xP_0+k_3}{\left[k_0^2-\mathcal{A}\right]^{\alpha+1}}, \tag{4.13}$$

where

$$\mathcal{A} = \left(k_3 - xP_3\right)^2 + x\left(\mathbf{k}_\perp - \mathbf{P}_\perp\right)^2 + x^2\left(P_0^2 - P_3^2\right) - x\mathbf{P}_\perp^2 - xM^2 - \mathrm{i}\eta - \mathrm{i}\delta, \tag{4.14}$$

We observe that the two regulators, η and δ have the same sign so they will displace the singularities in the same quadrant of the complex plane when we perform the Wick rotation. This procedure is used to transform the Minkowski-space integral into a Euclidean-space integral. This is implemented by rotating the integration path in Eq.(A.9) from the real axis to the complex imaginary axis. This can be done only if these two paths are equivalent, namely if we can perform this rotation avoiding the singularities in the complex plane k_0. The poles are placed in

$$k_0 = \pm\sqrt{\mathcal{A}} \simeq \pm\left(\sqrt{\lambda} + \mathrm{i}\,(\delta+\eta)\right), \tag{4.15}$$

where we used the fact that δ and η, being regularisation parameters, are small and

$$\lambda = \left(k_3 - xP_3\right)^2 + x\left(\mathbf{k}_\perp - \mathbf{P}_\perp\right)^2 + x^2\left(P_0^2 - P_3^2\right) - x\mathbf{P}_\perp^2 - xM^2. \tag{4.16}$$

We can always choose a region in the phase space where $\lambda \geq 0$ and then perform an analytic continuation to reach all the phase space. In this region, the two singularities are placed in the first and the third quadrant. Rotating the integration path clockwise we avoid these singularities and we get

$$I_{ML} = \frac{\Gamma(1+\alpha)}{\Gamma(\alpha)}\frac{1}{n_0}\int_0^1 dx\, x^{\alpha-1}\int \frac{d^{d-1}k}{(2\,\pi)^d}\int_{-\mathrm{i}\infty}^{+\mathrm{i}\infty} dk_0 \frac{xP_0+k_3}{\left[k_0^2-\mathcal{A}\right]^{\alpha+1}}. \tag{4.17}$$

At this point, we can change the integration variable to

$$k_E = \mathrm{i}k_0, \tag{4.18}$$

and get

$$I_{ML} = \frac{\Gamma(1+\alpha)}{\Gamma(\alpha)}\frac{\mathrm{i}(-1)^{\alpha+1}}{n_0}\int_0^1 dx\, x^{\alpha-1}\int \frac{d^{d-1}k}{(2\,\pi)^d}\int_{-\infty}^{+\infty} dk_E \frac{xP_0+k_3}{\left[k_E^2+\mathcal{A}\right]^{\alpha+1}}. \tag{4.19}$$

Once we perform this rotation we can take the limit $\eta \to 0$ and $\delta \to 0$ and we get a result independent of both regulators, in particular, it is independent of the regulator δ for the IR singularities due to the gauge choice. This is a significant difference between PV and ML prescriptions that is due to the fact that with ML prescription we can perform correctly the Wick rotation. This is why the ML prescription is formally the correct one to use.

4.2 Renormalisation in light-cone gauge

In this section, we will address the renormalization problem in light-cone gauge.

We start by briefly recalling how the resummation procedure works in the covariant gauges and then we will point out the differences when we choose a non-covariant gauge, like the light-cone gauge.

When we compute a one-loop amplitude in a gauge theory we find out that the loop integrals diverge in the ultraviolet. This is a problem because it prevents us from making predictions beyond the leading order. The procedure that, starting from these divergent contributions, allows us to get some finite result is called renormalization. We can call the non-renormalized Lagrangian the *bare* Lagrangian.

The renormalization is based on the observation that the parameters in the bare Lagrangian, like the mass of the particles, correspond to the physical parameter only at tree level. The mass of a particle, in fact, is defined as the pole of the propagator of the particle. If one does not take into account the quantum corrections, the pole of this propagator is identified with the lagrangian parameter. For example, if we consider a scalar field its propagator will be

$$G_2(q) = \frac{\mathrm{i}}{q^2 - m_0^2 + \mathrm{i}\eta}, \tag{4.20}$$

and so the lagrangian parameter m_0 can be identified as the mass of the field. If we take into account the quantum correction the two-point function, Eq.(4.20) changes and can be written as

$$G_2(q) = \frac{\mathrm{i}}{q^2 - m_0^2 - \Sigma(q^2, m_0^2) + \mathrm{i}\eta}, \tag{4.21}$$

where $\Sigma(q^2, m_0^2)$ is the one-loop correction to the propagator. We can notice that the pole of the propagator is now shifted, and so the definition for the physical mass of the particle is now

$$m_{\mathrm{F}}^2 = m_0^2 + \Sigma(q^2, m_0^2). \tag{4.22}$$

This means that the quantum corrections modify the lagrangian parameter but the physical value of the mass must be the the same. This is the key to solve this problem because we can always reparametrise the Lagrangian to write it as a function of the physical parameters. This is done, in practice, by adding some terms, called ultraviolet counterterms, at the Lagrangian that cancel the singularities so that we are left only with finite quantities. Of course, this method has its subtleties, like for instance, the fact that there is not a unique way to redefine the parameters. For a more complete discussion on this topic, one can see [40, 41] or any other standard QFT textbook.

Not in every theory this procedure can be systematically performed at all orders in perturbation theory. The theories that allow the implementation of this procedure are called *renormalizable* theories. It has been shown that a renormalizable theory has a global gauge symmetry called BRST symmetry [90–93]. Using this symmetry we can provide a more formal definition of the renormalization procedure.

In a covariant gauge the counterterms, since the lagrangian is Lorentz invariant, the counterterms must respect this invariance and then it is simple to derive them by

looking at the structure of the other terms in the lagrangian. For axial gauges, things are more complicated. Since the gauge fixing term in Eq.(4.2) breaks the Lorentz covariance, the counterterms are no longer constrained by it and so they may acquire a dependence on the gauge vector n. This is what we witness for example in light-cone gauge. To cancel the UV singularities of the amplitude in this gauge, we can not read the counterterms directly from the lagrangian but we have to compute the divergent contribution of each diagram and subtract it by hand. In Chapter 5 we will see how this works in an explicit calculation.

We want to emphasize the fact that we are allowed to proceed in this way because the complete lagrangian respects the BRST symmetry also when the gauge fixing term is the one in Eq.(4.2). In this sense, the counterterms can also be derived by using imposing this symmetry in a more formal procedure. A more complete analysis of this problem can be found in [88].

In the following, we will present a simple example of this procedure in order to show the difference between the renormalization procedure in the two prescriptions we discussed above.

4.2.1 Counterterms with PV prescription

Since with PV prescription we are not able to perform the Wick rotation correctly, we have to face the problem of the presence of spurious UV singularities, due to the failing of the power counting, and the dependence on δ of the UV counterterms.

We show the procedure to derive a gauge-dependent counterterm in the easiest possible case: the fermion self-energy. We compute the singular part of the diagram in Fig.4.1. We will see that this contribution has a gauge dependence in the UV part that must be canceled by defining an appropriate gauge-dependent counterterm. This result is also reported in [81], so we can check our results against theirs. We will work in the limit where the quark mass is negligible.

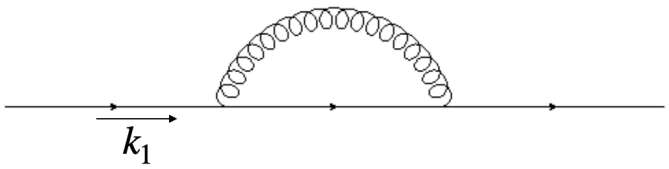

Figure 4.1: One-loop contribution to the fermion self-energy.

The quantity we want to compute is the singular part of

$$\Sigma(k_1, n) = \mathrm{i}g^2 C_F \int \frac{d^d k}{(2\pi)^d} \frac{\gamma^\nu (\not{k}_1 - \not{k}) \gamma^\mu}{k^2 (k_1 - k)^2} \left(-g_{\mu\nu} + \frac{k_\mu n_\nu + k_\nu n_\mu}{k \cdot n} \right). \tag{4.23}$$

We take the quark momentum k_1 to be off-shell, to avoid any infrared singularities. Contracting the indices and doing some algebra with the γ-matrices we get

$$\Sigma(k_1, n) = \mathrm{i}g^2 C_F \left[\frac{d-2}{2} B_{00}(k_1) \not{k}_1 + \frac{2k_1^2}{k_1 \cdot n} \left(k_1 \cdot n \, B_{10a}(k_1) - B_{00}(k_1) \right) \not{n} \right], \tag{4.24}$$

where

$$\begin{aligned} B_{00} &= \int \frac{d^d k}{(2\pi)^d} \frac{1}{k^2 (k-k_1)^2}; \\ B_{10a} &= \int \frac{d^d k}{(2\pi)^d} \frac{1}{k^2 (k-k_1)^2 k \cdot n}. \end{aligned} \tag{4.25}$$

In Eq.(4.24), we used Passarino-Veltmann decomposition to reduce tensorial integrals to scalar integrals. Since we are only interested in the singular part of this quantity, we compute the integrals in Eq.(4.25) using the techniques illustrated in Appendix A and retaining only their singular part. We get

$$\Sigma(k_1, n)|_{\text{UV}} = -\frac{\alpha}{4\pi} C_F \left[\frac{1}{\epsilon} \not{k}_1 + \frac{k_1^2}{2 k_1 \cdot n} \frac{1}{\epsilon} (4 I_0 - 4) \not{n} \right] + O(\epsilon), \tag{4.26}$$

where

$$I_0 = \int_0^1 dz \frac{z}{z^2 + \delta^2} = -\ln(\delta) + O(\delta), \tag{4.27}$$

comes from the fact that we used the PV prescription. This result is different from the one in Feynman gauge for two reasons. The first is the dependence on the PV parameter δ. As we argued before, this dependence is a symptom of the fact that this prescription is not the correct one to use when working in light-cone gauge. The other is the dependence on the gauge vector n. This dependence on the counterterm can not be derived by the terms in the lagrangian and this is the reason why we call the counterterms gauge-dependent.

In the following section, we will perform the calculation of the same counterterms but using the ML prescription. We will see that, while the δ dependence will disappear, we still have the dependence on the gauge vector n.

4.2.2 Counterterms with ML prescription

The problem of defining the counterterms for the light-cone gauge also appears when we work with ML prescription. The calculations are very similar to the ones in the previous section, in the following, we will point out the main differences between the two calculations.

The starting point is the same as the one in the previous section, and with the same calculations we get to

$$\Sigma(k_1, n) = \mathrm{i} g^2 C_F \left[\frac{d-2}{2} B_{00}(k_1) \not{k}_1 + \frac{2 k_1^2}{k_1 \cdot n} \left(k_1 \cdot n \, B_{10a}(k_1) - B_{00}(k_1) \right) \not{n} \right], \tag{4.28}$$

where the first integral,

$$B_{00} = \int \frac{d^d k}{(2\pi)^d} \frac{1}{k^2 (k-k_1)^2}, \tag{4.29}$$

is the same as in the PV case, since it does not contain any non-covariant contribution. The second integral instead become

$$B_{10a} = \int \frac{d^d k}{(2\pi)^d} \frac{1}{k^2 (k-k_1)^2} \frac{k \cdot \bar{n}}{k \cdot n \, k \cdot \bar{n} + \delta^2}, \tag{4.30}$$

where we used the ML prescription to regularise the gauge-dependent IR singularities. At this point the integral in Eq.(4.29) can be computed using the customary covariant loop-integrals integration techniques, while the integral in Eq.(4.30) can be computed using the techniques reported in Appendix A. Since we are only interested in the singular part of the Eq.(4.28), we note that we can directly neglect the non-covariant integral because its contribution is finite. The final result is

$$\Sigma(k_1, n)|_{\text{UV}} = -\frac{\alpha}{4\pi}\frac{C_F}{\epsilon}\left[\not{k}_1 - \frac{2k_1^2}{k_1 \cdot n}\not{n}\right] + O\left(\epsilon^0\right). \tag{4.31}$$

This result is different from the one in the previous section because it does not depend on the regulator for the gauge-dependent singularities δ. This is due to the fact, discussed in Section 4.1, that using ML prescription we can perform the Wick rotation correctly and then take the limit for $\delta \to 0$.

However, this result is also different from the one in Feynman gauge because we have the dependence on the gauge vector n. As we discussed above, this dependence can not be derived by the terms in the lagrangian and this is the reason why we call the counterterms gauge-dependent. This dependence is present with both prescriptions since it derives from the form of the gauge-fixing Lagrangian.

Chapter 5

Higgs-induced DIS

We want to test if the resummation formula presented in Chapter 2,

$$C_g(N,\alpha_s) = \int_0^\infty dk_\perp^2\, \mathcal{C}\left(N,k_\perp^2,Q^2,\alpha_s\right)\, \mathcal{U}\left(N,k_\perp^2,Q^2\right), \tag{5.1}$$

still works if we apply it to resum NLL terms in the coefficient function. This formula has two components. The first, $\mathcal{C}\left(N,k_\perp^2,Q^2,\alpha_s\right)$, as we explained in Chapter 2 is the off-shell coefficient function and it is process-dependent. The second, $\mathcal{U}\left(N,k_\perp^2,Q^2\right)$, is the evolutor that encodes the ladder of gluon emissions by the incoming parton. As we discussed in Chapter 3, to test Eq.(5.1) at NLL accuracy, we have to compute the off-shell coefficient function at one loop in light-cone gauge and verify that it is free from small-x logarithms. Then, we have to compute the evolutor $\mathcal{U}$ resummed at the required accuracy.

To compute the off-shell coefficient function we have to choose a suitable process. We choose the deep-inelastic scattering initiated by a Higgs-boson (Higgs-induced DIS). This process is suitable for studying small-x resummation because it involves only gluons, so the small-x logarithms appear already in the leading order. Moreover, we will work in the limit where $n_f \to 0$, namely a pure gluon theory, in order to avoid complications due to the presence of quark in loops at higher order.

The Higgs-induced deep inelastic scattering is a process similar to the usual deep-inelastic scattering that, instead of being initiated by a photon, has in the initial state an off-shell Higgs boson. Namely, the process we want to compute is

$$g^{(*)}(k_1) + H^{(*)}(q) \to g(k_2). \tag{5.2}$$

where the initial state gluon, of momentum k_1, is off-shell. Fig.(5.1) shows a schematic representation of it.

We start by giving a more detailed definition of the process and the kinematics in Section 5.1. Then we present the result for the one-loop on-shell coefficient function in Section 5.2. This calculation is preliminary to the one of the off-shell coefficient function. Then, in Section 5.3 we compute the counterterms for this process, as we discussed in Chapter 4. In Section 5.4, then, we will compute off-shell virtual amplitude for this process. Finally, in Section 5.5, we will present the next step we intend to take to improve this work.

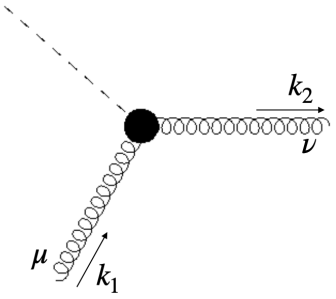

Figure 5.1: Higgs induced DIS. The incoming gluon of momentum k_1 is off-shell.

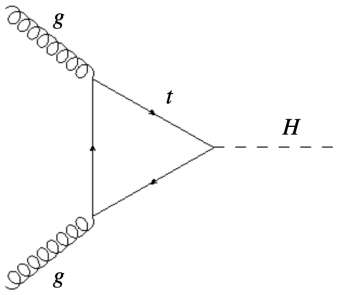

Figure 5.2: Leading order contribution to $gg \to H$ with finite top mass.

5.1 Higgs-induced DIS: kinematic and definitions

In this section, we describe the kinematics of the process and we set some notations that will be useful throughout all the calculations presented in this chapter.

Higgs boson does not directly interact with a gluon. This process is mediated by a quark as shown in Fig.(5.2). Since the coupling of the Higgs boson with a particle is proportional to its mass, the main contribution in the loop of Fig.(5.2) is given by the top quark. We are interested in the dominant soft contribution that does not resolve the gluon-gluon-Higgs (ggH) coupling induced by the top loop. Then we can evaluate QCD corrections quite accurately in the limit $m_t \to \infty$. The calculation simplifies considerably in this limit because the coupling becomes pointlike and the corresponding Feynman diagrams have one loop less. We can, then, describe the interaction between the Higgs boson and the gluon by the effective Lagrangian [94],

$$\mathcal{L} = \frac{\alpha_s \sqrt{\sqrt{2}\mathrm{G}_F}}{12\pi} \left(1 + \frac{\alpha_s}{4\pi}\frac{19}{3}C_A\right) \frac{H}{1+\delta} \mathrm{Tr}\{F^{\mu\nu}F_{\mu\nu}\} + \cdots , \tag{5.3}$$

where H is the Higgs boson field, $\delta = \frac{\alpha_s C_A}{4\pi}\frac{8}{3}$ and $F^{\mu\nu}$ is the gluon field strength tensor.

From the effective Lagrangian in Eq.(5.3), we extract the Feynman rule for the lowest order coupling between Higgs and gluons. Two vertexes will be useful to compute the NLO correction to the Higgs-induced DIS: the coupling of the Higgs with two gluons (Fig.5.3) and the coupling of the Higgs with three gluons (Fig.5.3). The vertex for the first diagram will be

$$M^{\mu\nu}_{ab}(k_1, k_2) = \mathrm{i}\, c\, (k_1^\nu k_2^\mu - g^{\mu\nu} k_1 \cdot k_2)\, \delta_{ab}, \tag{5.4}$$

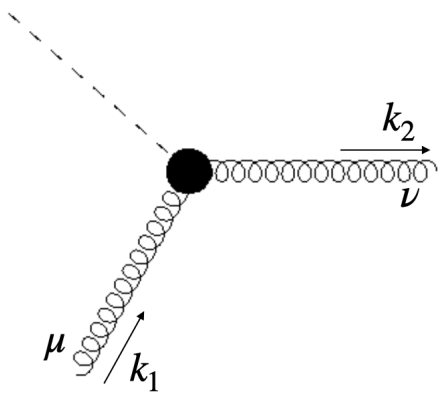

Figure 5.3: Feynman diagram for the Hgg coupling in the effective theory.

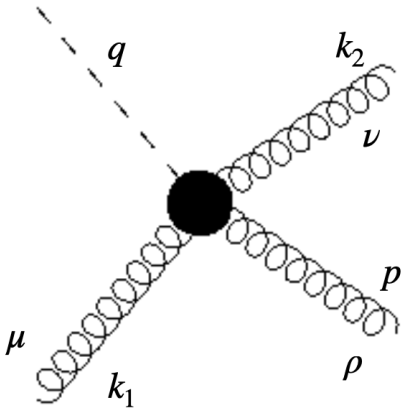

Figure 5.4: Feynman diagram for the $Hggg$ coupling in the effective theory.

where $c = \frac{\alpha_s \sqrt{\mathrm{G}_F \sqrt{2}}}{3\pi}$ and a, b are the colour indices. We refer to Fig.(5.3) for the momenta of the particles. The vertex for the second diagram will be

$$E^{\mu\nu\rho}_{abc}(k_1, k_2, p,) = c\, g_s\, f_{abc}\, [g^{\mu\nu}(k_1 + p)^\rho + g^{\nu\rho}(k_2 - p)^\mu - g^{\rho\mu}(k_2 + k_1)^\nu]\,, \tag{5.5}$$

where f_{abc} is the usual $SU(3)$ structure constant and k_1 is assumed to be incoming, while p_1 and p_2 are assumed to be outgoing.

To derive all the results presented in this chapter, we will use dimensional regularisation with $d = 4 - 2\epsilon$ and, as we already explained in Chapter 4, we will work in the light-cone gauge, defining a gauge vector n^μ so that $n^2 = 0$ and $A \cdot n = 0$, where A^μ is the field of the gluon.

We now clarify the kinematics of the process and we define some quantities that will be useful to derive the results presented in this chapter.

We will use the Sudakov parametrization for the momentum of the incoming parton:

$$k_1^\mu = z k^\mu + \beta n^\mu + k_t^\mu, \tag{5.6}$$

where we defined

$$\begin{aligned} &k^2 = n^2 = 0; \\ &k \cdot k_t = n \cdot k_t = 0; \\ &k_t^2 = -\mathbf{k}_t^2, \end{aligned} \tag{5.7}$$

and where n^μ is the gauge vector. It has been shown [18, 22] that, in the high-energy regime, the dominant integration region in the k_1 variable is the one where

$$k_1^2 \simeq -\mathbf{k}_t^2. \tag{5.8}$$

Following [18, 22], we will also limit our analysis to this kinematic region. We can, then, parameterize the momenta of the incoming particle in the process as

$$\begin{aligned} k_1 &= z\, k + k_t \\ q &= n - \rho\, k. \end{aligned} \tag{5.9}$$

Moreover, the off-shell Higgs must be time-like since it emerges from a scattering of two on-shell particles. This means $q^2 = -Q^2$, where $Q^2 > 0$. Form this relation we can derive that

$$\rho = \frac{Q^2}{2k \cdot n} = \frac{Q^2}{S}, \tag{5.10}$$

where

$$S = (k + n)^2 = 2k \cdot n. \tag{5.11}$$

We recognize in Eq.(5.10) the usual definition of the Bjorken x. In the limit where $S \gg Q^2$, this parameter goes to zero its logarithms in the coefficient function must be resummed to get a finite result.

Finally, we can define some other quantities that will be useful in the calculations:

$$\begin{aligned} \nu &= 2k_1 \cdot q = z\, S; \\ \xi &= \frac{\mathbf{k}_t^2}{Q^2}; \\ \tau &= \frac{\rho}{z}. \end{aligned} \tag{5.12}$$

In particular, when we consider the virtual contribution we can establish a relation between the parameter ξ and the parameter τ. Since the virtual contribution is a $2 \to 1$ process the integration of the amplitude on the phase space of the outgoing momentum, that we have to perform to get the cross-section, is quite simple. In particular, it can be done using the Dirac delta of momentum conservation that sets

$$k_2 = k_1 + q. \tag{5.13}$$

From the on-shell relation of the outgoing gluon, we get

$$(k_1 + q)^2 = 0, \tag{5.14}$$

from which, with a simple algebra, we get

$$\tau = \frac{1}{1 + \xi}. \tag{5.15}$$

This relation will be used to simplify the results in the following sections.

5.2 Next-to-leading order on-shell coefficient function

In this section, we compute the next-to-leading order (NLO) coefficient function for the Higg-induced DIS with the incoming gluon on-shell. This calculation allows us to show some features that will be useful in the more complicated off-shell calculation. Moreover, this is an example where the PV prescription can be safely applied since the real and the virtual contributions are separately gauge-invariant.

At NLO we always have two contributions to kinds the amplitude: the virtual correction and the real emissions. Since we set $n_f = 0$, we do not have to worry about the contribution from the quarks. In the following, we will compute these two contributions separately in light-cone gauge.

5.2.1 Real emission

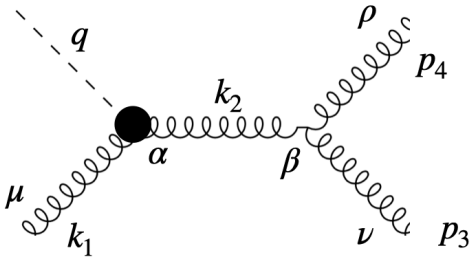

Figure 5.5: S-channel diagram contributing to NLO real correction. The momenta p_3 and p_4 are outgoing while the momentum k_1 is incoming.

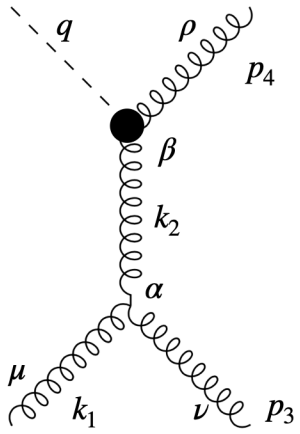

Figure 5.6: T-channel diagram contributing to NLO real correction. The momenta p_3 and p_4 are outgoing while the momentum k_1 is incoming.

Real emissions at NLO are made out of the combinations of four diagrams. The first is the s-channel diagram shown in Fig.(5.5) that, using Feynman rules can be written as

$$S^{\mu\nu\rho}_{abc} = M^{\mu\alpha}_{ad}(k_1, k_1+q)\frac{\mathrm{i}\delta_{de}d_{\alpha\beta}(k_1+q,n)}{(k_1+q)^2}V^{\beta\nu\rho}_{ebc}(k_1+q,-p_3,-p_4), \tag{5.16}$$

where

$$V^{\mu\nu\rho}(k_1,k_2,k_3) = g_s f_{abc}\left[g^{\mu\nu}(k_1^\rho - k_2^\rho) + g^{\nu\rho}(k_2^\mu - k_3^\mu) + g^{\rho\mu}(k_3^\nu - k_1^\nu)\right] \tag{5.17}$$

is the three gluon vertex, $M^{\mu\nu}(k_1, k_1+q)$ is the gluon-Higgs vertex defined in Eq.(5.4) and $d_{\alpha\beta}(k_1+q,q)$ is the numerator of the light-cone gauge gluon propagator,

$$d_{\alpha\beta}(k_1+q,n) = -g_{\alpha\beta} + \frac{(k_1+q)_\alpha n_\beta + (k_1+q)_\beta n_\alpha}{n\cdot(k_1+q)}. \tag{5.18}$$

The second diagram is the t-channel shown in Fig(5.6). Using Feynman rules this diagram can be written as

$$T^{\mu\nu\rho}_{abc} = V^{\mu\rho\nu}_{a,b,d}(k_1,-p_3,p_3-k_1)\frac{\mathrm{i}\delta_{de}d_{\alpha\beta}(k_1-p_3,n)}{(k_1-p_3)^2}M^{\beta\nu}_{ec}(k_1-p_3,p_4), \tag{5.19}$$

where the tensorial structures are the same as the ones defined for the s-channel diagram. The third contribution is the u-channel contribution, Fig.(5.7) that, using Feynman rules, can be written as

$$U^{\mu\nu\rho}_{abc} = V^{\mu\nu\alpha}_{a,c,d}(k_1,-p_4,p_4-k_1)\frac{\mathrm{i}\delta_{de}d_{\alpha\beta}(k_1-p_4,n)}{(k_1-p_4)^2}M^{\beta\rho}_{eb}(k_1-p_4,p_3), \tag{5.20}$$

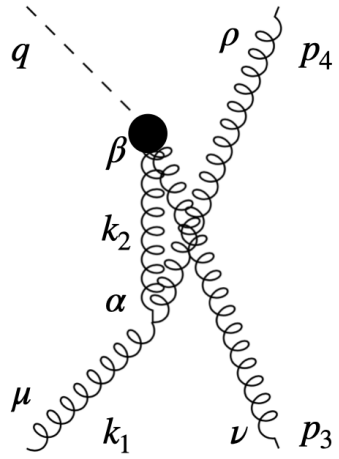

Figure 5.7: U-channel diagram contributing to NLO real correction. The momenta p_3 and p_4 are outgoing while the momentum k_1 is incoming.

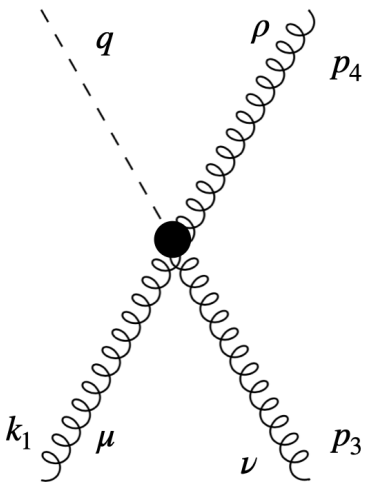

Figure 5.8: Three-gluons diagram contributing to NLO real correction. The momenta p_3 and p_4 are outgoing while the momentum k_1 is incoming.

that can be obtained from Eq.(5.19) by exchanging the two outgoing gluons p_3 and p_4. The last diagram is the contact term shown in Fig.(5.8). This can directly be written using Eq.(5.5).

To compute the on-shell coefficient function, we have to compute the amplitude for this process. This means that we have to compute

$$\mathcal{A}_{1,\text{on}} = \int d^4p_4 \int d^4p_3 |\mathcal{M}|^2 \delta^4(k_1 + q + p_3 + p_4) \delta^+\left(p_3^3\right) \delta^+\left(p_4^2\right), \tag{5.21}$$

where to get the squared matrix element we have to take all the possible combinations of the diagrams in Fig.(5.5), Fig.(5.6), Fig.(5.7) and Fig.(5.8). Since in this case, we are computing the on-shell coefficient function, the momentum k_1 of the incoming gluon is on-shell and the sum over the polarization of this gluon is given by the light-cone gauge polarization tensor,

$$d^{\mu\rho}(k_1, n) = -g^{\mu\nu} + \frac{k_1^\mu n^\nu + k_1^\nu n^\mu}{k_1 \cdot n}. \tag{5.22}$$

We define the Mandelstam invariants as

$$\begin{aligned} s &= (k_1 + q)^2 = (p_3 + p_4)^2 \\ t &= (k_1 - p_3)^2 = (p_4 - q)^2 \\ u &= (k_1 - p_4)^2 = (p_3 - q)^2. \end{aligned} \tag{5.23}$$

To compute the integrals we parametrize the momenta of the particles as

$$\begin{aligned} k_1 &= zk + k_t, \\ q &= n - \rho k\,, \\ p_3 &= z_1(1-\tau)k + z_2 n + p_{3\,t} \\ p_4 &= (1-z_1)(1-\tau)k + (1-z_2)n + k_t - p_{3\,t}, \end{aligned} \tag{5.24}$$

where we used the momentum conservation to write $p_4 = k_1 + q - p_3$. Of the two integrals in Eq.(5.21) one can be easily done using the momentum conservation Dirac delta, while the other can be simplified using the conditions derived by imposing that the momentum p_3 and p_4 must be on-shell. This calculation does not require the introduction of prescriptions to regularise the gauge-dependent singularities that we discussed in Chapter 4 and so can be done without much effort.

Once we have the amplitude, we can obtain the cross-section by dividing it by the initial state collinear flux,

$$F = 4k_1 \cdot q = \frac{2Q^2}{\tau}, \tag{5.25}$$

and averaging over the initial state gluon polarization. The coefficient function is linked to the cross-section by the relation

$$\mathcal{C}(Q^2) = \frac{Q^2}{\tau}\sigma(Q^2), \tag{5.26}$$

where τ is defined in Eq.(5.12). Doing all of these calculations we get

$$\begin{aligned}\mathcal{C}_{1,g\,R} = \left[\frac{\pi C^2 Q^2}{4}\right]\frac{\alpha_s C_A}{4\pi}\Bigg\{&\frac{4}{\epsilon^2}\delta(1-\tau) - \frac{1}{\epsilon}\left[4\left(\frac{1}{\tau} + \frac{1}{(1-\tau)_+} - 2 + \tau(1-\tau)\right)\right.\\ &\left.-\frac{11}{3}\delta(1-\tau)\right] + 4\left(\frac{1}{\tau} - 2 + \tau(1-\tau)\right)\ln(1-\tau) + 4\left(\frac{\ln(1-\tau)}{1-\tau}\right)_+\\ &-\frac{11}{3}\left(\frac{1}{\tau} + \frac{1}{(1-\tau)_+}\right) - 4\left(\frac{1}{\tau} + \frac{1}{(1-\tau)_+} - 2 + \tau(1-\tau)\right)\ln(\tau)\\ &+\left(\frac{67}{9} - 6\zeta_2\right)\delta(1-\tau) + \mathcal{O}\left(\epsilon^2\right)\Bigg\},\end{aligned} \tag{5.27}$$

where we factorized the Born-level contribution to the coefficient function. This contribution to the coefficient function as a double and a single IR pole. The double pole must be canceled by the virtual contribution as the part of the single pole proportional to the Dirac delta. The remaining singular contribution is the singular part of the splitting function of the gluon.

5.2.2 Virtual corrections

After having computed the real contribution, we now calculate the virtual one. The virtual diagrams that contribute to the NLO coefficient function are shown in Fig.(5.9), Fig.(5.10), Fig.(5.11) and Fig.(5.12). Before computing the contribution of each single diagram, we can make some observations.

First of all, we see that there are some contributions that we can set to zero from the beginning. We can consider the diagram in Fig.(5.12), the diagram with the bubble on the outgoing leg can be obtained by this one by exchanging k_1 with k_2. The contribution from this diagram will be proportional to

$$I_1 = \int \frac{d^d k}{(2\,\pi)^d}\frac{N(k, k_1, n)}{k^2(k-k_1)^2} \tag{5.28}$$

for the covariant part and to

$$I_2 = \int \frac{d^d k}{(2\,\pi)^d} \frac{N(k, k_1, n)}{k^2 (k - k_1)^2} \frac{1}{k \cdot n}, \tag{5.29}$$

for the non-covariant part. Since the incoming gluon is on-shell, the first integral is zero because we do not have any scale in the integral that can carry out the mass dimension of the integral. It could be only proportional to $(k_1^2)^\alpha$ but $k_1^2 = 0$. The second integral, if we use the principal value prescription to regularise the gauge singularity can be written, following Eq.(A.107) as

$$I_2 = \frac{i}{16\pi^2} \left(\frac{4\pi}{-k_1^2} \right)^\epsilon \frac{\Gamma(1+\epsilon)}{\epsilon} \int_0^1 dz f(l_+ z) z^{-\epsilon} (1-z)^{-\epsilon}. \tag{5.30}$$

Again, since $k_1^2 = 0$, this integral is vanishing. We conclude that the contribution form diagrams with a bubble on the incoming (or the outgoing) gluon give no contribution when we compute the on-shell one-loop coefficient function.

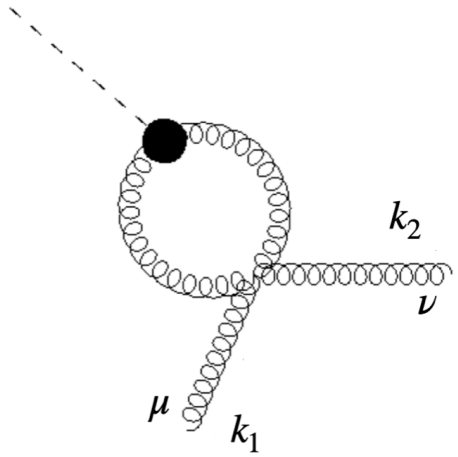

Figure 5.9: First diagram contributing to the NLO coefficient function. The momentum k_1 is taken to be incoming, the momentum k_2 is taken to be outgoing.

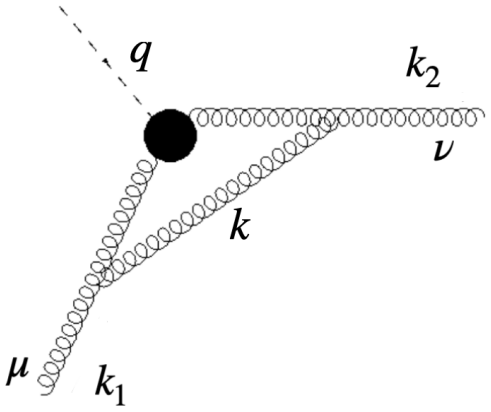

Figure 5.10: Triangle diagram. The momentum k_1 is taken to be incoming, the momentum k_2 is taken to be outgoing. The loop momentum is k.

We now concentrate on the contribution of the other three diagrams. We compute their contribution separately.

We start with the diagram in Fig.(5.9). The first step is to write the matrix element

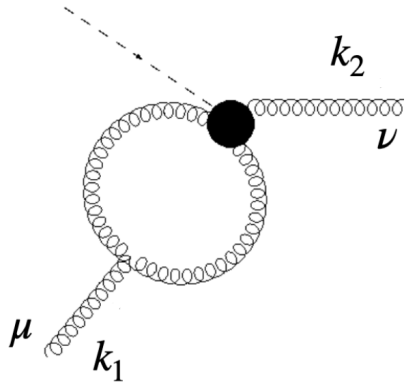

Figure 5.11: Three gluon effective vertex diagram. The momentum k_1 is taken to be incoming, the momentum k_2 is taken to be outgoing.

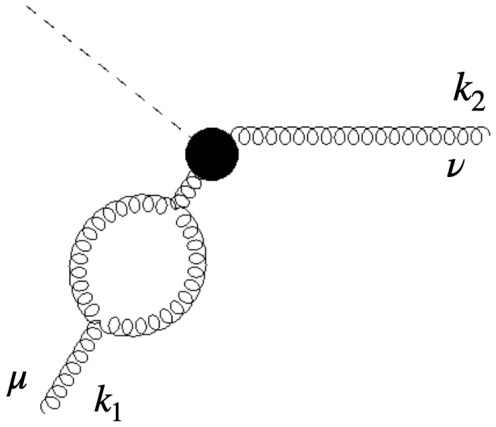

Figure 5.12: Bubble on the incoming gluon diagram. The diagram with the bubble on the outgoing gluon is the same as this when $k1$ is exchanged with k_2

for this diagram using Feynman rules. We get

$$\begin{aligned} A^{\mu\nu}_{a,b}(k_1,k_2,n) = &- c\, g^2 \mu^{2\epsilon} f^{a\,c\,d} f^{b}_{c\,d} \int \frac{d^d k}{(2\,\pi)^d} \frac{1}{(k-k_1)^2 (k-k_2)^2} \\ &\left[-g^{\mu\rho} g^{\nu\sigma} - g^{\mu\sigma} g^{\nu\rho} + 2 g^{\mu\nu} g^{\rho\sigma}\right] \\ &\left[(k_2-k)^\beta (k_1-k)^\alpha - g^{\alpha\beta} (k_1-k)\cdot(k_2-k)\right] \\ &\left[-g^{\rho\alpha} + \frac{(k_1-k)^\rho n^\alpha + (k_1-k)^\alpha n^\rho}{(k_1-k)\cdot n}\right] \\ &\left[-g^{\sigma\beta} + \frac{(k_2-k)^\sigma n^\beta + (k_2-k)^\beta n^\sigma}{(k_2-k)\cdot n}\right], \end{aligned} \tag{5.31}$$

where we notice the first issue of the light-cone gauge since the matrix element becomes more complicated. We also notice the presence of some non-covariant contributions. We discussed the techniques used to address gauge spurious singularities and non-covariant loop integrals in Chapter 4 and in Appendix A. We choose to regularise the gauge-dependent singularities using PV prescription. As we will show in the end, this prescription can be applied in this case because the virtual and the real contributions are separately gauge invariant. The dependence on the gauge singularities regulator, δ, vanishes at the level of the virtual contribution.

To get the NLO contribution to the cross-section, we need the squared matrix element,

$$|\mathcal{M}_A|^2 = 2Re\left\{A^{\mu\nu}(k_1,k_2,n) M^{*\,\rho\sigma}(k_1,k_2) d^{\mu\rho}(k_1,n) d^{\nu\sigma}(k_2,n)\right\}, \tag{5.32}$$

where $M^{*\,\rho\sigma}$ is the tree-level amplitude of the effective gluon-Higgs vertex, defined in Eq.(5.4) and $d^{\mu\rho}(k_i,n)$ are the sum over polarisations of the on-shell gluon in light-cone gauge defined in Eq.(5.22).

Contracted all the indices in Eq.(5.32), we have to integrate the resulting expression in the loop four-momentum k. We compute the covariant integrals with the usual techniques, while to compute the non-covariant ones we use the PV prescription and follow the method presented in Appendix A. The situation is quite simple since we have at most two covariant denominators because we have only two gluon propagators in Eq.(5.31). Once we compute all the integrals and put them all together we get

$$|M_A|^2 = 0. \tag{5.33}$$

We, then, are left with only two diagrams. The first is the one in Fig.(5.11). Clearly, also the same diagram but with the bubble on the outgoing gluon must be taken into account. For symmetry, however, once we have the contribution from the diagram in Fig.(5.11), we will get the other by exchanging k_1 with k_2. We repeat the same steps we followed to compute the contribution from the diagram in Fig.(5.9). First of all, we write the matrix element with Feynman rules

$$\begin{aligned} B^{\mu\nu}_{a,b}(k_1,k_2,n) = -c\,g^2\mu^{2\epsilon} f^{a\,c\,d} f^{b}_{c\,d} \int \frac{d^dk}{(2\,\pi)^d} \frac{1}{k^2(k-k_1)^2} \\ [g^{\rho\sigma}(k_1-2k)^\mu + g^{\mu\sigma}(k-2k_1)^\rho + g^{\mu\rho}(k-k_1)^\sigma] \\ \left[g^{\alpha\beta}(2k-k_1)^\nu - g^{\beta\nu}(k+k_1+k_2)^\alpha - g^{\alpha\nu}(k+k_2)^\beta\right] \\ \left[-g^{\sigma\beta} + \frac{(k_1-k)^\sigma n^\beta + (k_1-k)^\beta n^\sigma}{n\cdot(k_1-k)}\right] \\ \left[-g^{\rho\alpha} + \frac{k^\rho n^\alpha + k^\rho n^\alpha}{n\cdot k}\right] \end{aligned} \tag{5.34}$$

Then we compute the squared matrix element and we calculate the integrals. The calculations are analogous to the ones we did for the previous diagram. Also in this case, we get

$$|M_{DP}|^2 = 0. \tag{5.35}$$

This result is not surprising. We can see that this diagram is similar to the one in Fig.(5.12) that vanishes for dimensional reasons. Since this diagram gives no contribution to the coefficient function we can conclude that also the one with the bubble on the k_2 momentum is vanishing.

We have only one diagram that gives a contribution different from zero and it is the diagram with three gluon propagators shown in Fig.(5.10). To compute it, we write

the matrix element of this diagram using the Feynman rules

$$\begin{aligned} T^{\mu\nu} = & -c\, g^2 \mu^{2\epsilon} f^{a\,c\,d} f^{b}_{c\,d} \int \frac{d^d k}{(2\,\pi)^d} \frac{1}{k^2 (k-k_1)^2 (k-k_2)^2} \\ & \left[g^{\mu\sigma}(k_1+k)^\rho + g^{\rho\sigma}(k_1-2k)^\mu + g^{\mu\rho}(k-2k_1)^\sigma\right] \\ & \left[-g^{\nu\beta}(k_2+k)^\alpha + g^{\alpha\beta}(2k-k_2)^\nu + g^{\nu\alpha}(2k_2-k)^\beta\right] \\ & \left[(k_2-k)^\gamma (k_1-k)^\delta - g^{\gamma\delta}(k_1-k)\cdot(k_2-k)\right] \\ & \left[-g^{\sigma\beta} + \frac{k^\sigma n^\beta + k^\beta n^\sigma}{k\cdot n}\right] \\ & \left[-g^{\rho\gamma} + \frac{(k_1-k)^\rho n^\gamma + (k_1-k)^\gamma n^\rho}{(k_1-k)\cdot n}\right] \\ & \left[-g^{\alpha\delta} + \frac{(k_2-k)^\alpha n^\delta + (k_2-k)^\delta n^\alpha}{(k_2-k)\cdot n}\right]. \end{aligned} \tag{5.36}$$

Following what we did with the other diagrams, we now compute the squared matrix element and we integrate it over the loop momentum k. In this case, the number of integrals increases considerably. Luckily, all the contributions with three covariant denominators and a covariant part vanish and so the non-covariant part has the same structure as the one of simpler diagrams. By computing all the integrals and combining them all together we get

$$|M_T|^2 = g_s^2 c^2 C_A \delta_{a,b} \left[-\frac{1}{8}\left(\frac{\nu^2}{\epsilon} - \nu^2\right)\left(\frac{1}{\epsilon} + \ln\left(\frac{\mu^2}{\nu}\right)\right) + \frac{\nu^2}{8}\left(\zeta_2 - \ln^2\left(\frac{\mu^2}{\nu}\right)\right)\right], \tag{5.37}$$

where we used the MS renormalization scheme and $\nu = 2k_1 \cdot q = 2k_1 \cdot k_2$. It is interesting to notice that this result is free from the PV prescription parameter δ that regulates the gauge-dependent spurious singularities. This means that the virtual and the real contributions are separately gauge invariant. This is the reason why we can apply the PV prescription even if it generates spurious *delta*-dependent singularities.

To get the cross-section we now integrate this result divided by the incoming flux and mediated over the spin and polarisation of the incoming particle, in the one-particle phase space. The coefficient function will then be obtained by multiplying the cross-section by the scale Q^2, as we did for the real contribution. The result we get is

$$\mathcal{C}_{1\,\mathrm{V}} = -\left[\frac{\pi C^2 Q^2}{4}\right] \frac{C_A \alpha_s}{4\pi}\left(\frac{4}{\epsilon^2} - 2\zeta_2\right)\delta(1-\tau), \tag{5.38}$$

where we factorized the Born-level contribution to the coefficient function.

5.2.3 Charge renormalisation

The last ingredient is the contribution from the running of the QCD coupling encoded in the renormalization. This contribution takes into account the UV singularities of the amplitude and can be written as

$$\mathcal{C}_{1,\,\alpha_s} = \mathcal{C}_0 Z^2_{\alpha_s} = -\frac{\alpha_s}{4\pi}\frac{2}{\epsilon}\left(\frac{11}{3}C_A - \frac{2}{3}n_f\right)\mathcal{C}_0 + \mathcal{O}\left(\alpha_s^2\right), \tag{5.39}$$

where

$$\mathcal{C}_0 = \frac{\pi C^2 Q^2}{4}, \tag{5.40}$$

is the Born-level contribution to the coefficient function.

5.2.4 Complete NLO correction

Combining the results of the computations in the previous subsections we reconstruct

$$\begin{aligned}\mathcal{C}_{1,\text{on}} &= \mathcal{C}_{1,R} + \mathcal{C}_{1,V} + \mathcal{C}_{1,\alpha_s} \\ &= \left[\frac{\pi Q^2 C^2}{4}\right]\left[\frac{-1}{\epsilon}P_{gg}(\tau) + c_{hg,0}(\tau)\right],\end{aligned} \tag{5.41}$$

with the definitions

$$P_{gg}(z) = 4C_A\left[\frac{1}{(1-z)_+} + \frac{1}{z} - 2 + z(1-z)\right] + \frac{11}{3}C_A\delta(1-z) \tag{5.42}$$

$$\begin{aligned}c_{hg,0}(z) = C_A\Bigg[&4\left(\frac{1}{\tau} - 2 + \tau(1-\tau)\right)\ln(1-\tau) + 4\left(\frac{\ln(1-\tau)}{1-\tau}\right)_+ \\ &- 4\left(\frac{1}{\tau} + \frac{1}{1-\tau} - 2 + \tau(1-\tau)\right)\ln(\tau) - \frac{11}{3}\left(\frac{1}{\tau} + \frac{1}{(1-\tau)_+}\right) \\ &+ \left(\frac{67}{9} - 4\zeta_2\right)\delta(1-\tau)\Bigg]\end{aligned} \tag{5.43}$$

We worked in a pure gluon theory so we set $n_f = 0$ from the beginning. The results we found are in agreement with [83, 95], up to some algebraic gymnastics. We see that the IR double poles canceled between real and virtual contributions. Moreover, we reconstructed the splitting function of the gluon.

5.3 Renormalisation in light-cone gauge

In this section, we compute the gauge-dependent counterterm as discussed in Chapter 4. We perform this calculation using the ML prescriptions since, as we discussed in Chapter 4, this prescription displaces the spurious gauge singularities in the same way as the usual Feynman prescription. In this way, we are allowed to perform the Wick rotation and take the limit for the regulator that goes to zero. To define these counterterms we have to compute the UV pole of the following diagrams. To do so, we compute them with the incoming and the outgoing gluons off-shell. In this way, we avoid the IR singularities and all the poles we find are UV. The results computed using the PV prescription can be found in Appendix B for a comparison.

5.3.1 Counterterm for the gluon self-energy

We start by computing the counterterm for the gluon self-energy. This counterterm will be used in the following section to cancel the UV singularities of the diagram shown in Fig.(5.12).

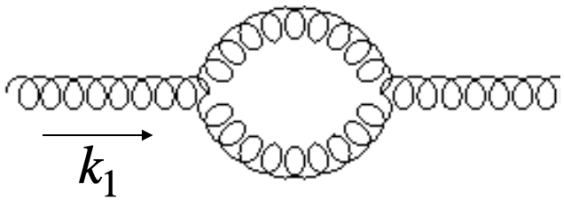

Figure 5.13: One-loop contribution to the gluon self-energy.

The starting point is the one-loop correction to the gluon propagator, represented in Fig.(5.13).

$$\Pi^{\mu\nu}(k_1,n) = \int \frac{d^dk}{(2\pi)^d} \frac{N^{\mu\nu\rho\sigma\alpha\beta}(k,k_1,n)}{k^2(k-k_1)^2} \left[-g_{\rho\alpha} + \frac{k_\alpha n_\rho + k_\rho n_\alpha}{k\cdot n}\right] \times \left[-g_{\sigma\beta} + \frac{(k_1-k)_\sigma n_\beta + (k_1-k)_\beta n_\sigma}{(k_1-k)\cdot n}\right], \tag{5.44}$$

where we omitted the $+i\eta$ Feynman prescription in the propagator of the gluons and

$$N^{\mu\nu\rho\sigma\alpha\beta}(k,k_1,n) = -\frac{g^2 C_A \delta_{a,b}}{2} \left[g^{\rho\sigma}(k_1-2k)^\mu + g^{\mu\sigma}(k-2k_1)^\rho + g^{\mu\rho}(k+k_1)^\sigma\right] \left[g^{\beta\nu}(2k_1-k)^\alpha - g^{\alpha\nu}(k+k_1)^\beta + g^{\alpha\beta}(2k-k_1)^\nu\right]. \tag{5.45}$$

From Eq.(5.44) we see that we have some spurious singularities due to the gauge choice. We regularise these singularities with the ML prescription. A detailed description of the method used to compute this contribution can be found in Section 5.4, while the procedure to compute these integrals is explained in detail in Appendix A. Here we point out the fact that, since we have two gluon propagators, we will have integrals with at most two covariant denominators. Moreover, we are only interested in the UV singularities so we will discard all the finite parts of these integrals. Doing all these calculations we get

$$\Pi^{\mu\nu}(k_1,n) = i\frac{\alpha_s}{4\pi}\frac{C_A\delta_{a,b}}{\epsilon}\left[\frac{11}{3}\left(k_1^\mu k_1^\nu - k_1^2 g^{\mu,\nu}\right) -4\left(k_1^\mu k_1^\nu - \frac{8k^2}{k_1\cdot n}\left(k_1^\mu n^\nu + k_1^\nu k_1^\mu\right) + \frac{8\left(k_1^2\right)^2}{\left(k_1\cdot n\right)^2} n^\mu n^\nu\right)\right]. \tag{5.46}$$

First of all, since the gluon we are considering is off-shell, the pole in Eq.(5.46) is UV. We notice that this expression depends on the gauge vector n. These terms, as we discussed in Chapter 4, can not be deduced by the terms in the lagrangian and are typical of the axial gauges since they break the Lorentz invariance. We also notice that this object is still transverse with respect to the gluon momentum k_1.

We can compare this result with the one obtained with the PV prescription, reported in Appendix B, Eq.(B.3). We see that the main difference is that here we do not have dependence on the parameter of the ML prescription: all the singularities are regularised by the regulator of the dimensional regularisation, ϵ. This is because with ML prescription we do not have spurious UV singularities.

At this point, we can define a gauge-dependent counterterm that cancels all the UV poles of this contribution:

$$\begin{aligned} CT^{\mu\nu}_{\text{self}}(k_1, n) = &- \mathrm{i}\frac{\alpha_s}{4\pi}\frac{C_A\delta_{a,b}}{\epsilon}\left[\frac{11}{3}\left(k_1^\mu k_1^\nu - k^2 g^{\mu,\nu}\right)\right. \\ &\left. -4\left(k^\mu k^\nu - \frac{8k^2}{k\cdot n}\left(k^\mu n^\nu + k^\nu k^\mu\right) + \frac{8\left(k^2\right)^2}{\left(k\cdot n\right)^2}n^\mu n^\nu\right)\right]. \end{aligned} \tag{5.47}$$

In the following section, we will use this same procedure to define gauge-dependent counterterms for the Higgs-DIS effective vertex that will be useful to compute the off-shell NLO virtual contribution to the process.

5.3.2 Renormalization of the effective vertex

In this section, we derive the counterterm for the Higgs-gluon effective vertex. We, therefore, isolate the UV divergent part of the one-loop contribution to the effective vertex.

To compute the UV divergent part of the one-loop contribution to the effective vertex, we perform the calculation keeping both the incoming and the outgoing gluons off-shell. In this way, we avoid IR singularities. This object, schematically represented in Fig.(5.14), receives a contribution from the diagrams that are shown in Fig.(5.15).

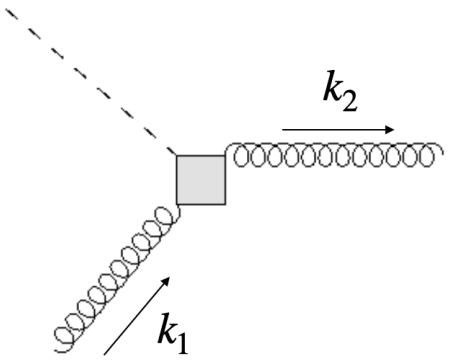

Figure 5.14: Schematic representation of the one-loop counterterm for the Higgs-gluon vertex.

In the following, we will compute the UV contribution diagram by diagram and then we will sum these up at the end to get the final result. The counterterm for the Higgs-gluon effective vertex will be defined as this UV contribution with the opposite sign so that all the UV divergences are canceled.

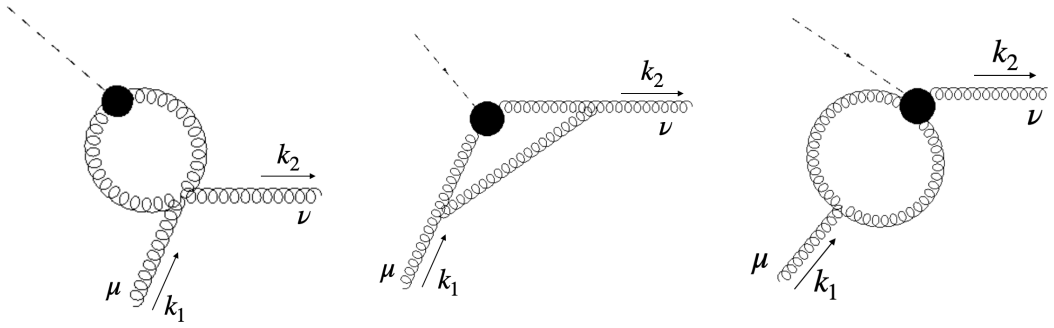

Figure 5.15: Diagrams contributing to the one-loop correction to the Higgs-gluon effective vertex. Here is not represented the fourth diagram that is the same as the third but with the bubble on the outgoing leg.

We start from the contribution of the first diagram in Fig.(5.15). Using Feynman rules, we write the contribution from this diagram as

$$C^{\mu\nu}(k_1,k_2,n) = \int \frac{d^dk}{(2\,\pi)^d}\frac{N^{\mu\nu\alpha\beta\rho\sigma}(k_1,k_2,n)}{(k-k_1)^2(k-k_2)^2}\left[-g_{\rho\alpha}+\frac{(k_1-k)_\alpha n_\rho+(k_1-k)_\rho n_\alpha}{(k_1-k)\cdot n}\right] \times\left[-g_{\sigma\beta}+\frac{(k_2-k)_\beta n_\sigma+(k_2-k)_\sigma n_\beta}{(k_2-k)\cdot n}\right], \tag{5.48}$$

where

$$N^{\mu\nu\alpha\beta\rho\sigma}(k_1,k_2,n) = \mathrm{i}\frac{g^2 c\, C_A \delta_{a,b}}{2}\left[(k_1-k)^\beta(k_2-k)^\alpha - g^{\alpha\beta}(k_1-k)\cdot(k_2-k)\right] \times\left[2g^{\mu\nu}g^{\rho\sigma}-g^{\mu\rho}g^{\nu\sigma}-g^{\mu\sigma}g^{\nu\rho}\right], \tag{5.49}$$

and the overall factor $\frac{1}{2}$ is due to symmetry. Since we kept both k_1 and k_2 off-shell, all the poles of this contribution are UV. Moreover, since we are interested in computing only the UV pole of this diagram we can discard all the finite contributions from the integrals. As we can see from Eq.(5.48), we are again in the case where we do not have contributions from integrals with three covariant denominators and a non-covariant term.

To compute the UV contribution from this diagram, we first use ML prescription to regulate the gauge singularities in Eq.(5.48). We, then, contract the indices in Eq.(5.48) and we use Passarino-Veltmann decomposition to reduce all the integrals to scalar ones. Finally, we compute the scalar integrals with the techniques shown in Appendix A.

Once we put all the terms together, we find out that the ultraviolet pole of this diagram is null. This means that the counterterm will be zero. The corresponding contribution in the amplitude will therefore have only infrared poles and a finite part.

We now move on to the second diagram in Fig.(5.15). This is the most complicated because it has three gluon propagators and one more gluon vertex compared to the other diagrams. Since we are interested in computing the counterterm, we compute this diagram keeping the incoming and the outgoing legs off-shell. In this way, all the are

poles ultraviolet and, again, we can read the counterterm simply from the coefficient of the pole.

Using Feynman rules we can write the contribution from this diagram as:

$$\begin{aligned} T^{\mu\nu}(k_1,k_2,n) = &\int \frac{d^dk}{(2\,\pi)^d}\frac{N^{\mu\nu\alpha\sigma\beta\gamma\rho\delta}(k_1,k_2,n)}{k^2(k-k_1)^2(k-k_2)^2} \\ &\times\left[-g_{\rho\delta}+\frac{k_\delta n_\rho+k_\rho n_\delta}{k\cdot n}\right]\left[-g_{\sigma\alpha}+\frac{(k_1-k)_\alpha n_\sigma+(k_1-k)_\sigma n_\alpha}{(k_1-k)\cdot n}\right] \\ &\times\left[-g_{\gamma\beta}+\frac{(k_2-k)_\beta n_\gamma+(k_2-k)_\gamma n_\beta}{(k_2-k)\cdot n}\right], \end{aligned} \tag{5.50}$$

where

$$\begin{aligned} N^{\mu\nu\alpha\sigma\beta\gamma\rho\delta}(k_1,k_2,n) =& \mathrm{i}g^2c\,C_A\delta_{a,b}\left[g^{\mu\rho}(k+k_1)^\sigma+g^{\mu\sigma}(k-2k_1)^\rho+g^{\rho\sigma}(k_1-2k)^\mu\right] \\ &\times\left[g^{\gamma\delta}(k_2-2k)^\nu+g^{\gamma\nu}(k-2k_2)^\delta+g^{\delta\nu}(k+k_2)^\gamma\right] \\ &\times\left[(k_1-k)^\beta(k_2-k)^\alpha-g^{\alpha,\beta}(k_1-k)\cdot(k_2-k)\right]. \end{aligned} \tag{5.51}$$

As we did before, use ML prescription to regularise gauge-dependent IR singularities. We note that, even if in principle from Eq.(5.75) we can have contributions from integrals with three covariant denominators and a non-covariant part, we can see from power counting that they will only give a finite contribution or an IR pole. For this reason, we can simplify our calculation by discarding these contributions.

The next step is to contract the indices in Eq.(5.50) and to compute the integrals with the techniques introduced in Appendix A. We write the result as:

$$\begin{aligned} &T^{\mu\nu}(k_1,k_2,n) = -\mathrm{i}\frac{\alpha_s c\,C_A\delta_{a,b}}{4\pi\,\epsilon}\left[\left(\frac{1}{3}-2x\right)k_1^\mu k_1^\nu+\left(\frac{1}{x}+\frac{1}{3}\right)k_2^\mu k_2^\nu\right. \\ &+\left(\frac{k_1^2x(9x+13)+k_2^2(13x+9)}{6x}\right)g^{\mu\nu}+\left(\frac{-2x^3+2x^2-3x+2}{x-x^2}\right)k_1^\mu k_2^\nu \\ &\frac{k_1^\mu n^\nu}{2k_1\cdot n}\left(\frac{2k_2^2\left(-k_1^2(x+1)x^2+4k_1\cdot k_2x+k_2^2\left(x^3-x^2-2\right)\right)}{x^2(x(k_1^2x-2k_1\cdot k_2)+k_2^2)}+\right. \\ &\left.+\frac{k_1^2\left(-5x^3+17x^2-9x+3\right)+4k_1\cdot k_2x\left(x^2-3x-1\right)+k_2^2\left(-4x^3+12x^2-6x+4\right)}{(x-1)^3}\right) \\ &+\frac{n^\mu k_1^\nu}{2k_1\cdot n}\left(\frac{2k_2^2\left(-k_1^2(x+1)x^2+4k_1\cdot k_2x+k_2^2\left(x^3-x^2-2\right)\right)}{x^2(x(k_1^2x-2k_1\cdot k_2)+k_2^2)}+\right. \\ &\left.\frac{k_1^2\left(-5x^3+17x^2-9x+3\right)+4k_1\cdot k_2x\left(x^2-3x-1\right)+k_2^2\left(-4x^3+12x^2-6x+4\right)}{(x-1)^3}\right) \\ &+\frac{k_2^\mu n^\nu}{2k_1\cdot n}\left(\frac{k_1^2\left(-3x^3+13x^2-17x+1\right)+k_1\cdot k_2\left(-12x^2+20x+4\right)+2k_2^2(2x-5)}{(x-1)^3}\right. \\ &\left.\left.+\frac{2\left(k_1^2\left(2k_1\cdot k_2x^2+k_2^2\left(-2x^2+x-1\right)\right)+(k_2^2-2k_1\cdot k_2)(2k_1\cdot k_2x-k_2^2(x+1))\right)}{x(x(k_1^2x-2k_1\cdot k_2)+k_2^2)}\right)\right. \end{aligned}$$

$$
\begin{aligned}
&+\frac{n^\mu k_2^\nu}{2x^2 k_1\cdot n}\left(\frac{k_2^2\left(x^3-5x^2+3x-1\right)-2k_1^2x^2\left(2x^3-4x^2+2x+1\right)}{(x-1)^2}\right.\\
&-\frac{2xk_1\cdot k_2\left(x^2-4x+1\right)}{(x-1)^2}-\frac{x\left(4(k_1^2)^2x^2-2k_1^2k_1\cdot k_2x(x+4)+k_1^2k_2^2\left(5x^2-2x+6\right)\right)}{x(k_1^2x-2k_1\cdot k_2)+k_2^2}\\
&\left.-\frac{x\left(4\left(k_1\cdot k_2\right)^2x-2k_1\cdot k_2(5k_2^2x+k_2^2)+\left(k_2^2\right)^2(2x+3)\right)}{x(k_1^2x-2k_1\cdot k_2)+k_2^2}\right)\\
&\frac{n^\mu n^\nu}{2x^3\left(k_1\cdot n\right)^2}\left(\frac{x^3\left((k_1^2)^2\left(5x^4-20x^3+83x^2-18x+4\right)\right)}{(x-1)^4}\right.\\
&+\frac{x^3\left(-k_1^2k_1\cdot k_2\left(x^4-4x^3+108x^2+122x-11\right)+12(k_1\cdot k_2)^2\left(2x^2+15x+1\right)\right)}{(x-1)^4}\\
&+\frac{k_2^2\left(2k_1^2\left(2x^4-8x^3+22x^2+29x+9\right)x^3+k_1\cdot k_2\left(5x^4-134x^3-90x^2+4x-1\right)x\right)}{(x-1)^4}\\
&+\frac{(k_2^2)^2\left(-2x^5+15x^4+29x^3+22x^2-13x+3\right)}{(x-1)^4}\\
&+\frac{k_2^2x\left(4(k_1^2)^2x^2+k_1^2\left(2k_1\cdot k_2(x-5)x+k_2^2\left(3x^2-2x+6\right)\right)\right)}{x(k_1^2x-2k_1\cdot k_2)+k_2^2}\\
&\left.+\frac{x(k_2^2)^2(-2k_1\cdot k_2x(x+2)+2k_2^2x+k_2^2)}{x(k_1^2x-2k_1\cdot k_2)+k_2^2}\right)\Bigg],
\end{aligned}
\tag{5.52}
$$

where we used $x=\frac{k_1\cdot n}{k_2\cdot n}$. This result is quite complicated but we can make some observations. The first is the fact that we do not have a dependence on the ML regulator δ. This is the main difference between this result and the one obtained using PV prescription, which you can find in Appendix D. We notice also that, like in PV prescription, we have some tensorial structures that depend on the gauge vector n. These terms cannot be derived directly from the Lagrangian and are typical of the axial gauges, as we discussed above. We can also observe that the coefficients of the tensorial structures that do not involve that gauge vector n are quite simple compared to the ones of the structures that depend on n.

Finally, we compute the last contribution, the one of the third diagram in Fig.(5.15). The diagram with the bubble on the outgoing leg will give the same contribution if we exchange k_1 (incoming momentum) with k_2 (outgoing momentum). For this reason, we can compute explicitly only the contribution from this diagram.

Using Feynman rules, we can write the contribution from this diagram as:

$$
\begin{aligned}
B_1^{\mu\nu}(k_1,k_2,n)=&\int\frac{d^dk}{(2\,\pi)^d}\frac{N^{\mu\nu\alpha\beta\rho\sigma}(k_1,k_2,n)}{k^2(k-k_1)^2}\\
&\times\left[-g_{\rho\alpha}+\frac{k_\alpha n_\rho+k_\rho n_\alpha}{k\cdot n}\right]\left[-g_{\sigma\beta}+\frac{(k_1-k)_\beta n_\sigma+(k_1-k)_\sigma n_\beta}{(k_1-k)\cdot n}\right],
\end{aligned}
\tag{5.53}
$$

where

$$N^{\mu\nu\alpha\beta\rho\sigma}(k_1,k_2,n) = \mathrm{i}\frac{\mathrm{g}^2 c\, C_A \delta_{a,b}}{2}\left[g^{\beta\nu}(k_1+k_2-k)^\alpha + g^{\alpha\beta}(2k-k_1)^\nu - g^{\alpha\nu}(k+k_2)^\beta\right] \\ \left[g^{\mu\rho}(k+k_1)^\sigma + g^{\mu,\sigma}(k-2k_1)\rho + g^{\rho\sigma}(k_1-2k)^\mu\right], \tag{5.54}$$

and the overall factor $\frac{1}{2}$ is due to symmetry.

Since both legs are off-shell, all the poles are ultraviolet. The contribution to the counterterm will be, as for the other diagrams, its divergent part with the opposite sign. As we did with the other diagrams, we first use ML in Eq.(5.91) to regularise the gauge singularities, and then we compute the resulting integrals with the techniques presented in Section 4.1.2. The result is

$$B_1^{\mu\nu}(k_1,k_2,n) = \mathrm{i}\frac{\alpha_s c\, C_A \delta_{a,b}}{8\pi\,\epsilon}\left[-\frac{2}{3}\,k_1^\mu k_1^\nu - \frac{k_1^2(9x+13)}{3}g^{\mu\nu} + \frac{5k_1^2}{k_1\cdot n}\,k_1^\mu n^\nu \right. \\ \left. + \frac{(5-x)k_1^2 + 4k_1\cdot k_2}{k_1\cdot n}k_1^\nu n^\mu + \frac{3k_1^2}{k_1\cdot n}k_2^\mu n^\nu - \frac{k_1^2(5k_1^2+3k_1\cdot k_2)}{(k_1\cdot n)^2}n^\mu n^\nu\right], \tag{5.55}$$

Also in this case we reported in Appendix B the result computed using PV prescription. This contribution is simpler than the one in Eq.(5.52), but also in this case we notice the presence of tensorial structures depending on the gauge vector n.

The contribution from the diagram with the bubble on the outgoing leg can be obtained from this one by exchanging k_1 with k_2. It will be:

$$B_2^{\mu\nu}(k_1,k_2,n) = \mathrm{i}\frac{\alpha_s c\, C_A \delta_{a,b}}{8\pi\,\epsilon}\left[-\frac{2}{3}\,k_2^\mu k_2^\nu - \frac{k_2^2(9+13x)}{3x}g^{\mu\nu} + \frac{5k_2^2}{k_2\cdot n}\,k_2^\mu n^\nu \right. \\ \left. + \frac{(5x-1)k_2^2 + 4xk_1\cdot k_2}{x\,k_2\cdot n}k_2^\nu n^\mu + \frac{3k_2^2}{k_2\cdot n}k_2^\mu n^\nu - \frac{k_2^2(5k_2^2+3k_1\cdot k_2)}{(k_2\cdot n)^2}n^\mu n^\nu\right]. \tag{5.56}$$

To get the total counterterm we have to sum the result we found in Eq.(5.52),

Eq.(B.7) and Eq.(B.14) with the opposite sign to cancel te Uv singularities. We get

$$
\begin{aligned}
CT^{\mu\nu}_{\text{eff}}(k_1,k_2,n) = \mathrm{i}\frac{\alpha_s c\, C_A \delta_{a,b}}{4\pi\,\epsilon}\Bigg[& -2x\,k_1^\mu k_1^\nu + \frac{1}{x}k_2^\mu k_2^\nu + \frac{-2x^3+2x^2-3x+2}{x(1-x)}k_1^\mu k_2^\nu \\
& + \frac{k_1^\mu n^\nu}{2k_1\cdot n}\Bigg(\frac{2k_2^2\left(-k_1^2(x+1)x^2+4k_1\cdot k_2 x+k_2^2\left(x^3-x^2-2\right)\right)}{x^2(x(k_1^2x-2k_1\cdot k_2)+k_2^2)} + 5k_1^2 + \frac{3k_2^2}{x} \\
& + \frac{k_1^2\left(-5x^3+17x^2-9x+3\right)+4k_1\cdot k_2 x\left(x^2-3x-1\right)+k_2^2\left(-4x^3+12x^2-6x+4\right)}{(x-1)^3}\Bigg) \\
& + \frac{k_1^\nu n^\mu}{2k_1\cdot n}\Bigg(\frac{2k_2^2\left(-k_1^2(x+1)x^2+4k_1\cdot k_2 x+k_2^2\left(x^3-x^2-2\right)\right)}{x^2(x(k_1^2x-2k_1\cdot k_2)+k_2^2)} + (5-x)k_1^2 + 4k_1\cdot k_2 \\
& + \frac{k_1^2\left(-5x^3+17x^2-9x+3\right)+4k_1\cdot k_2 x\left(x^2-3x-1\right)+k_2^2\left(-4x^3+12x^2-6x+4\right)}{(x-1)^3}\Bigg) \\
& + \frac{k_2^\mu n^\nu}{2k_1\cdot n}\Bigg(\frac{k_1^2\left(-3x^3+13x^2-17x+1\right)+k_1\cdot k_2\left(-12x^2+20x+4\right)+2k_2^2(2x-5)}{(x-1)^3} \\
& + \frac{5k_2^2}{x} + 3k_1^2 + \frac{2k_1^2\left(2k_1\cdot k_2 x^2+k_2^2\left(-2x^2+x-1\right)\right)}{x(x(k_1^2x-2k_1\cdot k_2)+k_2^2)} \\
& + \frac{2(k_2^2-2k_1\cdot k_2)(2k_1\cdot k_2 x-k_2^2(x+1))}{x(x(k_1^2x-2k_1\cdot k_2)+k_2^2)}\Bigg) \\
& + \frac{k_2^\nu n^\mu}{2x^2k_1\cdot n}\Bigg(\frac{-2x^3(k_1^2)^2\left(2x^4-4x^3+4x^2-3x+2\right)}{(x-1)^2(x(k_1^2x-2k_1\cdot k_2)+k_2^2)} \\
& + \frac{4x^2k_1^2k_1\cdot k_2\left(2x^4-3x^3+3x^2-2x+2\right)}{(x-1)^2(x(k_1^2x-2k_1\cdot k_2)+k_2^2)} \\
& + \frac{-8x^2(k_1\cdot k_2)^2\left(x^2-x+1\right)+xk_1^2k_2^2\left(-3x^4+4x^3-9x^2+10x-6\right)}{(x-1)^2(x(k_1^2x-2k_1\cdot k_2)+k_2^2)} \\
& + \frac{-2k_2^2k_1\cdot k_2 x\left(x^3-8x^2+7x-4\right)+(k_2^2)^2\left(-2x^4+7x^3-12x^2+7x-2\right)}{(x-1)^2(x(k_1^2x-2k_1\cdot k_2)+k_2^2)}\Bigg) \\
& \frac{n^\mu n^\nu}{2\,k_1\cdot n}\Bigg(\frac{(k_1^2)^2\left(5x^4-20x^3+83x^2-18x+4\right)}{(x-1)^4} - k_1^2(5k_1^2+3k_1\cdot k_2) \\
& + \frac{-k_1^2k_1\cdot k_2\left(x^4-4x^3+108x^2+122x-11\right)}{(x-1)^4} - \frac{k_2^2(3k_1\cdot k_2+5k_2^2)}{x^2} \\
& + \frac{12(k_1\cdot k_2)^2\left(2x^2+15x+1\right)+2k_1^2k_2^2\left(2x^4-8x^3+22x^2+29x+9\right)}{(x-1)^4} \\
& + \frac{(k_2^2)^2\left(-2x^5+15x^4+29x^3+22x^2-13x+3\right)}{(x-1)^4x^3} \\
& + \frac{xk_1\cdot k_2k_2^2\left(5x^4-134x^3-90x^2+4x-1\right)}{(x-1)^4x^3} + \frac{(k_2^2)^2(k_2^2(1+2x)-2k_1\cdot k_2x(x+2))}{x^2(x(k_1^2x-2k_1\cdot k_2)+k_2^2)} \\
& + \frac{k_2^2\left(4(k_1^2)^2x^2+k_1^2\left(2k_1\cdot k_2(x-5)x+k_2^2\left(3x^2-2x+6\right)\right)\right)}{x^2(x(k_1^2x-2k_1\cdot k_2)+k_2^2)}\Bigg)\Bigg]
\end{aligned}
\tag{5.57}
$$

where we again used the definition $x = \frac{k_1\cdot n}{k_2\cdot n}$. From this expression, we can notice that the coefficients of the tensorial structures that do not involve the gauge vector n simplify

a lot. In particular, we see that the coefficient of $g^{\mu\nu}$ vanishes. On the other hand, the coefficient of structures depending on the gauge vector n are still quite complicated. Comparing this result with the one obtained using PV prescription (Appendix (B), we can see that this is quite simpler and does not have the dependence on the regulator of the gauge-dependent infrared singularities, as we discussed in Chapter 5.

This counterterm will be used in the following section to compute the virtual NLO contribution to the Higgs-induced deep-inelastic scattering.

5.4 Next-to-leading order off-shell virtual contribution to the coefficient function

In Section 5.2 we studied the one-loop contribution to the Higgs-induced DIS in the on-shell limit. This has been helpful because we learned how to deal with some features of the calculation, like for instance the non-covariant gauge integrals, that will also be present in the off-shell calculation.

In this section, we compute the one-loop virtual contribution to the Higgs-induced Deep Inelastic Scattering (DIS) in light-cone gauge. Since in this thesis we are particularly interested in studying how the choice of light-cone gauge affects the calculations, we find it interesting to concentrate on the virtual contribution. It is in the loop integrals, in fact, that we have to choose a prescription to regularise the gauge-dependent singularities we discussed in Chapter 4. In this section, we will see that, since the virtual and the real contributions are not separately gauge-invariant, we have to choose the Mandelstam Leibbrandt prescription to regularise the singularities. This will make the integral quite more complicated to compute but, on the other hand, will allow us to get a result free from spurious singularities.

Before addressing the calculation, we have to make another remark. Since our final goal is to compute the off-shell coefficient function for this process, we have to compute the squared matrix element with the incoming gluon off-shell. This forces us to understand how to deal with the counterpart of the sum over polarizations when we have an off-shell gluon. As we discussed in Chapter 4 Catani, Ciafaloni and Hautmann in [18] solve this problem by defining

$$d^{\mu\nu}(k) = (d-2)\frac{k_t^\mu k_t^\mu}{\mathbf{k}_\perp^2}, \tag{5.58}$$

This projector by construction selects the dominant part of the amplitude in the high-energy region and if we take the on-shell limit we get

$$\lim_{\bar{k}_\perp^2 \to 0} \langle d_{CH}^{\mu\nu} \rangle = g_\perp^{\mu\nu}, \tag{5.59}$$

that is the usual sum over polarizations of an on-shell gluon.

Since, as we discussed in Chapter 4, we want to test if this form for the projector still selects the dominant part of the amplitude at NLL, we have to find out the scaling of the coefficients of various tensorial structures that contribute to the amplitude. Namely, we define

$$\mathcal{A}_{1\,\text{off}} = \mathcal{M}_{1\,\text{off}}^{\mu\nu}(k_1, k_2, n) d_{\mu\nu}(k_1, n), \tag{5.60}$$

once we have $\mathcal{M}^{\mu\nu}_{1\,\text{off}}(k_1,k_2,n)$ we can see if the tensor of Eq.(5.58) still selects the dominant part in the small-x region. For this reason, here we present the calculation to get $\mathcal{M}^{\mu\nu}_{1\,\text{off}}(k_1,k_2,n)$.

The loop diagrams contributing to the off-shell amplitude, the same contribution as the on-shell one, are shown in Fig.(5.9), Fig.(5.10), Fig.(5.11), and Fig.(5.12). In this case, the diagrams with the bubble on the incoming gluon give a contribution different from zero, because this gluon is off-shell. In the following, we will present the main steps of the calculation to get the contribution to the amplitude of each diagram. Since, as we discussed in Chapter 4, the correct prescription that has to be used to regularise the spurious gauge singularities is the Mandelstam-Leibbrandt prescription, we present the calculations done in this way. In Appendix C, you can find the result obtained using PV prescription.

5.4.1 Diagram A

We start by computing the contribution from the diagram in Fig.(5.9), we name it diagram A. We write directly the contribution to the amplitude $\mathcal{M}^{\mu\nu}(k_1,k_2,n)$ that is given by

$$A^{\mu\rho} = \int \frac{d^dk}{(2\,\pi)^d} \frac{N^{\mu\nu\alpha\beta\gamma\sigma}(k_1,k_2,n)\,T^{\rho}_{\delta}(k_1,k_2)\,d_{\nu\delta}(k_2,n)}{(k-k_1)^2(k-k_2)^2} \times \left[-g_{\gamma\alpha} + \frac{(k_1-k)_\alpha n_\gamma + (k_1-k)_\gamma n_\alpha}{(k_1-k)\cdot n}\right]\left[-g_{\sigma\beta} + \frac{(k_2-k)_\beta n_\sigma + (k_2-k)_\sigma n_\beta}{(k_2-k)\cdot n}\right], \tag{5.61}$$

where $T^{\rho}_{\delta}(k_1,k_2)$ is the tree-level Higgs-gluon vertex defined in Eq.(5.4), $d_{\nu\delta}(k_2,n)$ is the sum over polarizations of the on-shell gluon with momentum k_2 defined in Eq.(5.22), and

$$N^{\mu\nu\alpha\beta\gamma\sigma}(k_1,k_2,n) = \mathrm{i}\frac{g^2c^2\,C_A\delta_{a,b}}{2}\left[(k_1-k)^\beta(k_2-k)^\alpha - g^{\alpha\beta}(k_1-k)\cdot(k_2-k)\right] \left[2g^{\mu\nu}g^{\gamma\sigma} - g^{\mu\gamma}g^{\nu\sigma} - g^{\mu\sigma}g^{\nu\gamma}\right], \tag{5.62}$$

is the remaining numerator, where we also included the symmetry factor $S = \frac{1}{2}$. As you see from Eq.(5.61), we have two possible non-covariant denominators where we use the ML prescription defined in Eq.(4.10).

The next step is to contract the indices in Eq.(5.61) and identify all the possible tensorial structures that contribute to $A^{\mu\rho}$. We get

$$\begin{aligned} A^{\mu\rho}(k_1,k_2,n) =& \mathrm{i}\frac{g^2c^2\,C_A\delta_{a,b}}{2}\int\frac{d^dk}{(2\,\pi)^d}\left[A_g(k,k_1,k_2,n)g^{\mu\nu} + A_{k_1\,k_1}(k,k_1,k_2,n)k_1^\mu k_1^\nu\right. \\ &+ A_{k_2\,k_2}(k,k_1,k_2,n)k_2^\mu k_2^\nu + \frac{1}{2}A_{k_1\,k_2}(k,k_1,k_2,n)\,(k_1^\mu k_2^\nu + k_1^\mu k_2^\nu) \\ &+ A_{k\,k}(k,k_1,k_2,n)k^\mu k^\nu + \frac{1}{2}A_{k\,k_1}(k,k_1,k_2,n)\,(k^\mu k_1^\nu + k_1^\mu k^\nu) \\ &\left.+\frac{1}{2}A_{k\,k_2}(k,k_1,k_2,n)\,(k^\mu k_1^\nu + k_2^\mu k^\nu)\right], \end{aligned} \tag{5.63}$$

where we dropped the tensorial structures proportional to n^μ since, as we discussed in Chapter 3, the projector with whom we will contract this amplitude should satisfy

$$d^{\mu\nu}(k_1,n)n^\mu = d^{\mu\nu}(k_1,n)n^\nu = 0. \tag{5.64}$$

We note that in Eq.(5.65) we have some tensorial integrals, the ones in the third and the fourth row, and some scalar integrals. The first step will then be to reduce all the integrals to be scalar using Passarino-Veltmann reduction and write Eq.(5.65) as

$$\begin{aligned} A^{\mu\rho}(k_1,k_2,n) = \mathrm{i}\frac{g^2c^2\,C_A\delta_{a,b}}{2}\Bigg[&g^{\mu\nu}\int\frac{d^dk}{(2\,\pi)^d}A'_g(k,k_1,k_2,n) \\ &+k_1^\mu k_1^\nu\int\frac{d^dk}{(2\,\pi)^d}A'_{k_1\,k_1}(k,k_1,k_2,n)+k_2^\mu k_2^\nu\int\frac{d^dk}{(2\,\pi)^d}A'_{k_2\,k_2}(k,k_1,k_2,n) \\ &+\frac{1}{2}\left(k_1^\mu k_2^\nu+k_1^\mu k_2^\nu\right)\int\frac{d^dk}{(2\,\pi)^d}A'_{k_1\,k_2}(k,k_1,k_2,n)\Bigg], \end{aligned} \tag{5.65}$$

where A'_i are the coefficients after the Passarino-Veltmann reduction and we emphasized the fact that now the integral acts only on these coefficients. These coefficients are still quite complicated and in general, we can decompose them as

$$\begin{aligned} A'_i = &\frac{N_1(k,k_1,k_2,n)}{k^2(k-k_1)^2}+\frac{N_2(k,k_1,k_2,n)}{k^2(k-k_2)^2}+\frac{N_3(k,k_1,k_2,n)}{k^2(k-k_1)^2(k-k_2)^2} \\ &+\frac{N_4(k,k_1,k_2,n)}{k^2(k-k_1)^2k\cdot n}+\frac{N_5(k,k_1,k_2,n)}{k^2(k-k_2)^2k\cdot n}+\frac{N_6(k,k_1,k_2,n)}{k^2(k-k_1)^2(k-k_2)^2k\cdot n} \\ &+\frac{N_7(k,k_1,k_2,n)}{k^2(k-k_1)^2(k\cdot n-k_1\cdot n)}+\frac{N_8(k,k_1,k_2,n)}{k^2(k-k_2)^2(k\cdot n-k_1\cdot n)} \\ &+\frac{N_9(k,k_1,k_2,n)}{k^2(k-k_1)^2(k-k_2)^2(k\cdot n-k_1\cdot n)} \\ &+\frac{N_{10}(k,k_1,k_2,n)}{k^2(k-k_1)^2(k\cdot n-k_2\cdot n)}+\frac{N_{11}(k,k_1,k_2,n)}{k^2(k-k_2)^2(k\cdot n-k_2\cdot n)} \\ &+\frac{N_{12}(k,k_1,k_2,n)}{k^2(k-k_1)^2(k-k_2)^2(k\cdot n-k_2\cdot n)}, \end{aligned} \tag{5.66}$$

where the numerators N_i can still contain different powers of the loop momentum k contracted with the other momenta in the process. In the first row, there are some covariant integrals that can be computed with the usual loop-integral techniques. In the other rows, we see the presence of different non-covariant integrals with a different non-covariant part. We already used the identity

$$\frac{1}{(k\cdot n)(k\cdot n-k_1\cdot n)}=\frac{1}{k_1\cdot n}\left(\frac{1}{k\cdot n-k_1\cdot n}-\frac{1}{k\cdot n}\right) \tag{5.67}$$

to separate terms with more than one non-covariant denominator. To compute these integrals use the ML prescription to regularise the spurious gauge singularities and then we compute the integrals with the techniques exposed in Appendix A. Here we want to emphasize the fact that those techniques can be applied to scalar integrals.

This means that we still have to write the N_i numerators without powers of the loop momentum. This is possible by exploiting the identity

$$k \cdot l = -\frac{1}{2}(k-l)^2 + \frac{k^2}{2} + \frac{l^2}{2}, \tag{5.68}$$

and by using again the Passarino-Veltmann decomposition. Due to the complexity of the numerators N_i, this procedure required careful handling.

Of course not all the diagram contributions are the same in terms of complexity. For example in the case we are considering now we do not have integrals with three covariant denominators, since we have only two gluon propagators. Those contributions, that are the most cumbersome to deal with appear only in the diagram in Fig.(5.10).

After having done all these complicated calculations, the result we get is

$$\begin{aligned} A^{\mu\rho} = -\frac{\alpha_s}{8\pi} c^2 C_A \delta_{a,b} \left[A_g(k_1,k_2,n) g^{\mu\nu} + A_{k_1\,k_1}(k_1,k_2,n) k_1^\mu k_1^\nu \right. \\ \left. + A_{k_2\,k_2}(k_1,k_2,n) k_2^\mu k_2^\nu + \frac{1}{2} A_{k_1\,k_2}(k_1,k_2,n) \left(k_1^\mu k_2^\nu + k_1^\mu k_2^\nu\right) \right], \end{aligned} \tag{5.69}$$

where the coefficients of the tensorial structures are

$$A_g = \frac{3Q^4}{2\epsilon}(\xi - 1) + \frac{1}{2}(\xi - 1)Q^4; \tag{5.70}$$

$$A_{k_1 k_1} = 0; \tag{5.71}$$

$$A_{k_2 k_2} = -\frac{Q^2}{\epsilon}\frac{2(\xi+1)}{\xi} + \frac{\left(\pi^2\xi^2 + (\pi^2 - 6)\,\xi + 6\right) Q^2}{3\xi}; \tag{5.72}$$

and

$$A_{k_1 k_2} = \frac{Q^2}{\epsilon}\frac{2\xi - 1}{\xi} + \frac{\left(\pi^2\left(2\xi^2 - \xi + 1\right) - 12(\xi+1)\right) Q^2}{6\xi}, \tag{5.73}$$

were we set $\mu^2 = Q^2$ and $\xi = \frac{\mathbf{k}_1^2}{Q^2}$. We simplified these coefficients using the kinematic of the process. As we discussed in Section 5.1, since this is a $2 \to 1$ process we can impose

$$k_2^2 = (k_1 + q)^2 = 0. \tag{5.74}$$

This relation allows us to write the coefficients of the tensorial structures only as a function of the parameter ξ. We will use this relation also in the following results presented in this section.

We notice that, in this case, the result is quite simple. The parameter ϵ regularises the infrared singularities since, as we saw in Section 5.3, this diagram does not have ultraviolet divergences. We also notice that, as we expected, we do not have any dependence on the ML regulator δ. This is a difference from the result in PV prescription in Appendix C.

We also note that even though some of the integrals that contribute to this diagram have a double IR pole (see Appendix A), this final result has only a single pole. This means that the double poles cancel diagram by diagram.

5.4.2 Diagram B

We do the same procedure to compute the contribution from the second diagram, the one in Fig.(5.10). For simplicity, we name this integral B. We can write this contribution as

$$\begin{aligned} B^{\mu\rho}(k_1,k_2,n) = & \int \frac{d^dk}{(2\,\pi)^d} \frac{N^{\mu\nu\alpha\sigma\beta\gamma\rho\delta}(k_1,k_2,n)\, T_{\gamma\delta}(k_1,k_2)\, d_{\nu\delta}(k_2,n)}{k^2(k-k_1)^2(k-k_2)^2} \\ & \times \left[-g_{\rho\delta} + \frac{k_\delta n_\rho + k_\rho n_\delta}{k\cdot n}\right] \left[-g_{\sigma\alpha} + \frac{(k_1-k)_\alpha n_\sigma + (k_1-k)_\sigma n_\alpha}{(k_1-k)\cdot n}\right] \\ & \times \left[-g_{\gamma\beta} + \frac{(k_2-k)_\beta n_\gamma + (k_2-k)_\gamma n_\beta}{(k_2-k)\cdot n}\right], \end{aligned} \tag{5.75}$$

where the tree level Higgs-gluon vertex, $T_{\gamma\delta}(k_1,k_2)$, and the sum over the polarizations of the on-shell gluon, $d_{\nu\delta}(k_2,n)$, are the same as the ones used for the previous diagram, while the numerator is

$$\begin{aligned} N^{\mu\nu\alpha\sigma\beta\gamma\rho\delta}(k_1,k_2,n) = & \mathrm{i}g^2c^2\, C_A\delta_{a,b}\left[g^{\mu\rho}(k+k_1)^\sigma + g^{\mu\sigma}(k-2k_1)^\rho + g^{\rho\sigma}(k_1-2k)^\mu\right] \\ & \left[g^{\gamma\delta}(k_2-2k)^\nu + g^{\gamma\nu}(k-2k_2)^\delta + g^{\delta\nu}(k+k_2)^\gamma\right] \\ & \left[(k_1-k)^\beta(k_2-k)^\alpha - g^{\alpha\beta}(k_1-k)\cdot(k_2-k)\right]. \end{aligned} \tag{5.76}$$

In this case, the situation is quite more involved since we have three gluon propagators. The procedure we follow is the same as the one illustrated in the previous section. Here we do not repeat all the calculations, we simply point out the fact that in this case also the integrals with three covariant denominators must be taken into account.

We proceed by using the ML prescription in the non-covariant part of the gluon propagators. Then, we contract the indices and compute the integrals using the techniques explained in Appendix A. In this case, the result is quite more complicated and can be written as

$$\begin{aligned} B^{\mu\rho}(k_1,k_2,n) = -\frac{\alpha_s}{4\,\pi}c^2C_A\delta_{a,b}Q^2 \Big[& B_{k_1k_1}k_1^\mu k_1^\rho + B_{k_2k_2}k_2^\mu k_2^\rho + \frac{1}{2}B_{k_1k_2}(k_1^\mu k_2^\rho + k_2^\mu k_1^\rho) \\ & + B_g Q^2 g^{\mu\rho} + \ldots\Big], \end{aligned} \tag{5.77}$$

where we dropped the tensorial structures proportional to the gauge vector n because they will vanish once contracted with the tensor that selects the dominant part of the amplitude in the high-energy region. The calculations to get these coefficients are quite complicated due to the presence of integrals with three covariant denominators and a non-covariant part. Computing these integrals with ML prescription is challenging and a procedure to deal with them is presented in Appendix A. As we discuss in this appendix, the strategy we found to compute these integrals depends on the form of the non-covariant part. We find out that, in the end, only two integrals of this type contribute to the diagram,

$$T_{01} = \int \frac{d^dk}{(2\,\pi)^d} \frac{1}{k^2(k-k_1)^2(k-k_2)^2} \frac{1}{k\cdot n} \tag{5.78}$$

and

$$T_{01a} = \int \frac{d^d k}{(2\,\pi)^d} \frac{1}{k^2 (k-k_1)^2 (k-k_2)^2} \frac{1}{k\cdot n - k_1 \cdot n}. \tag{5.79}$$

In Appendix A we give a method to compute both the integrals. In Appendix A there are more details on these calculations, here we want to point out that since the non-covariant part of these integrals is different we could not exploit the result of one integral to compute the second. We had to compute them separately.

In this section, since the coefficients of the tensorial structures are in this case quite involved, we report only their divergent part. The finite part can be found in Appendix D. We have:

$$\begin{aligned} B_{k_1 k_1} = \frac{(\xi-1)}{24(\xi+1)^2\epsilon} \big[& 3\xi \left(20\xi^6 + 30\xi^5 + 32\xi^4 + 43\xi^3 + 19\xi^2 + 3\xi + 5\right) \ln(\xi) \\ & - 2\left(36\xi^5 + 90\xi^4 + 63\xi^3 - 16\xi^2 + 3(2\xi+1)\xi^2 \ln(\xi+2) - 29\xi - 4\right) \\ & -6\left(8\xi^6 + 12\xi^5 + 8\xi^4 + 10\xi^3 + 4\xi^2 - 3\xi - 1\right)\xi \ln(\xi+1)\big]\,; \end{aligned} \tag{5.80}$$

$$\begin{aligned} B_{k_2 k_2} = \frac{1}{12\xi(\xi+1)\epsilon} \big[& -6\left(4\xi^8 + 6\xi^7 + 6\xi^6 + 8\xi^5 + 4\xi^4 + 2\xi^3 + 6\xi^2 + 5\xi + 1\right) \ln(\xi+1) \\ & - 2\left(18\xi^6 + 45\xi^5 + 33\xi^4 + 22\xi^3 + 59\xi^2 - 3\left(2\xi^2 + 4\xi + 1\right)\xi \ln(\xi+2) + 64\xi + 21\right) \\ & +3\left(10\xi^8 + 15\xi^7 + 21\xi^6 + 29\xi^5 + 19\xi^4 + 20\xi^3 + 30\xi^2 + 20\xi + 4\right) \ln(\xi)\big]\,; \end{aligned} \tag{5.81}$$

$$\begin{aligned} B_{k_1 k_2} = \frac{(\xi-1)}{8\epsilon^2} - \frac{1}{24\xi(\xi+1)\epsilon} \big[& -144\xi^6 - 216\xi^5 + 30\xi^4 + 70\xi^3 - 62\xi^2 \\ & - 6\left(16\xi^7 + 8\xi^6 + 4\xi^5 + 8\xi^4 - 19\xi^3 - 10\xi^2 + 6\xi + 1\right)\xi \ln(\xi+1) \\ & + 3\left(40\xi^7 + 20\xi^6 + 34\xi^5 + 33\xi^4 - 42\xi^3 - 3\xi^2 + 6\xi - 12\right)\xi \ln(\xi) + 26\xi + 20 \\ & -6\left(2\xi^2 - 3\xi + 2\right)\xi^2 \ln(\xi+2)\big]\,; \end{aligned} \tag{5.82}$$

$$\begin{aligned} B_g = \frac{(\xi-1)}{24(\xi+1)^2\epsilon} \big[& 3\left(10\xi^6 + 15\xi^5 + 21\xi^4 + 21\xi^3 - 5\xi^2 - 8\xi + 2\right) \ln(\xi) \\ & - 2\left(18\xi^4 + 5\xi^3 - 32\xi^2 - 16\xi + 3 + 3\left(2\xi^2 + 4\xi + 1\right)\xi \ln(\xi+2)\right) \\ & -6\left(4\xi^6 + 6\xi^5 + 6\xi^4 + 6\xi^3 - 2\xi^2 - 5\xi - 1\right) \ln(\xi+1)\big]\,, \end{aligned} \tag{5.83}$$

where we set the renormalization scale $\mu^2 = Q^2$ and we used Eq.(5.15) to simplify the results. As for the previous diagram, it is important to note that there is no dependence on the ML regulator in the coefficient. All the singularities, ultraviolet and infrared, are regulated by the dimensional regularisation parameter ϵ.

We also notice that there is only one coefficient of the tensorial structure, the one in Eq.(5.82), that has a double pole and its expression is quite simple. It is interesting to note that the cancellation of the double poles in the other structures is non-trivial and happens only once we sum the contributions of all the diagrams of each tensorial structure.

5.4.3 Diagram C

We repeat the calculation for the third diagram shown in Fig.(5.11), we call this diagram C. Using the Feynman rules, we can write this contribution as

$$\begin{aligned} C^{\mu\rho}(k_1,k_2,n) = \int \frac{d^dk}{(2\,\pi)^d} \frac{N^{\mu\nu\alpha\beta\gamma\sigma}(k_1,k_2,n)\,T_{\rho\delta}(k_1,k_2) d_{\nu\delta}(k_2,n)}{k^2(k-k_1)^2} \\ \times \left[-g_{\gamma\alpha} + \frac{k_\alpha n_\gamma + k_\gamma n_\alpha}{k\cdot n}\right]\left[-g_{\sigma\beta} + \frac{(k_1-k)_\beta n_\sigma + (k_1-k)_\sigma n_\beta}{(k_1-k)\cdot n}\right], \end{aligned} \tag{5.84}$$

where the tree level vertex, $T_{\rho\delta}(k_1,k_2)$, and the sum over polarizations of the on-shell gluon, $d_{\nu\delta}(k_2,n)$, are the same as the ones used for the other diagrams, while, in this case, the numerator is

$$\begin{aligned} N^{\mu\nu\alpha\beta\gamma\sigma}(k_1,k_2,n) = \mathrm{i}g^2c^2\,C_A\delta_{a,b}\,&[g^{\mu\rho}(k+k_1)^\sigma + g^{\mu\sigma}(k-2k_1)^\rho + g^{\rho\sigma}(k_1-2k)^\mu] \\ &\left[g^{\gamma\delta}(k_2-2k)^\nu + g^{\gamma\nu}(k-2k_2)^\delta + g^{\delta\nu}(k+k_2)^\gamma\right] \\ &\left[(k_1-k)^\beta(k_2-k)^\alpha - g^{\alpha\beta}(k_1-k)\cdot(k_2-k)\right]. \end{aligned} \tag{5.85}$$

As we did in the previous sections, first of all, we use ML to regularise the light-cone gauge singularities, then we contract the indices in Eq.(5.61) and we compute the resulting loop integrals with the techniques presented in Appendix A. The result can be written as

$$\begin{aligned} C^{\mu\rho} = -\frac{\alpha_s}{8\,\pi}c^2C_A\delta_{a,b}\Big[&C_{k_1\,k_1}k_1^\mu k_1^\rho + C_{k_2\,k_2}k_2^\mu k_2^\rho + \frac{1}{2}C_{k_1\,k_2}(k_1^\mu k_\rho + k_1^\rho k_2^\mu) \\ &+C_g g^{\mu\rho} + \ldots\Big], \end{aligned} \tag{5.86}$$

where, as in the previous cases, we dropped the tensorial structures proportional to the gauge vector n. The coefficients of the tensorial structures are

$$C_{k_1\,k_1} = \frac{Q^2}{\epsilon}\frac{\xi^2-6\xi+5}{3(\xi+1)} - \frac{Q^2(\xi-1)(-5\xi+3(\xi-5)\ln(\xi)+31)}{9(\xi+1)}; \tag{5.87}$$

$$C_{k_2\,k_2} = \frac{Q^2}{\epsilon}\frac{22\xi+7}{3} + \frac{Q^2(134\xi-3(22\xi+7)\ln(\xi)+35)}{9}; \tag{5.88}$$

$$\begin{aligned} C_{k_1\,k_2} =& -\frac{Q^2}{\epsilon}\frac{(23\xi^3+2\xi^2+\xi-5)}{3\xi(\xi+1)} \\ &+\frac{Q^2\left(-139\xi^3-4\xi^2+3\left(23\xi^3+2\xi^2+\xi-5\right)\ln(\xi)-5\xi+31\right)}{9\xi(\xi+1)}; \end{aligned} \tag{5.89}$$

$$C_g = -\frac{Q^4}{\epsilon}\frac{\xi\left(22\xi^2-15\xi-7\right)}{6(\xi+1)} + \frac{Q^4(\xi-1)\xi(-134\xi+3(22\xi+7)\ln(\xi)-35)}{18(\xi+1)}. \tag{5.90}$$

In these coefficients, we set $\mu^2 = Q^2$ and we used Eq.(5.15) to simplify the results. We see that here we do not have a dependence on the regulator of the ML prescription.

We can note that, even though some of the integrals that contribute to this diagram have a double IR pole (see Appendix A), this final result has only a single pole. This means that the double poles cancel diagram by diagram.

5.4.4 Diagram D

The last diagram is the one shown in Fig.(5.12), we name it diagram D. We could have also the contribution with the bubble on the outgoing gluon, k_2 but, since this gluon is on-shell this contribution is vanishing. Using the Feynman rules, we write the contribution from diagram D as

$$\begin{aligned} D^{\mu\rho}(k_1,k_2,n) = \int \frac{d^dk}{(2\,\pi)^d} \frac{N^{\mu\nu\alpha\beta\gamma\sigma\delta\eta}(k_1,k_2,n)\,T_{\rho\theta}(k_1,k_2) d_{\nu\theta}(k_2,n)}{k^2\,k_1^2(k-k_1)^2} \\ \times \left[-g_{\sigma\beta} + \frac{k_\sigma n_\beta + k_\beta n_\sigma}{k\cdot n}\right] \left[-g_{\eta\alpha} + \frac{(k_1-k)_\eta n_\alpha + (k_1-k)_\alpha n_\eta}{(k_1-k)\cdot n}\right], \\ \times \left[-g_{\gamma\delta} + \frac{k_{1\,\gamma} n_\delta + k_{1,\delta} n_\gamma}{k_1\cdot n}\right] \end{aligned} \tag{5.91}$$

where the tree level vertex, $T_{\rho\theta}(k_1,k_2)$, and the sum over polarizations of the on-shell gluon, $d_{\nu\theta}(k_2,n)$, are the same as the ones used for the other diagrams, while, in this case, the numerator is

$$\begin{aligned} N^{\mu\nu\alpha\beta\gamma\sigma\delta\eta}(k_1,k_2,n) = \mathrm{i}g^2c^2\,C_A\delta_{a,b}\,&[g^{\sigma\eta}(k_1-2k)^\mu + g^{\mu\sigma}(k+k_1)^\eta + g^{\mu\eta}(k-2k_1)^\sigma] \\ &\left[g^{\beta\gamma}(k+k_1)^\alpha - g^{\alpha\gamma}(2k_1-k)^\beta - g^{\alpha\beta}(2k-k_1)^\sigma\right] \\ &\left[k_1^\nu k_2^\delta - g^{\nu\delta}k_1\cdot k_2\right]. \end{aligned} \tag{5.92}$$

As we did in the previous sections, first of all, we use ML to regularise the light-cone gauge singularities, then we contract the indices in Eq.(5.61) and we compute the resulting loop integrals with the techniques presented in Appendix A. The result can be written as

$$\begin{aligned} D^{\mu\rho} = -\frac{\alpha_s}{8\,\pi}c^2C_A\delta_{a,b}\Big[&D_{1\,k_1\,k_1}k_1^\mu k_1^\rho + D_{1\,k_2\,k_2}k_2^\mu k_2^\rho + \frac{1}{2}D_{1\,k_1\,k_2}(k_1^\mu k_\rho + k_1^\rho k_2^\mu) \\ &+D_{1\,g}g^{\mu\rho} + \ldots\Big], \end{aligned} \tag{5.93}$$

where, as in the previous cases, we dropped the tensorial structures proportional to the gauge vector n. The explicit form for the coefficients of the tensorial structures are

$$D_{k_1\,k_1} = \frac{Q^2}{\epsilon}\frac{4Q^2(\xi-1)\xi}{\xi+1} - \frac{4(\xi-1)\xi(\ln(\xi)-2)}{\xi+1}; \tag{5.94}$$

$$D_{k_2\,k_2} = \frac{Q^2}{\epsilon}\frac{22\xi}{3} + \frac{2\xi Q^2(67-33\ln(\xi))}{9}; \tag{5.95}$$

$$D_{k_1\,k_2} = \frac{Q^2}{\epsilon}\frac{2\,(5-17\xi^2)}{3(\xi+1)} + \frac{2Q^2\,(-103\xi^2+3\,(17\xi^2-5)\ln(\xi)+31)}{9(\xi+1)}; \tag{5.96}$$

$$D_g = -\frac{Q^4}{\epsilon}\frac{11(\xi-1)^2}{6} + \frac{(33\ln(\xi)-67)(\xi-1)^2Q^4}{18}; \tag{5.97}$$

In these coefficients, we set $\mu^2 = Q^2$ and we used Eq.(5.15) to simplify the results. We note that even though some of the integrals that contribute to this diagram have a double IR pole (see Appendix A), this final result has only a single pole. This means that the double poles cancel diagram by diagram.

5.4.5 Ultraviolet singularities cancellation

The results presented in the previous section contain both infrared and ultraviolet singularities, both regularised by the principal value prescription parameter ϵ.

To cancel the UV divergence of the one-loop contribution to the Higgs-induced DIS, we have to sum the contribution of the counterterms to this process. There are two counterterms that must be added to this process. The first is the counterterm for the gluon self-energy on the incoming leg. To compute the contribution of this counterterm to the process we must calculate

$$CT^{\mu\rho}_{\mathcal{M}\,\mathrm{self}}(k_1,n) = CT^{\mu\alpha}_{\mathrm{self}}(k_1,n)\Pi^{\beta}_{\alpha}(k_1,n)T^{\nu}_{\beta}(k_1,k_2)d^{\sigma}_{\nu}(k_2,n)T^{\rho}_{\sigma}(k_1,k_2), \tag{5.98}$$

where $CT^{\mu\alpha}_{\mathrm{self}}(k_1,n)$ is the self-energy counterterm given in Eq.(5.47), $\Pi^{\beta}_{\alpha}(k_1,n)$ is the propagator of the off-shell gluon of momentum k_1 in light-cone gauge, $d^{\sigma}_{\nu}(k_2,n)$ is the sum over the polarisations of the on-shell gluon of momentum k_2, and $T^{\rho}_{\sigma}(k_1,k_2)$ is the Higgs-gluon effective vertex defined in Eq.(5.4).

The UV divergences of the other three diagrams, which are shown in Fig.(5.9), Fig.(5.10), and in Fig.(5.11), are all canceled by the counterterm for the effective vertex we computed in Eq.(5.57) in the previous section. The contribution from this counterterm to the amplitude is

$$CT^{\mu\rho}_{\mathcal{M}\,\mathrm{eff}}(k_1,n) = CT^{\mu\nu}_{\mathrm{eff}}(k_1,k_2,n)d^{\alpha}_{\nu}(k_2,n)T^{\rho}_{\alpha}(k_1,k_2), \tag{5.99}$$

where $CT^{\mu\nu}_{\mathrm{eff}}(k_1,k_2,n)$ is the counterterm for the effective vertex given in Eq.(5.57), $d^{\alpha}_{\nu}(k_2,n)$ is the sum over polarisation of the on-shell gluon k_2 and $T^{\rho}_{\alpha}(k_1,k_2)$ is the complex conjugate of the tree level vertex.

In the following section, we will sum the results for each diagram and the counterterms and we will give a result for the virtual contribution to the Higgs-induced DIS.

5.4.6 One-loop virtual contribution to Higgs induced DIS

Here we present the final result for the virtual NLO contribution to the off-shell amplitude for the Higgs-induced DIS. Since we included also the counterterms computed in the previous section, this result is free from UV singularities. The remaining IR singularities must be canceled once we add the NLO real emission.

We can write this result in terms of the tensorial structures we used in the previous sections as

$$\begin{aligned}\mathcal{M}^{\mu\nu}(k_1,k_2,n) = \frac{\alpha_s}{4\,\pi}c^2 C_A Q^2 \delta_{a,b}\Big[&\mathcal{M}_g Q^2 g^{\mu\nu} + \mathcal{M}_{k_1\,k_1}k_1^{\mu}k_1^{\nu} + \mathcal{M}_{k_2\,k_2}k_2^{\mu}k_2^{\nu} \\ &+\frac{1}{2}\mathcal{M}_{k_1\,k_2}\left(k_1^{\mu}k_2^{\nu}+k_1^{\nu}k_2^{\mu}\right)+\ldots\Big],\end{aligned} \tag{5.100}$$

where, once again, we dropped the tensorial structures depending on the gauge vector n. Since the coefficients are quite complicated, here we report only their divergent part,

the finite part can be found in Appendix E. The divergent part of these coefficients are:

$$\mathcal{M}_g = \frac{(\xi-1)}{4(\xi+1)^2\epsilon}\left[-6\xi^4-9\xi^3-6\xi^2-2\xi^3\ln(\xi+2)-4\xi^2\ln(\xi+2)\right.$$
$$\left.+\left(8\xi^4+8\xi^3+6\xi+6\right)\ln(\xi)-\left(4\xi^4+4\xi^3+3\xi+3\right)\ln(\xi+1)-7\xi-\xi\ln(\xi+2)-4\right] \tag{5.101}$$

$$\mathcal{M}_{k1k1} = \frac{(\xi-1)}{4(\xi+1)^2\epsilon}\left[-12\xi^5-30\xi^4-21\xi^3+2\xi^2-2\xi^3\ln(\xi+2)-\xi^2\ln(\xi+2)+11\xi\right.$$
$$\left.+6+2\left(8\xi^4+12\xi^3+6\xi^2+7\xi+5\right)\xi\ln(\xi)-\left(8\xi^4+12\xi^3+6\xi^2+7\xi+5\right)\xi\ln(\xi+1)\right]; \tag{5.102}$$

$$\mathcal{M}_{k_2k_2} = \frac{1}{2\xi(\xi+1)\epsilon}\left[-6\xi^6-15\xi^5-11\xi^4-4\xi^2+2\xi^3\ln(\xi+2)+4\xi^2\ln(\xi+2)\right.$$
$$-11\xi+\xi\ln(\xi+2)-5+2\left(4\xi^6+6\xi^5+6\xi^4+10\xi^3+10\xi^2+5\xi+1\right)\ln(\xi)$$
$$\left.-\left(4\xi^6+6\xi^5+6\xi^4+10\xi^3+10\xi^2+5\xi+1\right)\ln(\xi+1)\right]; \tag{5.103}$$

$$\mathcal{M}_{k_1k_2} = \frac{(\xi-1)}{8\epsilon^2}-\frac{1}{24\xi(\xi+1)\epsilon}\left[-144\xi^6-216\xi^5+30\xi^4+410\xi^3+66\xi^2\right.$$
$$-6\left(2\xi^2-3\xi+2\right)\xi^2\ln(\xi+2)+3\left(64\xi^5+28\xi^4-2\xi^3+47\xi^2-24\xi-37\right)\xi\ln(\xi)$$
$$\left.-6\left(16\xi^5+6\xi^4-3\xi^3+10\xi^2-6\xi-9\right)\xi\ln(\xi+1)-62\xi+36\right]. \tag{5.104}$$

In these coefficients we set the renormalization scale $\mu^2 = Q^2$ and we used Eq.(5.15) to simplify the results.

The first observation we can make is that only one coefficient, the one in Eq.(5.102), has a double pole. The coefficient of this double pole is simple and must vanish once we add the contribution from the real emission, similarly to what happened in Section 5.2 with the on-shell calculation. It is also interesting to notice that the cancellation of the double pole of the other coefficients happened diagram by diagram in a non-trivial way.

To give a complete result for the off-shell NLO cross section for the Higgs-induced DIS, we have to add the contribution from the real emission. In the following section, we will present the next steps we are intended to take.

5.5 Outlook

In this section, we want to summarise the results presented in this long chapter and present some solutions to the main problems we faced.

The first calculation we presented is the on-shell calculation for the coefficient function of the HDIS in light-cone gauge. This was useful to show how the light-cone gauge modifies the loop-integral in a simplified situation. Moreover, it offered us the opportunity to show an example where the PV prescription actually gives the correct result.

The main progress made in this chapter regards the understanding of the loop calculations in light-cone gauge. We now are able to compute a broad list of differ-

ent non-covariant integrals both using Mandelstam Leibbrandt and Principal Value prescription. The different methods we used are described in detail in Appendix A, together with a list of the integrals we computed.

In this chapter, we presented the calculation of the virtual contribution to the NLO off-shell amplitude for the Higgs-induced DIS. Of course to get the off-shell coefficient function we need to add the contribution from the NLO real emission. In this thesis, we focused on the study of the effects of the choice of the light-cone gauge and the prescription to regulate the gauge-dependent singularities. For the real emission, we do not have the problem of spurious singularities in the calculation of non-covariant loop integrals. In this case, the structure of the calculation is similar to the on-shell calculation but, since the incoming gluon is off-shell, the phase space integration is challenging. Some details on this calculation can be found in [46] where there is also a result for the NLO off-shell real emission computed using Principal Value prescription.

We do not have yet a final result for the NLO off-shell amplitude but, at this stage of the calculation we can, make some observations. A first check of the real and the virtual calculation will be the cancellation of the IR singularities, in particular of the double poles. We expect that the poles of the virtual contribution, see Eq.(5.101) to Eq.(5.104), cancel with the corresponding real divergent part.

The next step of this work will be to combine together the real emission and the virtual correction to get the complete NLO off-shell amplitude for the Higgs-induced DIS.

Once we have the complete NLO off-shell amplitude we will be able to study its properties as we anticipated in Chapter 3. In particular, we will be able to determine the scaling of the coefficient of each tensorial structure and we will verify if the projector introduced by Catani Ciafaloni and Hautmann [18, 22] is still valid to select the dominant contribution beyond LL. With this projector, we will be able to define the off-shell coefficient function and we will be finally able to verify the resummation formula for the coefficient function,

$$C(x,Q^2) = \int dk_\perp^2 \int_x^1 \frac{dz}{z} \mathcal{C}\left(\frac{x}{z}, k_\perp^2, Q^2\right) \mathcal{U}\left(z, k_\perp^2, Q^2\right), \tag{5.105}$$

at NLL.

We think that the calculations presented in this chapter are an important step towards the complete understanding of the off-shell coefficient function in light-cone gauge. They allowed us to face and solve many problems due to the gauge choice, like the regularisation of spurious gauge singularities, the definition of gauge-dependent counterterms, and the calculation of non-covariant loop integrals.

Chapter 6

Conclusions

In this final chapter, we want to recap the main results we presented in this thesis and give some prospects on how we can improve and continue this work.

First of all, in Chapter 2 and Chapter 3 we introduced the main topic of this thesis, the small-x resummation of logarithmic enhancements in the coefficient functions of partonic processes. First, we reviewed the state of the art of this technique of resummation by discussing the factorization properties on which it is based and the general strategy to achieve it. In particular, we focused our attention on the High-energy factorization theorem. By explaining in detail its derivation at leading logarithmic accuracy, we pointed out what is still missing for its application to resum next-to-leading logarithms in perturbative coefficient functions. In particular, by deriving the definition of the off-shell coefficient function, $\mathcal{C}$, and the evolution operator, $\mathcal{U}$, we show how the main ingredient that is missing is an accurate definition of the off-shell coefficient function computed at NLO. This was the starting point of this thesis.

We have decided to focus on the calculation of the NLO off-shell coefficient function for a specific process. This is important because it allows us to discuss and resolve several details, both conceptual and technical, of the calculation. First of all, it is important to compute this quantity in a physical gauge, like the light cone gauge. The first thing that we want to verify is that this quantity is free from logarithmic enhancements when computed in a physical gauge, as in the case of the LL resummation. This is not obvious, because at NLO we can have different gluon emissions that modify the *ladder* configuration we introduced in Chapter 3. Moreover, the NLO off-shell coefficient function can have a different scaling in the coefficients of its tensorial structures and, for this reason, it is important to verify which are the dominant ones in the high-energy region. In this way, we can see if the projector introduced by Catani, Ciafaloni, and Hautmann [18] is still able to select the dominant contributions or if it has to be modified.

In Chapter 5, we presented our calculation for the NLO off-shell coefficient function for the Higgs-induced Deep-inelastic scattering in light-cone gauge. We presented the progress we made in the calculation of the virtual contribution. In particular, we learned how to deal with non-covariant loop integrals and spurious gauge singularities. We also reported in Appendix A a general method to compute these integrals. As we discussed in Appendix A, the calculation of loop integrals with three covariant

denominators and a non-covariant part was particularly complicated, especially in the case of the Mandelstam-Leibbrandt prescription. In this case, we were not able to give a method independent of the form of the non-covariant part, so each integral must be computed individually. We were, however, able to compute both the integrals of this type that contribute to the virtual correction. In the future, we can study these integrals more carefully, and possibly give a general formula to compute them, as we did for all integrals regulated with the Principal Value prescription and for the simpler ones regulated with Mandelstam-Leibbrandt.

In the end, however, we were able to give a final result for the NLO virtual correction for the amplitude of this process. The next step will be to combine the virtual result provided in this thesis with the one of the real emission, to get the complete NLO off-shell amplitude for the Higgs-induced DIS. Having the complete NLO off-shell amplitude, we will be able to study its properties as we discussed in Chapter 3 and we will be able to properly define the NLO off-shell coefficient function for this process.

This thesis also allowed us to study the light-cone gauge in detail. This gauge is not much used in the literature and by using it for a NLO calculation we could point out some of its characteristics. First of all, as we discussed in Chapter 4, we faced the problem of spurious gauge singularities and how to regularise them. In this thesis, we have presented a detailed study of the two prescriptions that are most used in literature, the Mandelstam-Leibbrandt and the Principal Value prescription. In Chapter 4, we discussed their definition and their properties, and we explained why the correct one to use is the ML prescription, although is quite more complicated to apply in loop calculations than the PV prescription. We also discussed the problem of the renormalization in this gauge and the definition of the gauge-dependent counterterms.

In the final pages of this thesis, we placed some appendices. We already discussed the content of Appendix A which is the most interesting. In the others, we reported some results that were too long to be placed in the main corp of the thesis.

In conclusion, even if at this stage we are not able to give a complete result for the resummed coefficient function for a specific process, we think that this thesis is an important step in this direction. We especially want to point out all the progress we made in the understanding of a gauge, the light-cone gauge, that is not commonly used to perform loop calculations. The breaking of the Lorentz-invariance and the presence of spurious gauge singularities are a serious challenge that we overcame in Chapter 4 and in Appendix A where we gave a general method to compute a large class of non-covariant loop integral both using PV and ML prescriptions. Some work is still to be done, but, once we carefully combine the real and the virtual contributions, we will be able to give a final result for the NLO off-shell coefficient function for the HDIS in light-cone gauge. As we discussed in Chapter 3, this is the main ingredient that is still missing to achieve the resummation of the coefficient function of this process. This thesis was an important step toward the resummation of high-energy next-to-leading logarithms in QCD.

Appendix A

Integrals in light-cone gauge

In this chapter, we present a method to compute the non-covariant loop integrals that one has to face when competing NLO amplitudes in light-cone gauge.

These techniques have been used to compute the result we presented in Chapter 5 for the NLO on-shell and off-shell coefficient function for the Higgs-induced DIS calculated in light-cone gauge.

As we already discussed in Chapter 4, we will present techniques to compute the integral with both the Principal Value and the Mandelstam-Leibbrandt prescriptions. We refer to Chapter 4 for a discussion on why the ML prescription should be the correct one to use in a general light-cone gauge calculation.

The structure of the chapter is the following: we will start by studying the non-covariant integrals with ML prescription in Section A.2. Then, in Section A.1 we will also derive a different method to address loop integrals regularised with PV prescription. We present both methods, even if the ML is the formally correct one, because in some cases the PV prescription gives the correct result ([81]) and it is simpler to use.

A.1 Non-covariant one loop integrals with Mandelstam Leibbrandt prescription

In this section we address integrals regularised with the Mandelstam Leibbrandt prescription. We aim to remain as independent as possible of the particular form of the non-covariant part.

As we already discussed in Chapter 4, differently from the case where we use PV prescription, here we can make a Wick rotation and then take the limit for the regulator that goes to zero obtaining expressions that do not depend on δ anymore.

We start by considering

$$I_{\mathrm{ML}} = \int \frac{d^d k}{(2\pi)^d} \frac{1}{(k^2 - 2P\cdot k + M^2 + \mathrm{i}\eta)^\alpha} \frac{k\cdot\bar{n}}{(k\cdot n)(k\cdot\bar{n}) + \mathrm{i}\delta}, \tag{A.1}$$

where the $\mathrm{i}\eta$ term in the covariant denominator is the usual Feynman prescription for the propagator of the gluons. As we discussed in Chapter 4, is crucial the fact that, using the ML, this term has the same sign as the regulator of the spurious gauge singularities. This allows us to perform the Wick rotation as in the covariant case.

As you can see, a covariant integral with any number of covariant denominators can be reduced to this form using Feynman parametrization. Moreover, if we have one non-covariant denominator it can always be written in this form by a proper shift of the integration momentum, k. If we have more than one non-covariant denominator, instead, we can always separate the integrand into two integrands with one non-covariant denominator using the identity:

$$\begin{aligned}&\frac{k\cdot\bar{n}}{(k\cdot n)\,(k\cdot\bar{n})+i\delta}\frac{(k-p)\cdot\bar{n}}{((k-p)\cdot n)\,((k-p)\cdot\bar{n})+i\delta}\\&=\frac{1}{p\cdot n}\left[\frac{k\cdot\bar{n}}{(k\cdot n)\,(k\cdot\bar{n})+i\delta}+\frac{(k-p)\cdot\bar{n}}{((k-p)\cdot n)\,((k-p)\cdot\bar{n})+i\delta}\right].\end{aligned}\tag{A.2}$$

The form of Eq.(A.1) is, then, the most general form that a one-loop integral regularized with ML prescription can take.

To compute this integral, the first step is to choose a direction for the gauge vector and to specify all the scalar products. This helps us to identify the singularities in the complex plane k_0. At the end, we will combine back the contributions we find to give the result as a function of covariant structures. We then choose, as already specified in Chapter 4,

$$\begin{aligned}n^\mu&=(n_0,\,\overrightarrow{0},n_0)\\\bar{n}^\mu&=(n_0,\,\overrightarrow{0},-n_0)\end{aligned}\tag{A.3}$$

to simplify the calculations. We also used the fact that in the light-cone gauge $n^2=0$. The scalar products in Eq.(A.1) become

$$\begin{aligned}k\cdot n&=n_0(k_0-k_3)\\k\cdot\bar{n}&=n_0(k_0+k_3)\\(k\cdot n)(k\cdot\bar{n})&=n_0^2(k_0^2-k_3^2)\end{aligned}\tag{A.4}$$

The integral in Eq.(A.1) becomes

$$I_{ML}=\frac{1}{n_0}\int\frac{d^dk}{(2\,\pi)^d}\frac{1}{(k^2-2P\cdot k+M^2)^\alpha}\frac{k_0+k_3}{k_0^2-k_3^2+\mathrm{i}\delta},\tag{A.5}$$

where we used the fact that the parameter δ is small. At this point, we use the Feynman parametrization to write this integral with only one denominator. We get

$$I_{\mathrm{ML}}=\frac{\Gamma(1+\alpha)}{\alpha}\frac{1}{n_0}\int_0^1 dx\,x^{\alpha-1}\int\frac{d^dk}{(2\,\pi)^d}\frac{k_0+k_3}{\left[(k_0-xP_0)^2-\mathcal{A}\right]^{\alpha+1}},\tag{A.6}$$

where

$$\mathcal{A}=(k_3-xP_3)^2+x\left(\mathbf{k}_\perp-\mathbf{P}_\perp\right)^2+x^2\left(P_0^2-P_3^2\right)-x\mathbf{P}_\perp^2-xM^2-\mathrm{i}\delta,\tag{A.7}$$

and to get this result we completed the square for every integration variable. We now make a shift in the integration k_0, namely

$$k_0'=k_0-x\,P_0.\tag{A.8}$$

We get

$$I_{\mathrm{ML}} = \frac{\Gamma(1+\alpha)}{\alpha}\frac{1}{n_0}\int_0^1 dx\, x^{\alpha-1}\int\frac{d^{d-1}k}{(2\,\pi)^d}\int_{-\infty}^{+\infty}dk_0\frac{xP_0+k_3}{\left[k_0^2-\mathcal{A}\right]^{\alpha+1}}, \tag{A.9}$$

where we dropped odd powers of the integration variable in the numerator. At this point, we perform the Wick rotation as we explained in Chapter 4 and we get

$$I_{\mathrm{ML}} = \frac{\Gamma(1+\alpha)}{\Gamma(\alpha)}\frac{\mathrm{i}(-1)^{\alpha+1}}{n_0}\int_0^1 dx\, x^{\alpha-1}\int\frac{d^{d-1}k}{(2\,\pi)^d}\int_{-\infty}^{+\infty}dk_E\frac{xP_0+k_3}{\left[k_E^2+\mathcal{A}\right]^{\alpha+1}}. \tag{A.10}$$

This integral can now be computed by calculating the integrals in each variable:

$$\begin{aligned} I_{\mathrm{ML}} =& \frac{\Gamma(1+\alpha)}{\Gamma(\alpha)}\frac{\mathrm{i}(-1)^{\alpha+1}}{n_0}\int_0^1 dx\, x^{\alpha-1} \\ & \int_{-\infty}^{+\infty}dk_E\int_{-\infty}^{+\infty}dk_3\int\frac{d^{d-2}\mathbf{k}_\perp}{(2\,\pi)^d}\frac{xP_0+k_3}{\left[x\left(\mathbf{k}_\perp-\mathbf{P}_\perp\right)^2+\mathcal{B}\right]^{\alpha+1}}, \end{aligned} \tag{A.11}$$

where

$$\mathcal{B} = \left(k_3-xP_3\right)^2+k_E^2+x^2\left(P_0^2-P_3^2\right)-x\mathbf{P}_\perp^2-xM^2-\mathrm{i}\delta. \tag{A.12}$$

Making the shift

$$\mathbf{k}'_\perp = \mathbf{k}_\perp-\mathbf{P}_\perp, \tag{A.13}$$

we can reduce this integral to

$$\begin{aligned} I_{\mathrm{ML}} =& \frac{\mathrm{i}(-1)^{\alpha+1}}{(4\pi)^{\frac{d}{2}}}\frac{\Gamma(1+\alpha)}{\Gamma(\alpha)\Gamma\left(\frac{d}{2}-1\right)}\frac{1}{\pi n_0}\int_0^1 dx\, x^{\alpha-1} \\ & \int_{-\infty}^{+\infty}dk_E\int_{-\infty}^{+\infty}dk_3\int_0^{+\infty}d\mathbf{k}_\perp^2\frac{\left(\mathbf{k}_\perp^2\right)^{\frac{d-4}{2}}\left(xP_0+k_3\right)}{\left[x\,\mathbf{k}_\perp^2+\mathcal{B}\right]^{\alpha+1}}, \end{aligned} \tag{A.14}$$

where we computed the $d\Omega_{d-2}$ integral since the angular dependence was trivial. To compute the three integrals in the second row of Eq.(A.14), we can exploit the following identity:

$$\int_0^\infty dz\frac{z^{\mu-1}}{(p+q\,z^\nu)^\rho} = \frac{1}{\nu p^\rho}\left(\frac{p}{q}\right)^{\frac{\mu}{\nu}}\frac{\Gamma\left(\frac{\mu}{\nu}\right)\Gamma\left(\rho-\frac{\mu}{\nu}\right)}{\Gamma(\rho)}. \tag{A.15}$$

Starting with the $\mathbf{k}_\perp$-integral,

$$I_{\mathbf{k}_\perp} = \int_0^{+\infty}d\mathbf{k}_\perp^2\frac{\left(\mathbf{k}_\perp^2\right)^{\frac{d-4}{2}}\left(xP_0+k_3\right)}{\left[x\,\mathbf{k}_\perp^2+\mathcal{B}\right]^{\alpha+1}}, \tag{A.16}$$

applying this formula we get

$$I_{\mathbf{k}_\perp} = \frac{xP_0+k_3}{x^{\frac{d}{2}-1}}\frac{\Gamma\left(\frac{d}{2}-1\right)\Gamma\left(\alpha+2-\frac{d}{2}\right)}{\Gamma(\alpha+1)}\frac{1}{\left[\left(k_3-xP_3\right)^2+\mathcal{C}\right]^{\alpha+2-\frac{d}{2}}}, \tag{A.17}$$

where

$$\mathcal{C} = k_E^2+x^2\left(P_0^2-P_3^2\right)-x\mathbf{P}_\perp^2-xM^2-\mathrm{i}\delta. \tag{A.18}$$

The newt integral to compute is the one in the integration variable k_3,

$$I_{k_3} = \int_{-\infty}^{+\infty} dk_3 \frac{xP_0 + k_3}{x^{\frac{d}{2}-1}} \frac{1}{\left[(k_3 - xP_3)^2 + \mathcal{C}\right]^{\alpha+2-\frac{d}{2}}}. \tag{A.19}$$

First of all, we shift the integration variable to get

$$I_{k_3} = \int_{-\infty}^{+\infty} dk_3 \frac{P_0 + P_3}{x^{\frac{d}{2}-2}} \frac{1}{\left[k_3^2 + \mathcal{C}\right]^{\alpha+2-\frac{d}{2}}} = 2\int_{0}^{+\infty} dk_3 \frac{P_0 + P_3}{x^{\frac{d}{2}-2}} \frac{1}{\left[k_3^2 + \mathcal{C}\right]^{\alpha+2-\frac{d}{2}}}, \tag{A.20}$$

where we set to zero terms with an odd power of the integration variable in the numerator and we changed the extremes of integration exploiting the symmetry of the integrand. We can now apply Eq.(A.15) to get

$$I_{k_3} = \frac{P_0 + P_3}{x^{\frac{d}{2}-2}} \frac{\Gamma\left(\frac{1}{2}\right)\Gamma\left(\alpha - \frac{d-3}{2}\right)}{\Gamma\left(\alpha + 2 - \frac{d}{2}\right)} \frac{1}{\left(k_E^2 + \mathcal{D}\right)^{\alpha-\frac{d-3}{2}}}, \tag{A.21}$$

where

$$\mathcal{D} = x^2\left(P_0^2 - P_3^2\right) - x\mathbf{P}_\perp^2 - xM^2 - \mathrm{i}\delta. \tag{A.22}$$

The last integral we have to compute is

$$I_{k_E} = \int_{-\infty}^{+\infty} dk_E \frac{1}{\left(k_E^2 + \mathcal{D}\right)^{\alpha-\frac{d-3}{2}}} = 2\int_{0}^{+\infty} dk_E \frac{1}{\left(k_E^2 + \mathcal{D}\right)^{\alpha-\frac{d-3}{2}}}, \tag{A.23}$$

where again we exploited the symmetry of the integrand to compute the integral between 0 and ∞. In this way, we can apply Eq.(A.15) to get

$$I_{k_E} = \frac{\Gamma\left(\frac{1}{2}\right)\Gamma\left(\alpha + 1 - \frac{d}{2}\right)}{\Gamma\left(\alpha - \frac{d-3}{2}\right)} \frac{1}{\left[x^2\left(P_0^2 - P_3^2\right) - x\mathbf{P}_\perp^2 - xM^2 - \mathrm{i}\delta\right]^{\alpha+1-\frac{d}{2}}}. \tag{A.24}$$

Now we can put together Eq.(A.17), Eq.(A.21) and Eq.(A.24) with Eq.(A.14) to get

$$I_{\mathrm{ML}} = \frac{\mathrm{i}(-1)^{\alpha+1}}{(4\pi)^{\frac{d}{2}}} \frac{\Gamma\left(\alpha + 1 - \frac{d}{2}\right)}{\Gamma(\alpha)} \frac{P_0 + P_3}{n_0} \int_0^1 dx \, \frac{x^{\alpha+1-\frac{d}{2}}}{\left[x^2\left(P_0^2 - P_3^2\right) - x\mathbf{P}_\perp^2 - xM^2 -\right]^{\alpha+1-\frac{d}{2}}}. \tag{A.25}$$

Here, we took the limit for the regularisation parameter δ that goes to zero so the final result does not depend on δ anymore. We could do this limit without problems because we performed the Wick rotation correctly. This same limit cannot be taken when we work with the PV prescription and this is the reason why the results in Section A.2 depend on δ.

To compute the last integral, we write the integrand as a function of covariant structures. To do so, we can exploit the following relations

$$\begin{aligned}
&P \cdot n = n_0\left(P_0 - P_3\right) \\
&P \cdot \bar{n} = n_0\left(P_0 + P_3\right) \\
&(P \cdot n)(P \cdot \bar{n}) = n_0^2\left(P_0^2 - P_3^2\right) \\
&P^2 = P_0^2 - \mathbf{P}_\perp^2 - P_3^2 \\
&n \cdot \bar{n} = 2n_0^2
\end{aligned} \tag{A.26}$$

We get

$$I_{\rm ML} = \frac{\mathrm{i}(-1)^{\alpha+1}}{(4\pi)^{\frac{d}{2}}} \frac{\Gamma\left(\alpha+1-\frac{d}{2}\right)}{\Gamma(\alpha)} \frac{2P\cdot\bar{n}}{n\cdot\bar{n}} \frac{1}{(P^2-M^2)^{\alpha+1-\frac{d}{2}}} \int_0^1 dx\ [1-(1-x)a]^{\frac{d}{2}-1-\alpha}\,, \tag{A.27}$$

where

$$a = \frac{2P\cdot nP\cdot\bar{n}}{n\cdot\bar{n}\,(P^2-M^2)}. \tag{A.28}$$

Computing the last integral we finally get

$$\begin{aligned} I_{\rm ML} &= \int \frac{d^dk}{(2\pi)^d} \frac{1}{(k^2-2P\cdot k+M^2)^\alpha} \frac{k\cdot\bar{n}}{(k\cdot n)(k\cdot\bar{n})+\mathrm{i}\delta} \\ &= \frac{\mathrm{i}(-1)^\alpha}{(4\pi)^{\frac{d}{2}}} \frac{\Gamma\left(\alpha-\frac{d}{2}\right)}{\Gamma(\alpha)} \frac{1}{(P^2-M^2)^{\alpha-\frac{d}{2}}} \frac{1}{P\cdot n} \left[1-\left(1-\frac{2P\cdot n\,P\cdot\bar{n}}{n\cdot\bar{n}(P^2-M^2)}\right)^{\frac{d}{2}-\alpha}\right]. \end{aligned} \tag{A.29}$$

This result is independent of the regulator δ for the IR singularities due to the gauge choice. This is a significant difference between PV and ML prescriptions that is due to the fact that with ML prescription we can perform correctly the Wick rotation. This is why the ML prescription is formally the correct one to use, even if PV prescription still works in some cases.

In the following sections, we apply Eq.(A.29) to compute useful integrals that appear frequently in loop integrals in the axial gauge.

A.1.1 One covariant denominator: ML prescription

We start by pointing out the first difference between integrals computed with ML prescription and computed with PV prescription. In fact, in PV prescription, integrals with one covariant denominator are always vanishing while this is not the case in ML prescription. A general integral with one covariant denominator can be written as

$$I_1 = \int \frac{d^dk}{(2\,\pi)^d} \frac{1}{(k-l)^2} \frac{1}{k\cdot n}. \tag{A.30}$$

If the non-covariant part is a more complicated function we can always make some shift in the integration variable k and write the integral in the form of Eq.(A.30). This integral can be computed using Eq.(A.29) with

$$\begin{aligned} &\alpha = 1 \\ &P^\mu = l^\mu \\ &M^2 = l^2. \end{aligned} \tag{A.31}$$

We get

$$I_1 = \frac{-\mathrm{i}}{(4\pi)^{\frac{d}{2}}} \frac{\Gamma\left(1-\frac{d}{2}\right)}{(P^2-M^2)^{1-\frac{d}{2}}} \frac{1}{l\cdot n} \left[1-\left(1-\frac{2l\cdot n\,l\cdot\bar{n}}{n\cdot\bar{n}(P^2-M^2)}\right)^{\frac{d}{2}-1}\right], \tag{A.32}$$

that can be split into two contributions. The first, where we take the 1 in the square bracket, is vanishing since $P^2 = M^2$. The second one, instead, gives

$$I_1 = \frac{\mathrm{i}}{(4\pi)^{\frac{d}{2}}} \frac{\Gamma\left(1-\frac{d}{2}\right)}{(n\cdot\bar{n})^{\frac{d}{2}-1}} \frac{(-2\,l\cdot\bar{n}\,l\cdot n)^{\frac{d}{2}-1}}{l\cdot n}. \tag{A.33}$$

This result, given $d = 4 - 2\epsilon$, can be expanded to the required power of ϵ.

A.1.2 Two covariant denominators: ML prescription

In this section, we move on to the case of two covariant denominators. This case is more complicated, than the previous one. We consider

$$I_2 = \int \frac{d^d k}{(2\,\pi)^d} \frac{1}{k^2 (k-l)^2} \frac{1}{k\cdot n}, \tag{A.34}$$

that, as long as we do not specify the momentum l^μ is a good generalization of all the possible non-covariant integrals with two covariant denominators. For the moment, we assume the simplest non-covariant function.

If the integral is in the form of Eq.(A.34), we can use Feynman parametrisation to get

$$I_2 = \int_0^1 dt \int \frac{d^d k}{(2\,\pi)^d} \frac{1}{\left[k^2 - 2t\,l\cdot k + t\,l^2\right]^2} \frac{1}{k\cdot n}. \tag{A.35}$$

Now we can use ML prescription ad apply Eq.(A.29) with

$$\begin{aligned} &\alpha = 2 \\ &P^\mu = t\,l^\mu \\ &M^2 = t\,l^2, \end{aligned} \tag{A.36}$$

we get

$$I_2 = \frac{\mathrm{i}}{(4\,\pi)^{\frac{d}{2}}} \frac{\Gamma\left(2-\frac{d}{2}\right)}{(-l^2)^{2-\frac{d}{2}}} \frac{1}{l\cdot n} \int_0^1 dx\, x^{\frac{d}{2}-3} (1-x)^{\frac{d}{2}-2} \left[1 - \left(1 - a\,\frac{x}{1-x}\right)^{\frac{d}{2}-2}\right], \tag{A.37}$$

where

$$a = \frac{l\cdot n\, l\cdot\bar{n}}{n\cdot\bar{n}(-l^2)}. \tag{A.38}$$

This case is more complicated because we have one integral left, the one in Feynman parameter t. To compute this integral, we can use $d = 4 - 2\epsilon$ to get

$$I_2 = \frac{\mathrm{i}}{(4\,\pi)^2} \left(\frac{4\pi}{-l^2}\right)^{\epsilon} \frac{\Gamma(\epsilon)}{l\cdot n} \int_0^1 dx\, x^{-1-\epsilon} (1-x)^{-\epsilon} \left[1 - \left(1 - a\,\frac{x}{1-x}\right)^{-\epsilon}\right]. \tag{A.39}$$

We can compute this integral noticing that can be written as a Hypergeometric function, and then expand up to the $\mathcal{O}(0)$ in ϵ. The result we get is

$$I_2 = \frac{\mathrm{i}}{(4\,\pi)^2} \frac{1}{l\cdot n} \left(\frac{\pi^2}{6} - \mathrm{Li}_2(a+1)\right), \tag{A.40}$$

where a is the parameter defined in Eq.(A.38). Despite the expression in Eq.(A.39) being quite complicated, the result in Eq.(A.40) is quite simple. Moreover, we get a finite result, as we expect from the power-counting. Here is the evident difference between the two prescriptions. The result we got for the same integral using the PV prescription (Eq.(A.107)) was UV divergent.

In the following section, we will compute the last integral that is involved in the one-loop calculation we performed in Chapter 5.

A.1.3 Three covariant denominators: ML prescription

Although up to two covariant denominators computing integrals with ML or PV prescription requires nearly the same effort, things are quite different when we face integrals with three non-covariant denominators. The growing number of integrals and scales complicates the ML calculations and makes it difficult to find a general formula to compute those integrals independently from the non-covariant part.

To show an example of calculations and to keep the computations as simple as possible, we consider a particular integral,

$$\begin{aligned} I_3 &= \int \frac{d^d k}{(2\,\pi)^d} \frac{1}{k^2 (k-k_1)^2 (k-k_2)^2} \frac{1}{k\cdot n} \\ &= \int \frac{d^d k}{(2\,\pi)^d} \frac{1}{k^2 (k-k_1)^2 (k-k_2)^2} \frac{k\cdot \bar{n}}{k\cdot n\, k\cdot \bar{n} + \delta^2}, \end{aligned} \tag{A.41}$$

where we applied the ML prescription to the non-covariant part. First, we apply Feynman parametrization to the covariant part of Eq.(A.41) and we get

$$\begin{aligned} I_3 =& 2 \int_0^1 d\,t_1 \int_0^{1-t_1} d\,t_2 \\ &\times \int \frac{d^d k}{(2\,\pi)^d} \frac{1}{\left[k^2 - 2(k_1\,t_1 + k_2\,t_2)\cdot k + t_1\,k_1^2 + t_1\,k_2^2\right]^3} \frac{k\cdot \bar{n}}{k\cdot n\, k\cdot \bar{n} + \delta^2}. \end{aligned} \tag{A.42}$$

To compute the integral on the loop momentum k we use Eq.(A.29) with

$$\begin{aligned} P^\mu &= k_1 t_1 + k_2 t_2, \\ M^2 &= t_1\,k_1^2 + t_1\,k_2^2. \end{aligned} \tag{A.43}$$

We get

$$\begin{aligned} I_3 =& \frac{-\mathrm{i}\Gamma\left(3-\frac{d}{2}\right)}{(4\pi)^{\frac{d}{2}}} \\ &\times \int_0^1 d\,t_1 \int_0^{1-t_1} d\,t_2 \frac{1}{\left[2t_1t_2k_1\cdot k_2 - k_1^2 t_1(1-t_1) - k_2^2 t_2(1-t_2)\right]^{3-\frac{d}{2}}} \frac{1}{t_1 k_1\cdot n + t_2 k_2\cdot n} \\ &\times \left[1 - \left(1 - \frac{2\,(t_1k_1\cdot n + t_2k_2\cdot n)\,(t_1k_1\cdot \bar{n} + t_2k_2\cdot \bar{n})}{n\cdot\bar{n}\,(2t_1t_2k_1\cdot k_2 - k_1^2t_1(1-t_1) - k_2^2t_2(1-t_2))}\right)^{\frac{d}{2}-3}\right], \end{aligned} \tag{A.44}$$

where at this level we made no assumption on the parametrization of the momenta k_1 and k_2. Ideally, if we are able to compute this integral, we can get a general result valid for any parametrization of k_1 and k_2. Unfortunately, this expression is too complicated and to compute this integral we have to make some assumptions on the kinematic. First of all, we assume that one of the two momenta, k_2, is on-shell. With this assumption, however, we have still too many scales in the integral. Then, we assume a particular kinematic having in mind the $2 \to 1$ process we computed in Chapter 5. Making these kinematic assumptions, however, means that we lose generality and then we can not use this result to compute an integral different from the one in Eq.(A.41). We choose

$$\begin{aligned} k_1^\mu &= z\,\bar{n}^\mu + k_{1\,t}^\mu \\ q^\mu &= n^\mu - \rho\,\bar{n}^\mu \\ k_2^\mu &= k_1^\mu + q^\mu \\ n\cdot\bar{n} &= \frac{S}{2}. \\ k_1^2 &= -\mathbf{k}_{1\perp} \\ k_2^2 &= 0. \end{aligned} \tag{A.45}$$

Moreover, we can also define

$$\begin{aligned} \tau &= \frac{\rho}{z} = \frac{Q^2}{zS}; \\ \xi &= \frac{\mathbf{k}_{1\perp}^2}{Q^2}. \end{aligned} \tag{A.46}$$

Under these assumptions, the integral becomes

$$\begin{aligned} I_3 = \frac{-2\mathrm{i}}{(4\,\pi)^2}\left(\frac{4\,\pi}{Q^2}\right)^{\epsilon}\frac{\Gamma(1+\epsilon)}{Q^4}\int_0^1 d\,t_1\int_0^{1-t_1} d\,t_2 \frac{t_1^{-1-\epsilon}\left(\xi(1-t_1)+\frac{t_2}{\tau}\right)^{-1-\epsilon}}{t_1+(1-\tau)t_2} \\ \left[1-\left(1-\frac{1}{\tau}\frac{t_2(t_1+(1-\tau)t_2)}{\xi(1-t_1)+\frac{t_2}{\tau}}\right)^{-1-\epsilon}\right]. \end{aligned} \tag{A.47}$$

This integral is still too complicated due to the presence of the two independent parameters τ and ξ. We can further simplify this expression by keeping in mind that we want to use this integral to compute a contribution to the cross-section of a $2 \to 1$ scattering. This means that we can use the one-body phase-space Dirac-delta that gives

$$(k_1+q)^2 = 0 \to \tau = \frac{1}{1+\xi}. \tag{A.48}$$

Implementing this relation in Eq.(A.47) we get

$$\begin{aligned} I_3 = \frac{-2\mathrm{i}}{(4\,\pi)^2}\left(\frac{4\,\pi}{Q^2}\right)^{\epsilon}\frac{\Gamma(1+\epsilon)}{Q^4}\int_0^1 d\,t_1 t_1^{-\epsilon}\int_0^{1-t_1} d\,t_2 \frac{(1+\xi)\left[\xi(1-t_1)+t_2(1+\xi)\right]^{-1-\epsilon}}{(1+\xi)t_1+\xi t_2} \\ \left[1-\left(1-\frac{t_2\left[(1+\xi)t_1+\xi t_2\right]}{\xi(1-t_1)+(1+\xi)t_2}\right)^{-1-\epsilon}\right]. \end{aligned} \tag{A.49}$$

In this expression, we have only one parameter left, ξ, but we have lost the generality of Eq.(A.41). Making the shift $t_2 \to (1+t_1)t_2$ we get

$$I_3 = \frac{-2\mathrm{i}}{(4\,\pi)^2}\left(\frac{4\,\pi}{Q^2}\right)^{\epsilon}\frac{\Gamma(1+\epsilon)}{Q^4}I, \tag{A.50}$$

where we defined

$$I = \int_0^1 d\,t_1 t_1^{-\epsilon}(1-t_1)^{-1-\epsilon}J \tag{A.51}$$

where

$$\begin{aligned} J &= \int_0^1 d\,t_2 \frac{[t_2(1-\xi)+\xi]^{-1-\epsilon}}{t_1(1+\xi)\,+t_2(1-t_1)\xi}\left[1-\left(1-\frac{t_2\,[(1+\xi)t_1+\xi(1-t_1)t_2]}{t_1\,(t_2(1-\xi)+\xi)}\right)^{-1-\epsilon}\right] \\ &= \int_0^1 d\,t_2 \frac{[t_2(1-\xi)+\xi]^{-1-\epsilon}}{t_1(1+\xi)\,+t_2(1-t_1)\xi}\left[1-\left(\frac{t_1\,(t_2(1-\xi)+\xi)}{\xi\,[t_1(1-t_2)^2+t_2^2]}\right)^{-1-\epsilon}\right]. \end{aligned} \tag{A.52}$$

To compute this integral we can notice that there are some singular points:

- $t_1 = 0$;
- $t_2 = \frac{\xi}{1-}$, that is always outside the integration range
- $t_2 = -\frac{\sqrt{t_1}}{1-\sqrt{t_1}} < 0$, that is also always outside the integration range;
- $t_2 = -\frac{\sqrt{t_1}}{1-\sqrt{t_1}}\left[0,\frac{1}{2}\right]$ that is inside the integration range, but it is an integrable singularity;
- $t_1 = -\frac{(1+\xi)t_1}{(1-t_1)\xi} \leq 0$, which is present only when $t_1 = 0$.

To determine the leading singular behavior, we can compute the integral in Eq.(A.52) with $\epsilon = 0$. This simplifies the calculation and we get

$$J = -\frac{\ln(t_1)}{2\xi^2}, \tag{A.53}$$

that means that the lowest order in the ϵ-expansion of Eq.(A.49) is

$$I_3 = \frac{\mathrm{i}}{(4\pi)^2}\frac{1}{Q^4}\frac{1}{2\xi^2}\frac{1}{\epsilon^2} + \mathcal{O}\left(\frac{1}{\epsilon}\right). \tag{A.54}$$

We note that this leading ϵ behavior is determined by both terms in the squared bracket. Indeed, by splitting the integral into two parts, we have

$$J = J_1 + J_2, \tag{A.55}$$

where

$$J_1 \equiv \int_0^1 dt_2\,\frac{[t_2(1-\xi)+\xi]^{-1-\epsilon}}{t_1(1+\xi)+t_2(1-t_1)\xi} = \frac{\ln(t_1)-\ln(\xi)+\ln\left(\frac{1+\xi}{t_1+\xi}\right)}{t_1-\xi^2} + \mathcal{O}(\epsilon), \tag{A.56}$$

and

$$\begin{aligned} J_2 &\equiv -\left(\frac{t_1}{\xi}\right)^{1+\epsilon} \int_0^1 dt_2 \, \frac{[\sqrt{t_1}-(1+\sqrt{t_1})t_2]^{-1-\epsilon}[\sqrt{t_1}+(1-\sqrt{t_1})t_2]^{-1-\epsilon}}{t_1(1+\xi)+t_2(1-t_1)\xi} \\ &= \frac{-\frac{1}{2}\ln(t_1) - \ln\left(\frac{1+\xi}{t_1+\xi}\right)}{t_1-\xi^2} + \mathcal{O}(\epsilon). \end{aligned} \tag{A.57}$$

Both integrals contain a $\ln(t_1)$ term in the $t_1 \to 0$ limit that is responsible for the double pole.

We are now interested in computing the full ϵ-expansion of Eq.(A.49). This calculation is quite complicated. The strategy we follow is to compute the contributions from the two parts, J_1 and J_2 separately. This calculation can be done by writing the function J_i as

$$J_i = A_i(\epsilon)\ln t_1 + \hat{J}_i(t_1,\epsilon) \tag{A.58}$$

with $\hat{J}_i(0)$ a finite constant. The first part is responsible for the double pole, while the second for the rest of the ϵ-expansion. In this way, we can split also the integral I into two parts, each of which can be derived from the J_i integral as

$$I_i = I_{0,i} + \hat{I}_i, \tag{A.59}$$

where

$$\begin{aligned} I_{0,i} &\equiv A_i(\epsilon)\int_0^1 dt_1 \, \frac{t_1^{-1-\epsilon}}{(1-t_1)^\epsilon}\,\ln(t_1), \\ \hat{I}_i &\equiv \int_0^1 dt_1 \, \frac{t_1^{-1-\epsilon}}{(1-t_1)^\epsilon}\,\hat{J}_i(t_1,\epsilon). \end{aligned} \tag{A.60}$$

The first integral can be computed as

$$I_{0_i} = A_i(\epsilon)\frac{d}{d\eta}\int_0^1 dt_1 \, \frac{t_1^{-1-\epsilon+\eta}}{(1-t_1)^\epsilon} = -A_i(\epsilon)\left[\frac{1}{\epsilon^2}+\mathcal{O}(\epsilon)\right]. \tag{A.61}$$

The other contribution is regular in $t_1 = 0$, so we can regulate the singularity as

$$t_1^{-1-\epsilon} = -\frac{1}{\epsilon}\delta(t_1) + \left[\frac{1}{t_1}\right]_+ + \mathcal{O}(\epsilon). \tag{A.62}$$

Finally, we get

$$\begin{aligned} \hat{I}_i &= -\frac{1}{\epsilon}\hat{J}_i(0,\epsilon) + \int_0^1 \frac{dt_1}{t_1}\,\left[\frac{\hat{J}_i(t_1,\epsilon)}{(1-t_1)^\epsilon} - \hat{J}_i(0,\epsilon)\right] + \mathcal{O}(\epsilon) \\ &= -\frac{1}{\epsilon}\hat{J}_i(0,0) - \hat{J}_i^{(1)}(0,0) + \int_0^1 \frac{dt_1}{t_1}\,\left[\hat{J}_i(t_1,0) - \hat{J}_i(0,0)\right] + \mathcal{O}(\epsilon) \end{aligned} \tag{A.63}$$

where $\hat{J}_i^{(1)}(t_1,\epsilon)$ is the first derivative with respect to the second argument ϵ. We observe that for the sake of producing the expansion up to $\mathcal{O}(\epsilon^0)$ it is sufficient that the decomposition Eq.(A.58) holds up to $\mathcal{O}(\epsilon)$.

The calculation can be performed separately for J_1 and J_2 by finding the correct expression for $A_i(\epsilon)$ and $\hat{J}_i(t_1, \epsilon)$. From Eq.(A.56) and Eq.(A.57), we already know that

$$\begin{aligned} A_1(0) &= -\frac{1}{\xi^2}, \\ A_2(0) &= \frac{1}{2\xi^2}, \end{aligned} \tag{A.64}$$

we guess

$$\begin{aligned} A_1(\epsilon) &= -\frac{1}{\xi^{2+\epsilon}}, \\ A_2(\epsilon) &= \frac{1}{2\xi^{2+\epsilon}}, \end{aligned} \tag{A.65}$$

If our guess is not correct we will find some singularities. Under these assumptions, we write the other contribution in Eq.(A.58), J_i and we can compute the various contributions that enter in Eq.(A.63). The results of the two integrals are

$$\begin{aligned} I_1 = \frac{1}{\xi^2}\Bigg[\frac{1}{\epsilon^2} + \frac{1}{\epsilon}\ln\left(\frac{\xi}{1+\xi}\right) + \zeta_2 + \frac{1}{2}\ln^2(\xi) + \frac{1}{2}\ln^2\left(\frac{\xi}{1+\xi}\right) \\ + \mathrm{Li}_2\left(\frac{\xi-1}{\xi}\right) + \mathrm{Li}_2(1-\xi) + \mathcal{O}(\epsilon)\Bigg], \end{aligned} \tag{A.66}$$

and

$$I_2 = -\frac{1}{\xi^2}\left[\frac{1}{2\epsilon^2} + \frac{1}{\epsilon}\ln\left(\frac{1+\xi}{\xi\sqrt{\xi}}\right) + \frac{\zeta_2}{2} + \ln^2\left(\frac{1+\xi}{\xi\sqrt{\xi}}\right) + \mathrm{Li}_2\left(\frac{1}{1+\xi}\right) + \mathcal{O}(\epsilon)\right]. \tag{A.67}$$

Summing the results in Eq.(A.66) and in Eq.(A.67) we get the final result for the integral I defined in Eq.(A.50). Finally, we can use Eq.(A.50) to get the final result for the integral we wanted to compute. We get

$$\begin{aligned} I_3 &= \int \frac{d^dk}{(2\,\pi)^d}\frac{1}{k^2(k-k_1)^2(k-k_2)^2}\frac{k\cdot\bar{n}}{k\cdot n\, k\cdot\bar{n}+\delta^2} \\ &= \frac{-\mathrm{i}}{(4\pi)^2}\frac{1}{Q^2\xi^2}\left[\frac{1}{\epsilon^2} + \frac{1}{\epsilon}\left(5\ln(\xi) - 4\ln\left(\xi+1\right)\right) + 2\ln^2(\xi) - \ln^2(\xi+1)\right. \\ &\left. -2\ln(\xi+1)\ln(\xi) + 3\ln(\xi) + 2\mathrm{Li}_2(1-\xi) + 2\mathrm{Li}_2\left(\frac{\xi-1}{\xi}\right) - 2\mathrm{Li}_2\left(\frac{1}{\xi+1}\right) + \frac{\pi^2}{6}\right], \end{aligned} \tag{A.68}$$

where we set the renormalization scale $\mu^2 = Q^2$, to simplify the result.

In this way, we get the result of a specific integral with three covariant denominators and a non-covariant part. Integrals of this kind will be used to compute the process described in Chapter 5. In particular, they enter in the contribution from the diagram shown in Fig.(5.10). Considering the calculation of this diagram, we find out that only two integrals contribute to the final result,

$$T_{01} = \int \frac{d^dk}{(2\,\pi)^d}\frac{1}{k^2(k-k_1)^2(k-k_2)^2}\frac{1}{k\cdot n} \tag{A.69}$$

that is precisely the integral we computed in this section, and

$$T_{01a} = \int \frac{d^dk}{(2\,\pi)^d} \frac{1}{k^2(k-k_1)^2(k-k_2)^2} \frac{1}{k\cdot n - k_1\cdot n}. \tag{A.70}$$

Since to get the result in Eq.(A.68) we used the kinematic assumptions in Eq.(A.45), we can not exploit this result to compute the second integral. To calculate the integral in Eq.(A.70), then, we have to follow once again the steps we just illustrated. First of all, to use ML prescription and the general formula in Eq.(A.29), we have to shift the loop-momentum in Eq.(A.70) to get

$$\begin{aligned} T_{01a} =& \int \frac{d^dk}{(2\,\pi)^d} \frac{1}{k^2(k+k_1)^2(k+k_1-k_2)^2} \frac{1}{k\cdot n} \\ =& \int \frac{d^dk}{(2\,\pi)^d} \frac{1}{k^2(k+k_1)^2(k+k_1-k_2)^2} \frac{k\cdot\bar{n}}{k\cdot n\, k\cdot\bar{n}+\delta^2}. \end{aligned} \tag{A.71}$$

We can use Feynman parametrization in the covariant part of Eq.(A.70) to get

$$T_{01a} = 2\int_0^1 dt_1 \int_0^{1-t_1} dt_2 \int \frac{d^dk}{(2\,\pi)^d} \frac{1}{[k^2 - 2(t_2q - t_1k_1)\cdot k + t_1k_1^2 + t_2q^2]} \frac{k\cdot\bar{n}}{k\cdot n\, k\cdot\bar{n}+\delta^2}, \tag{A.72}$$

where we used the fact that, in the kinematic of the process considered in Chapter 5, we have $q^\mu = k_2^\mu - k_1^\mu$. At this point, we apply the formula in Eq.(A.29) to get

$$\begin{aligned} T_{01a} = \frac{\mathrm{i}\Gamma\,(1+\epsilon)}{(4\pi)^2}\left(\frac{4\pi}{Q^2}\right)^\epsilon \frac{2}{Q^4} \int_0^1 dt_1 \int_0^{1-t_1} dt_2 \frac{[\xi t_1(1-t_1) + t_2(1-t_2) - t_1t_2(1+\xi)]^{-1-\epsilon}}{t_2 + (1+\xi)t_1} \\ \left[1 - \left(1 + \frac{t_2\,(t_2 + (1+\xi)t_1)}{\xi t_1(1-t_1) + t_2(1-t_2) - t_1t_2(1+\xi)}\right)^{-1-\epsilon}\right], \end{aligned} \tag{A.73}$$

where we used the kinematic in Eq.(A.45) to simplify the expression and we also used $d = 4-\epsilon$. We can also make the change of variable $t_2 \to (1-t_1)t_2$ to get

$$\begin{aligned} T_{01a} =& \frac{\mathrm{i}\Gamma\,(1+\epsilon)}{(4\pi)^2}\left(\frac{(4\pi)^2}{Q^2}\right)^\epsilon \frac{2}{Q^4} \int_0^1 dt_1 (1-t_1)^{-\epsilon} \\ & \times \int_0^1 dt_2 \frac{(1-t_2)^{-1-\epsilon}\,[(1-t_1)t_2 + \xi t_1]^{-1-\epsilon}}{t_2(1-t_1) + (1+\xi)t_1} \\ & \times \left[1 - \left(1 + \frac{t_2\,((1-t_1)t_2 + (1+\xi)t_1)}{(1-t_2)\,((1-t_1)t_2 + \xi t_1)}\right)^{-1-\epsilon}\right]. \end{aligned} \tag{A.74}$$

This expression can be simplified and we obtain

$$\begin{aligned} T_{01a} =& \frac{\mathrm{i}\Gamma\,(1+\epsilon)}{(4\pi)^2}\left(\frac{(4\pi)^2}{Q^2}\right)^\epsilon \frac{2}{Q^4} \int_0^1 dt_1 (1-t_1)^{-\epsilon} \\ & \times \int_0^1 dt_2 \frac{(1-t_2)^{-1-\epsilon}\,[(1-t_1)t_2 + \xi t_1]^{-1-\epsilon}}{t_2(1-t_1) + (1+\xi)t_1} \\ & \times \left[1 - \left(\frac{t_2 + \xi t_1}{(1-t_2)\,((1-t_1)t_2 + \xi t_1)}\right)^{-1-\epsilon}\right]. \end{aligned} \tag{A.75}$$

Here the calculations are more complicated with respect to the ones in Eq.(A.52). This is due to the fact that, while in the integral T_{10} we had one of the two momenta on-shell ($k_2^2 = 0$), in this case, both momenta in the covariant denominators are off-shell. This means that we have one more scale in the integral. Again we can separate the integral into two parts and compute the contributions separately. We get

$$T_{01a} = \frac{\mathrm{i}\Gamma(1+\epsilon)}{(4\pi)^2}\left(\frac{(4\pi)^2}{Q^2}\right)^{\epsilon}\frac{2}{Q^4}\left(I_1^{[2]} + I_2^{[2]}\right), \tag{A.76}$$

where

$$I_1^{[2]} = \int_0^1 dt_1(1-t_1)^{-\epsilon}\int_0^1 dt_2 \frac{(1-t_2)^{-1-\epsilon}\left[(1-t_1)t_2 + \xi t_1\right]^{-1-\epsilon}}{t_2(1-t_1)+(1+\xi)t_1} \tag{A.77}$$

and

$$I_2^{[2]} = -\int_0^1 dt_1(1-t_1)^{-\epsilon}\int_0^1 dt_2 \frac{\left[t_2+\xi t_1\right]^{-1-\epsilon}}{t_2(1-t_1)+(1+\xi)t_1}. \tag{A.78}$$

In this case, the integral in Eq.(A.78) is not too complicated while the one in Eq.(A.77) requires more careful handling. However, we can give also for these two integral a final result:

$$\begin{aligned} I_1^{[2]} = {} & \frac{2}{\epsilon}\ln\left(\frac{1+\xi}{\xi}\right) - \zeta_2 - \frac{1}{2}\ln^2(1+\xi) - \ln(1+\xi)\ln\xi + \frac{1}{2}\ln^2\xi \\ & + \mathrm{Li}_2(1-\xi) - 3\mathrm{Li}_2(-\xi) - \mathrm{Li}_2\left(1-\frac{1}{\xi}\right) - \mathrm{Li}_2\left(\frac{1}{1+\xi}\right) + \mathcal{O}(\epsilon), \end{aligned} \tag{A.79}$$

and

$$I_2^{[2]} = \frac{1}{\epsilon}\ln\left(\frac{\xi}{1+\xi}\right) + \zeta_2 - \frac{1}{2}\ln^2\xi + 2\ln(1+\xi)\ln\xi - \ln^2(1+\xi) + \mathrm{Li}_2(-\xi) + \mathcal{O}(\epsilon). \tag{A.80}$$

Summing these two results and using Eq.(A.78) we get the final result for this integral

$$\begin{aligned} T_{01a} = {} & \int \frac{d^dk}{(2\,\pi)^d}\frac{1}{k^2(k+k_1)^2(k+k_1-k_2)^2}\frac{k\cdot\bar{n}}{k\cdot n\, k\cdot\bar{n}+\delta^2} \\ = {} & \frac{\mathrm{i}}{(4\pi)^2}\frac{1}{Q^2}\left[\frac{2}{\epsilon}\left(\ln(\xi+1)-\ln(\xi)\right) - 3\ln^2(\xi+1) + 2\ln(\xi)\ln(\xi+1)\right. \\ & \left. +2\mathrm{Li}_2(1-\xi) - 2\mathrm{Li}_2\left(\frac{\xi-1}{\xi}\right) - 4\mathrm{Li}_2(-\xi) - 2\mathrm{Li}_2\left(\frac{1}{\xi+1}\right)\right], \end{aligned} \tag{A.81}$$

where we set $\mu^2 = Q^2$ to simplify the expression. We notice that this integral does not have a double pole.

With the integrals in Eq.(A.69) and in Eq.(A.70) we are able to compute the complete NLO off-shell virtual contribution to the Higgs-induced DIS.

A.2 Non-covariant one loop integrals with principal value prescription

The usual techniques to compute loop integrals strongly rely on the Lorentz invariance, and so they will fail when we face some non-covariant loop integrals. The aim of this section is to present a method to compute non-covariant loop integrals that can be applied when one works with the PV prescription. This method aims to be as independent as possible of the particular form of the non-covariant part.

To avoid confusion, we start by clarifying the notation. First of all, the most general non-covariant one loop-integral can be written as:

$$I = \int \frac{d^dk}{(2\pi)^d} \frac{N(k, l_1, \dots, l_m, n, q_1 \dots q_j)}{k^2(k-l_1)^2(\dots)(k-l_m)^2(k\cdot n - q_1\cdot n)^{\alpha_1}(\dots)(k\cdot n - q_j\cdot n)^{\alpha_j}}, \quad \text{(A.82)}$$

where the covariant denominators are $m+1$, the non-covariant denominators are j and the numerator can be a function of all the momenta. In the following, we will analyze the case where $N(k, l_1, \dots, l_m, n, q_1 \dots q_j) = 1$, because integrals with more powers of the loop momentum in the numerator can be reduced to scalar integrals using Passarino-Veltmann reduction.

We will also use the following notation for the integrals:

$$I_{i,j} = \int \frac{d^dk}{(2\pi)^d} \frac{1}{k^2(k-l_2)^2(\dots)(k-l_i)^2(k_+ - q_{1+})^{\alpha_1}(\dots)(k_+ - q_{j+})^{\alpha_i}}, \quad \text{(A.83)}$$

where i is the number of covariant denominators and j is the number of non-covariant denominators. The projection of a momentum on the gauge vector is denoted by $q_+ = q\cdot n$.

As we anticipated in Chapter 4, to compute these integrals, we will exploit the identity [89]:

$$\begin{aligned} S &= \int \frac{d^dk}{(2\pi)^d} \frac{1}{(k^2 - 2P\cdot k + M^2 + \mathrm{i}\eta)^\alpha} \frac{1}{(k\cdot n)^\beta} \\ &= \frac{\mathrm{i}(-1)^\alpha}{(4\pi)^{\frac{d}{2}}} \frac{\Gamma\left(\alpha - \frac{d}{2}\right)}{\Gamma(\alpha)} \frac{1}{(P^2 - M^2)^{\alpha - \frac{d}{2}}(P\cdot n)^\beta}, \end{aligned} \quad \text{(A.84)}$$

where α and β are natural numbers and we also assumed $n^2 = 0$, for the light-cone gauge. The strength of this formula is that gives a result quite similar to the one obtained with covariant integrals,

$$C = \int \frac{d^dk}{(2\pi)^d} \frac{1}{(k^2 - 2P\cdot k + M^2)^\alpha} = \frac{i(-1)^\alpha}{(4\pi)^{\frac{d}{2}}} \frac{\Gamma\left(\alpha - \frac{d}{2}\right)}{\Gamma(\alpha)} \frac{1}{(P^2 - M^2)^{\alpha - \frac{d}{2}}}. \quad \text{(A.85)}$$

This is helpful because we can see it as a generalization of the covariant result in the presence of a non-covariant denominator and we can exploit many techniques we use for covariant loop integrals.

The result in Eq.(A.84) can be obtained starting by using Feynman parametrization in

$$S = \int \frac{d^dk}{(2\pi)^d} \frac{1}{(k^2 - 2P\cdot k + M^2 + \mathrm{i}\eta)^\alpha} \frac{1}{(k\cdot n)^\beta} \quad \text{(A.86)}$$

getting

$$S = \frac{\Gamma(\alpha+\beta)}{\Gamma(\alpha)\Gamma(\beta)} \int_0^1 dx \frac{(1-x)^{\beta-1}}{x^{\beta+1}} \int \frac{d^dk}{(2\pi)^d} \frac{1}{\left[k^2 - 2\left(P - \frac{1-x}{2x}n\right)\cdot k + M^2\right]^{\alpha+\beta}}. \quad \text{(A.87)}$$

The next step is to calculate the integral in the loop momentum k in the usual way, using Wick rotation:

$$\begin{aligned} S =& \frac{i(-1)^{\alpha+\beta}}{(4\pi)^{\frac{d}{2}}} \frac{\Gamma\left(\alpha+\beta-\frac{d}{2}\right)}{\Gamma(\alpha)\Gamma(\beta)} \frac{1}{(P^2-M^2)^{\alpha+\beta-\frac{d}{2}}} \\ &\times \int_0^1 dx \frac{(1-x)^{\beta-1}}{x^{\beta+1}} \left[1 - \frac{1-x}{x}\frac{P\cdot n}{P^2-M^2}\right]^{\frac{d}{2}-\alpha-\beta}, \end{aligned} \quad \text{(A.88)}$$

where we exploited the fact that in light-cone gauge $n^2 = 0$. Note that, for this step, is crucial that the non-covariant parts are linear in $k \cdot n$. Here the Wick rotation is not an issue, because, since we do not have yet introduced a regularisation for the gauge singularities, the non-covariant part does not have an imaginary part. For this reason, the singular structure of the k_0 component is the same as the usual covariant loop integrals.

We now perform the change of variable $x = \frac{a}{t+a}$, where $a = -\frac{P\cdot n}{P^2-M^2}$. In this way, we recover the integral representation of the Beta function,

$$B(1+m, 1+n) = \int_0^\infty \frac{dt\, t^m}{(1+t)^{m+n+2}}. \quad \text{(A.89)}$$

In the end, using the properties of the Beta function, we get

$$S = \frac{i(-1)^\alpha}{(4\pi)^2} \frac{\Gamma\left(\alpha-\frac{d}{2}\right)}{\Gamma(\alpha)} \frac{1}{(P\cdot n)^\beta} \frac{1}{(P^2-M^2)^{\alpha-\frac{d}{2}}}, \quad \text{(A.90)}$$

this expression matches the one presented in [89]. We already discussed in Chapter 4 how to get this result is crucial to introduce the PV prescription only after having performed the Wick rotation.

In the following, we will concentrate on the most common integrals that can show up in loop calculations. These are the integrals with one, two, or three covariant denominators.

A.2.1 One covariant denominator: PV prescription

Starting from the integral with one covariant denominator, we can point out that, using this formula, they are always vanishing. This is because they can be written as

$$I = \int \frac{d^dk}{(2\pi)^d} \frac{1}{(k^2 - 2k\cdot l + l^2)^2 (k\cdot n)}, \quad \text{(A.91)}$$

and so the term that appears in Eq.(A.84),

$$(P^2-M^2)^{\frac{d}{2}-1}, \quad \text{(A.92)}$$

vanish, since $P^2 = M^2 = l^2$. This happens no matter what is the form of the non-covariant part. We will see that this will not be true if we use the ML prescription.

A.2.2 Two covariant denominators: PV prescription

In this section, we want to give a general formula to compute integrals with two covariant denominators and an arbitrary non-covariant part.

We start by analyzing the case of an integral with two covariant denominators and one non-covariant denominator,

$$I_{2,1} = \int \frac{d^dk}{(2\pi)^d} \frac{1}{k^2(k-l)^2(k\cdot n)}, \tag{A.93}$$

where we assume in general $l^2 \neq 0$. After Feynman parametrization, the integral becomes

$$I_{2,1} = \int_0^1 dx \int \frac{d^dk}{(2\pi)^d} \frac{1}{k\cdot n} \frac{1}{\left[k^2 - 2P\cdot n + M^2\right]^2}, \tag{A.94}$$

where $P^\mu = x\, l^\mu$ and $M^2 = x\, l^2$. Here we can apply Eq.(4.8) to get

$$I_{2,1} = \frac{i}{16\pi^2}\left(\frac{4\pi}{-l^2}\right)^\epsilon \frac{\Gamma(1+\epsilon)}{\epsilon} \int_0^1 dx \frac{1}{x\, l_+} x^{-\epsilon}(1-x)^{-\epsilon}, \tag{A.95}$$

where we set $d = 4 - 2\epsilon$. Note that if $l^2 = 0$, this integral vanishes.

The generalization of this result to the case where the non-covariant denominator appears at some power β is straightforward. We can therefore state that

$$\int \frac{d^dk}{(2\pi)^d} f(k_+) \frac{1}{k^2(k-l)^2} = \frac{i}{16\pi^2}\left(\frac{4\pi}{-l^2}\right)^\epsilon \frac{\Gamma(1+\epsilon)}{\epsilon} \int_0^1 dx f(l_+z) z^{-\epsilon}(1-z)^{-\epsilon}, \tag{A.96}$$

where we defined $f(k_+) = \frac{1}{(k_+)^\beta}$.

We now show that Eq.(A.96) holds for a larger class of function $f(k_+)$. First of all, it is still valid when we add a constant term in the covariant denominator:

$$\int \frac{d^dk}{(2\pi)^d} \frac{1}{(k_+ - q_+)^\beta} \frac{1}{k^2(k-l)^2} = \int \frac{d^dk}{(2\pi)^d} \frac{f(k_+ - q_+)}{k^2(k-l)^2}. \tag{A.97}$$

In order to apply Eq.(4.8), we have to shift the loop momentum,

$$\int \frac{d^dk}{(2\pi)^d} \frac{f(k_+)}{(k+q)^2(k-(l-q))^2}, \tag{A.98}$$

and use Feynman parametrization. Now we can apply Eq.(4.8) to get

$$\int \frac{d^dk}{(2\pi)^d} \frac{f(k_+ - p_+)}{k^2(k-l)^2} = \frac{i}{16\pi^2}\left(\frac{4\pi}{-l^2}\right)^\epsilon \frac{\Gamma(1+\epsilon)}{\epsilon} \int_0^1 dx f(l_+z - p_+z) z^{-\epsilon}(1-z)^{-\epsilon}. \tag{A.99}$$

Note that this is the same expression we get in Eq.(A.96), the only difference is in the form of the function $f(k_+)$. This means that, as long as we can write the non-covariant part as

$$f(k_+) = \frac{1}{(k_+ - q_+)^\beta}, \tag{A.100}$$

where q is a generic momentum that does not depend on k, we can directly write the result with Eq.(A.96). This is the case when we have more than one non-covariant denominator. Taking as an example the case of two non-covariant denominators we have:

$$f(k_+) = \frac{1}{(k_+)(k_+ - q_+)}. \tag{A.101}$$

In the integrand, we can always use Feynman parametrization to get

$$I_{2,2} = \int \frac{d^dk}{(2\,\pi)^d} \frac{1}{k^2(k-l)^2(k_+)(k_+ - q_+)} = \int_0^1 dx \int \frac{d^dk}{(2\,\pi)^d} \frac{1}{k^2(k-l)^2(k_+ - x\,q_+)^2}. \tag{A.102}$$

The non-covariant part is now in the correct form to apply Eq.(A.96). We get:

$$I_{2,2} = \frac{i}{16\pi^2} \left(\frac{4\pi}{-l^2}\right)^\epsilon \frac{\Gamma(1+\epsilon)}{\epsilon} \int_0^1 dx \int_0^1 dz \frac{z^{-\epsilon}(1-z)^{-\epsilon}}{(zl_+ - xq_+)^2}. \tag{A.103}$$

We notice that the only dependence on the Feynman variable x is in the denominator, then, we can first compute this integral to get

$$I_{2,2} = \frac{i}{16\pi^2} \left(\frac{4\pi}{-l^2}\right)^\epsilon \frac{\Gamma(1+\epsilon)}{\epsilon} \int_0^1 dz \frac{z^{-\epsilon}(1-z)^{-\epsilon}}{l_+ z(l_+ z - p_+)}. \tag{A.104}$$

Now we identify in the integrand

$$f(l_+ z) = \frac{1}{l_+ z(l_+ z - q_+)}. \tag{A.105}$$

We can conclude that

$$I_{2,2} = \frac{i}{16\pi^2} \left(\frac{4\pi}{-l^2}\right)^\epsilon \frac{\Gamma(1+\epsilon)}{\epsilon} \int_0^1 dz f(l_+\,z) z^{-\epsilon}(1-z)^{-\epsilon}, \tag{A.106}$$

where $f(l_+)$ has the form of Eq.(A.101). It is straightforward to generalize this example to the case of any number of non-covariant denominators. We conclude that

$$\begin{aligned} I_{2,j} =& \int \frac{d^dk}{(2\,\pi)^d} \frac{1}{k^2(k-l)^2} \frac{1}{(k\cdot n - l_1\cdot n)^{\alpha_1} \ldots (k\cdot n - l_k \cdot n)^{\alpha_j}} \\ =& \frac{i}{16\pi^2} \left(\frac{4\pi}{-l^2}\right)^\epsilon \frac{\Gamma(1+\epsilon)}{\epsilon} \int_0^1 dz f(l_+\,z) z^{-\epsilon}(1-z)^{-\epsilon}, \end{aligned} \tag{A.107}$$

where

$$f(l_+ z) = \frac{1}{(l_+ z - q_1\cdot n)^{\alpha_1} \ldots (l_+ z - q_j \cdot n)^{\alpha_j}}. \tag{A.108}$$

It is remarkable that the assumption on the form of the non-covariant part is quite general and includes all the possible expressions for $f(k_+)$ that we encounter computing non-covariant loop integrals. The Eq.(A.107) allows us to insert the specific form of the non-covariant part only in the last integral on the Feynman parameter. In this sense, the calculation is similar to the one in covariant gauge, the only difference is

this last step. We recall that in this approach one regularises the IR gauge divergences using the PV prescription at this stage and not at the stage of the gluon propagators. This implies that the result will depend on the IR regulator δ.

Note that the result in Eq.(A.108) has a UV pole. This is a violation of the power-counting principle from which we expected this integral to be finite. This violation is due to the fact that with the PV the Wick rotation does not work and so we get some spurious UV singularities.

A.2.3 Three covariant denominators: mass-less case

The case of one and two covariant denominators is not too difficult once one understands Eq.(A.84). Things become more complex when we want to compute integrals with three non-covariant denominators. In this section analyse a particular case,

$$I_{3,j} = \int \frac{d^d k}{(2\,\pi)^d} \frac{1}{k^2 (k-l)^2 (k-p)^2 (k\cdot n - l_1\cdot n)^{\alpha_1} \dots (k\cdot n - l_j \cdot n)^{\alpha_j}}, \tag{A.109}$$

where $p^2 = 0$ and $(p-l)^2 = 0$. This means that $2p\cdot l = l^2$, and so we have only one scale. This provides an important simplification in the calculations. Since we proved that Eq.(A.84) can be applied if

$$f(k_+) = \frac{1}{(k\cdot n - l_1\cdot n)^{\alpha_1} \dots (k\cdot n - l_j \cdot n)^{\alpha_j}}, \tag{A.110}$$

we compute directly

$$I_{3,j} = \int \frac{d^d k}{(2\,\pi)^d} \frac{f(k_+)}{k^2 (k-l)^2 (k-p)^2}, \tag{A.111}$$

where $f(k_+)$ as the form in Eq.(A.110). The first step is, again, to apply Feynman parametrization and Eq.(A.84) in Eq.(A.111). We get

$$I_{3,j} = \frac{i}{16\pi^2} \left(\frac{4\pi}{-l^2}\right)^{\epsilon} \frac{\Gamma(1+\epsilon)}{l^2} \int_0^1 dt_1 \int_0^{1-t_1} dt_2 f\left(l_+(t_1 + x t_2)\right) \left[t_1(1-t_1) - t_1 t_2\right]^{-1-\epsilon}, \tag{A.112}$$

where we defined $x = \frac{p_+}{l_+}$. Since we want to give a result valid for a generic function $f(l_+)$, we want to make the argument of the non-covariant function dependent only on one integration variable. To do so, we change the order of integration and we change the integration variable to

$$t_1' = t_1 + x t_2. \tag{A.113}$$

We get

$$\begin{aligned} I_{3,j} = {} & \frac{i}{16\pi^2} \left(\frac{4\pi}{-l^2}\right)^{\epsilon} \frac{\Gamma(1+\epsilon)}{l^2} x^{\epsilon} \\ & \times \int_0^1 dt_2 \int_{x t_2}^{1-t_2(1-x)} dt_1 f(l_+ t_1) (t_1 - x t_2)^{-1-\epsilon} \left(1 - t_1 - t_2(1-x)\right)^{-1-\epsilon}. \end{aligned} \tag{A.114}$$

We change again the order of the integrals so that we can first compute the integral in the variable that does not appear in the argument of the non-covariant function. In

doing this, we must pay attention to the limits of integration. In particular, we see that the integral splits into two different parts:

$$\begin{aligned} I_{3,j} = & \frac{i}{16\pi^2}\left(\frac{4\pi}{-l^2}\right)^{\epsilon}\frac{\Gamma(1+\epsilon)}{l^2} \\ & \times\left[\int_0^x dt_1 f(l_+t_1)\int_0^{\frac{t_1}{x}} dt_2 (t_1-xt_2)^{-1-\epsilon}\left(1-t_1-t_2(1-x)\right)^{-1-\epsilon}\right. \\ & \left.+\int_x^1 dt_1 f(l_+t_1)\int_0^{\frac{1-t_1}{1-x}} dt_2 (t_1-xt_2)^{-1-\epsilon}\left(1-t_1-t_2(1-x)\right)^{-1-\epsilon}\right]. \end{aligned} \tag{A.115}$$

At this point, we reduce the limits of the integration between 0 and 1 in both the t_2-integrals. We have to make a change variable: in the first integral, we set $t_2 = \frac{t_1}{x}t$, while in the second we set $t_2 = \frac{1-t_1}{1-x}t$. We get

$$\begin{aligned} I_{3,j} = & \frac{i}{16\pi^2}\left(\frac{4\pi}{-l^2}\right)^{\epsilon}\frac{\Gamma(1+\epsilon)}{l^2} \\ & \times\left[\frac{1}{x}\int_0^x dt_1 f(l_+t_1)(1-t_1)^{-1-\epsilon}t_1^{-\epsilon}\int_0^1 dt\,(1-t)^{-1-\epsilon}\left(1-\frac{1-x}{x}\frac{t_1}{1-t_1}t\right)^{-1-\epsilon}\right. \\ & \left.+\frac{1}{(1-x)}\int_x^1 dt_1 f(l_+t_1)(1-t_1)^{-\epsilon}t_1^{-1-\epsilon}\int_0^1 dt(1-t)^{-1-\epsilon}\left(1-\frac{x}{1-x}\frac{1-t_1}{t_1}t\right)^{-1-\epsilon}\right]. \end{aligned} \tag{A.116}$$

In both integrals, we recognize the integral representation of the Hypergeometric function. This brings us to our final result:

$$\begin{aligned} I_{3,j} = & \frac{i}{16\pi^2}\left(\frac{4\pi}{-l^2}\right)^{\epsilon}\frac{1}{-l^2}\frac{\Gamma(1+\epsilon)}{\epsilon} \\ & \times\left[\frac{1}{x}\int_0^x dz f(l_+z)(1-z)^{-1-\epsilon}z^{-\epsilon}{}_2F_1\left(1+\epsilon,1;1-\epsilon;\frac{1-x}{x}\frac{z}{1-z}\right)\right. \\ & \left.+\frac{1}{1-x}\int_x^1 dy f(l_+y)(1-y)^{-\epsilon}y^{-1-\epsilon}{}_2F_1\left(1+\epsilon,1;1-\epsilon;\frac{1-x}{x}\frac{y}{1-y}\right)\right], \end{aligned} \tag{A.117}$$

where

$$f(k_+) = \frac{1}{(k_+-q_{1+})^{\alpha_1}\ldots(k_+-q_{j,+})^{\alpha_j}}. \tag{A.118}$$

A.2.4 Three covariant denominators: massive case

We now consider the case with three covariant denominators in the more general case where $p^2 = 0$ but $(p-l)^2 \neq 0$. This means that we have an additional scale: $2l\cdot p \neq l^2$. To simplify the notation we set $b = \frac{l^2}{2p\cdot l}$.

As we did before, we study the case where

$$I_{3,j} = \int \frac{f(k_+)}{k^2(k-l)^2(k-p)^2}, \tag{A.119}$$

where

$$f(k_+) = \frac{1}{(k_+ - q_{1+})^{\alpha_1} \dots (k_+ - q_{j,+})^{\alpha_j}}. \tag{A.120}$$

We can directly use the most general non-covariant part because we showed that Eq.(4.8) is still valid in this case.

The first step is the same as the case with one scale: we use Feynman parametrization and apply Eq.(4.8) to get

$$I_{3,j} = \frac{i}{16\pi^2}\left(\frac{4\pi}{-2l\cdot p}\right)^{\epsilon}\frac{\Gamma(1+\epsilon)}{2l\cdot p}\int_0^1 dt_1 \int_0^{1-t_1} dt_2 f\left(l_+(t_1+xt_2)\right)\left[b\,t_1(1-t_1)-t_1\,t_2\right]^{-1-\epsilon}, \tag{A.121}$$

where again we defined $x = \frac{p_+}{l_+}$. Now we follow steps very similar to what we did for the case with only one scale. We, then, change variable so that function f will depend only on t_1. After steps analogous to the one we did before, we get

$$\begin{aligned} I_{3,j} = &\frac{i}{16\pi^2}\left(\frac{4\pi}{-2l\cdot p}\right)^{\epsilon}\frac{\Gamma(1+\epsilon)}{2l\cdot p} \\ &\times \int_0^x dt_1 f(l_+t_1)\int_0^{\frac{t_1}{x}} dt_2\,(t_1 - x\,t_2)^{-1-\epsilon}\left[b(1-t_1)-t_2(1-b\,x)\right]^{-1-\epsilon} \\ &+ \frac{i}{16\pi^2}\left(\frac{4\pi}{-2l\cdot p}\right)^{\epsilon}\frac{\Gamma(1+\epsilon)}{2l\cdot p} \\ &\times \int_x^1 dt_1 f(l_+t_1)\int_0^{\frac{1-t_1}{1-x}} dt_2\,(t_1 - x\,t_2)^{-1-\epsilon}\left[b(1-t_1)-t_2(1-b\,x)\right]^{-1-\epsilon}. \end{aligned} \tag{A.122}$$

Now, we change variables to set the limits of the t_2 integration between 0 and 1 in both integrals. In the first we set $t_2 = \frac{t_1}{x}\,t$ while in the second $t_2 = \frac{1-t_1}{1-x}\,t$. We get:

$$\begin{aligned} I_{3,j} = &\frac{i}{16\pi^2}\left(\frac{4\pi}{-2l\cdot p}\right)^{\epsilon}\frac{\Gamma(1+\epsilon)}{2l\cdot p}\,\frac{b^{-1-\epsilon}}{x}\int_0^x dt_1 f(l_+t_1)t_1^{-\epsilon}(1-t_1)^{-1-\epsilon} \\ &\times \int_0^1 dt\,(1-t)^{-1-\epsilon}\left[1-\frac{1-b\,x}{b\,x}\frac{t_1}{1-t_1}t\right]^{-1-\epsilon} \\ &+ \frac{i}{16\pi^2}\left(\frac{4\pi}{-2l\cdot p}\right)^{\epsilon}\frac{\Gamma(1+\epsilon)}{2l\cdot p}\,\frac{b^{-1-\epsilon}}{(1-x)}\int_x^1 dt_1 f(l_+t_1)t_1^{-1-\epsilon}(1-t_1)^{-\epsilon} \\ &\times \int_0^1 dt\left(1-\frac{1-b\,x}{b(1-x)}t\right)^{-1-\epsilon}\left(1-\frac{x(1-t_1)}{(1-x)t_1}t\right)^{-1-\epsilon}. \end{aligned} \tag{A.123}$$

In the first integral, we recognize the integral representation of the Hypergeometric function. The second integral can also be written as a sum of two Hypergeometric

functions after some manipulations. This allows us to write the final result as

$$
\begin{aligned}
I_{3,j} &= \frac{i}{16\pi^2}\left(\frac{4\pi}{-2l\cdot p}\right)^{\epsilon}\frac{1}{-2l\cdot p}\frac{\Gamma(1+\epsilon)}{\epsilon}\frac{b^{-1-\epsilon}}{x}\\
&\times\int_0^x dz f(l_+ z) z^{-\epsilon}(1-z)^{-1-\epsilon}{}_2F_1\left(1+\epsilon,1;1-\epsilon;\frac{(1-b\,x)}{b\,x}\frac{z}{1-z}\right)\\
&-\frac{i}{16\pi^2}\left(\frac{4\pi}{-2l\cdot p}\right)^{\epsilon}\frac{1}{-2l\cdot p}\frac{\Gamma(1+\epsilon)}{\epsilon}\,b^{-\epsilon}(b\,x-1)^{\epsilon}\\
&\times\int_x^1 dy f(l_+ y)(1-y)^{-\epsilon}(b\,x-y)^{-1-\epsilon}{}_2F_1\left(1+\epsilon,-\epsilon;1-\epsilon;\frac{(1-y)b\,x}{b\,x-y}\right)\\
&+\frac{i}{16\pi^2}\left(\frac{4\pi}{-2l\cdot p}\right)^{\epsilon}\frac{1}{-2l\cdot p}\frac{\Gamma(1+\epsilon)}{\epsilon}\,\frac{(b\,x-1)^{\epsilon}(1-x)^{\epsilon}}{(b-1)^{\epsilon}}\\
&\times\int_x^1 dy f(l_+ y)(1-y)^{-\epsilon}(b\,x-y)^{-1-\epsilon}{}_2F_1\left(1+\epsilon,-\epsilon;1-\epsilon;\frac{(b-1)\,x}{(1-x)}\frac{(1-y)}{(b\,x-y)}\right),
\end{aligned}
\tag{A.124}
$$

where we remind you that

$$
f(k_+) = \frac{1}{(k_+ - q_{1+})^{\alpha_1}\ldots(k_+ - q_{j,+})^{\alpha_j}}. \tag{A.125}
$$

Appendix B

Counterterms computed with PV prescription

In this appendix, we report the counterterms relevant for the off-shell HDIS coefficient function computed with PV prescription. They are listed diagram by diagram and we will comment on the dependence on the PV regulator δ that is due to the fact that with PV prescription the Wick rotation fails. The counterterm for the diagram in Fig.(5.11), as we already saw in Chapter 5 is null because the diagram does not have UV divergences.

B.1 Counterterm for the gluon self-energy

We start by presenting the calculation for the simplest diagram, the self-energy of the gluon.

If we consider a pure gluon theory, the only non-zero one-loop contribution to the gluon self-energy is the diagram in Fig.(5.13). Using Feynman rules we can write the contribution from this diagram as:

$$\begin{aligned}\Pi^{\mu\nu}(k_1,n) = \int \frac{d^dk}{(2\pi)^d} \frac{N^{\mu\nu\rho\sigma\alpha\beta}(k,k_1,n)}{k^2(k-k_1)^2} \left[-g_{\rho\alpha} + \frac{k_\alpha n_\rho + k_\rho n_\alpha}{k\cdot n}\right] \\ \times \left[-g_{\sigma\beta} + \frac{(k_1-k)_\sigma n_\beta + (k_1-k)_\beta n_\sigma}{(k_1-k)\cdot n}\right],\end{aligned} \tag{B.1}$$

where

$$\begin{aligned}N^{\mu\nu\rho\sigma\alpha\beta}(k,k_1,n) = -\frac{\mathrm{g}^2 C_A \delta_{a,b}}{2} \left[g^{\rho\sigma}(k_1-2k)^\mu + g^{\mu\sigma}(k-2k_1)^\rho + g^{\mu\rho}(k+k_1)^\sigma\right] \\ \left[g^{\beta\nu}(2k_1-k)^\alpha - g^{\alpha\nu}(k+k_1)^\beta + g^{\alpha\beta}(2k-k_1)^\nu\right],\end{aligned} \tag{B.2}$$

and the overall factor $\frac{1}{2}$ is due to the symmetry.

We can contract the indices and compute the non-covariant integrals using the techniques explained in Appendix A. When we find some tensorial integrals we reduce them to scalar using Passarino-Veltmann decomposition. As in the previous case, since

the gluon is off-shell, all the poles will be ultraviolet. We can, then, write the divergent part of this integral as

$$\begin{aligned}\Pi^{\mu\nu}(k_1,n) = \mathrm{i}\frac{\alpha_s}{4\pi}\frac{C_A\delta_{a,b}}{\epsilon}\Bigg[\left(\frac{11}{3}-4I_0\right)\left(k_1^\mu k_1^\nu - k_1^2 g^{\mu\nu}\right) \\ -4\left(1-I_0\right)\left(k_1^\mu k_1^\nu - \frac{k_1^2}{k_1\cdot n}(k_1^\mu n^\nu + k_1^\nu n^\mu) + \frac{k_1^4}{(k_1\cdot n)^2}n^\mu n^\nu\right)\Bigg],\end{aligned} \tag{B.3}$$

where

$$I_0 = \int_0^1 du \frac{u}{u^2+\delta^2} = -\ln(\delta) + O(\delta). \tag{B.4}$$

This expression is quite different from the one in the Feynman gauge. First, we notice the dependence on the gauge vector n. This contribution cannot be derived by terms in the Lagrangian, we have to add it by hand. In particular, in Eq.(B.6) we recognize two terms. The first is similar to the Feynman gauge counterterm, the only difference is in the renormalization constant

$$Z_g = \frac{11}{3} - 4I_0 \tag{B.5}$$

that acquires a dependence on the principal value prescription regulator (δ). The second term explicitly depends on the gauge vector n. We want also to remark that the singular part of the gluon propagator in Eq.(B.6) is still transverse with respect to the gluon momentum k_1.

Following [81], we define a gauge-dependent counterterm that cancels all the UV poles. The counterterm will be

$$\begin{aligned}CT^{\mu\nu}(k_1,n) = -\mathrm{i}\frac{\alpha_s}{4\pi}\frac{C_A\delta_{a,b}}{\epsilon}\Bigg[\left(\frac{11}{3}-4I_0\right)\left(k_1^\mu k_1^\nu - k_1^2 g^{\mu\nu}\right) \\ -4\left(1-I_0\right)\left(k_1^\mu k_1^\nu - \frac{k_1^2}{k_1\cdot n}(k_1^\mu n^\nu + k_1^\nu n^\mu) + \frac{k_1^4}{(k_1\cdot n)^2}n^\mu n^\nu\right)\Bigg],\end{aligned} \tag{B.6}$$

B.2 Counterterm for the effective vertex

As we did in chapter 5, we compute this counterterm by isolating the UV divergent part of the one-loop contribution to the effective vertex. We report here the contributions from each of the four diagrams that contribute to it.

B.2.1 Diagram with a bubble on the incoming (outgoing) leg

We start from the contribution in Fig.(5.12). The diagram with the bubble on the outgoing leg will give the same contribution if we exchange k_1 (incoming momentum) with k_2 (outgoing momentum). For this reason, here we compute explicitly only the contribution from this diagram.

The calculations are very similar to the ones reported in Chapter 5, the only difference is in the way of performing the integrals. For this reason, hare we present only

the final result. We get

$$B_1^{\mu\nu}(k_1,k_2,n) = -\frac{\alpha_s c\, C_A \delta_{a,b}}{8\pi\,\epsilon}\left[B_{1\,k_1k_1}k_1^\mu k_1^\nu + B_{g\,k_1k_1}g^{\mu\nu} + B_{1\,nk_1}n^\mu k_1^\nu \right. \\ \left. + B_{1\,k_2n}k_2^\mu n^\nu + B_{1\,nn}n^\mu n^\nu\right], \tag{B.7}$$

where the coefficients are

$$B_{1\,k_1k_1} = -\frac{2}{3}; \tag{B.8}$$

$$B_{1\,g} = -\frac{(12(x+1)\ln(\delta)+9x+13)\,k_1^2}{3}; \tag{B.9}$$

$$B_{1\,k_1n} = \frac{(4\ln(\delta)+5)k_1^2}{k_1\cdot n}; \tag{B.10}$$

$$B_{1\,nk_1} = \frac{(2(x+1)\ln(\delta)+3x+5)k_1^2}{k_1\cdot n}; \tag{B.11}$$

$$B_{1\,k_2n} = \frac{(2\ln(\delta)+3)k_1^2}{k_1\cdot n}; \tag{B.12}$$

$$B_{1\,nn} = -\frac{(2\ln(\delta)(k_1^2+k_1\cdot k_2)+5k_1^2+3k_1\cdot k_2)k_1^2}{(k_1\cdot n)^2}. \tag{B.13}$$

From these expressions, we get the counterterm for the diagram with the gluon on the outgoing leg:

$$B_2^{\mu\nu}(k_1,k_2,n) = -\frac{\alpha_s c\, C_A \delta_{a,b}}{8\pi\,\epsilon}\left[B_{2\,k_2k_2}k_2^\mu k_2^\nu + B_{2\,g}g^{\mu\nu} + B_{2\,nk_2}n^\mu k_2^\nu \right. \\ \left. + B_{2\,k_1n}k_1^\mu n^\nu + B_{2\,nn}n^\mu n^\nu\right], \tag{B.14}$$

where the coefficients are

$$B_{2\,k_2k_2} = -\frac{2}{3}; \tag{B.15}$$

$$B_{2\,g} = -\frac{1}{3}k_2^2\left(\frac{12(1+x)}{x}\ln(\delta)+\frac{9}{x}+13\right); \tag{B.16}$$

$$B_{2\,k_2n} = \frac{(4\ln(\delta)+5)k_2^2}{x\,k_1\cdot n}; \tag{B.17}$$

$$B_{2\,nk_2} = \frac{(2(x+1)\ln(\delta)+3+5x)k_2^2}{x^2\,k_1\cdot n}; \tag{B.18}$$

$$B_{2\,k_1n} = \frac{(2\ln(\delta)+3)k_2^2}{x\,k_1\cdot n}; \tag{B.19}$$

$$B_{1\,nn} = -\frac{(2\ln(\delta)(k_2^2+k_1\cdot k_2)+5k_2^2+3k_1\cdot k_2)k_2^2}{x^2(k_1\cdot n)^2}. \tag{B.20}$$

Summing these two diagrams we get the total contribution:

$$B^{\mu\nu}(k_1,k_2,n) = -\frac{\alpha_s c\, C_A \delta_{a,b}}{8\pi\,\epsilon}\left[B_{k_1k_1}k_1^\mu k_1^\nu + B_{k_2k_2}k_2^\mu k_2^\nu + B_g g^{\mu\nu} + B_{k_1n}k_1^\mu n^\nu \right. \\ \left. + B_{nk_1}n^\mu k_1^\nu + B_{k_2n}k_2^\mu n^\nu + B_{2\,nk_2}n^\mu k_2^\nu + B_{2\,nn}n^\mu n^\nu\right], \tag{B.21}$$

where the coefficients are:

$$B_{k_1k_1} = -\frac{2}{3}; \tag{B.22}$$

$$B_{k_2k_2} = -\frac{2}{3}; \tag{B.23}$$

$$B_g = -\frac{12(x+1)\ln(\delta)(k_1^2x+k_2^2)+k_1^2x(9x+13)+k_2^2(13x+9)}{3x}; \tag{B.24}$$

$$B_{k_1n} = \frac{(4\ln(\delta)+5)k_1^2}{k_1\cdot n} + \frac{(2\ln(\delta)+3)k_2^2}{x\,k_1\cdot n}; \tag{B.25}$$

$$B_{n\,k_1} = \frac{(2(1+x)\ln(\delta)+3x+5)k_1^2}{k_1\cdot n}; \tag{B.26}$$

$$B_{2\,k_2n} = \frac{(4\ln(\delta)+5)k_2^2}{x\,k_1\cdot n} + \frac{(2\ln(\delta)+3)k_1^2}{k_1\cdot n}; \tag{B.27}$$

$$B_{n\,k_2} = \frac{(2(1+x)\ln(\delta)+3+5x)k_2^2}{x^2\,k_1\cdot n}; \tag{B.28}$$

$$\begin{aligned} B_{1\,n\,n} = &-\frac{(2\ln(\delta)(k_1^2+k_1\cdot k_2)+5k_1^2+3k_1\cdot k_2)k_1^2}{(k_1\cdot n)^2} \\ &-\frac{(2\ln(\delta)(k_2^2+k_1\cdot k_2)+5k_2^2+3k_1\cdot k_2)k_2^2}{x^2(k_1\cdot n)^2}. \end{aligned} \tag{B.29}$$

We note that these coefficients depend on the regulator δ.

B.2.2 Triangle diagram

In this section, we report the results for the counterterm for the diagram in figure (5.10). As we did in the previous section, we report only the final result since the calculations are analogous to the one discussed in Chapter 5. The only difference is in the prescription used to regulate the gauge singularities. This means that the integrals will be computed using the result presented in Section A.2 of the Appendix A. The contribution from this diagram can be written as

$$\begin{aligned} T^{\mu\nu}(k_1,k_2,n) = &-\frac{\alpha_s c\, C_A\delta_{a,b}}{4\pi\,\epsilon}\left[T_{k_1k_1}k_1^\mu k_1^\nu + T_{k_2k_2}k_2^\mu k_2^\nu + T_g g^{\mu\nu} + T_{k_1k2}k_1^\mu k_2^\nu\right. \\ &\left. + T_{k_2k1}k_2^\mu k_1^\nu + T_{k_1n}k_1^\mu n^\nu + T_{nk_1}n^\mu k_1^\nu + T_{k_2n}k_2^\mu n^\nu + T_{2\,nk_2}n^\mu k_2^\nu + T_{2\,nn}n^\mu n^\nu\right]. \end{aligned} \tag{B.30}$$

The coefficients of these tensorial structures are:

$$\begin{aligned} T_{k_1k_1}(k_1,k_2,n) = &-4x\ln(\delta) + \frac{1}{3}(1-6x) \\ &+ \frac{1}{2(x(k_1^2x-2k_1\cdot k_2)+k_2^2)^2}\left[x\ln(1-x)\left[-2k_1\cdot k_2k_2^2(x-3)x+(k_2^2)^2(x-2)\right]\right. \\ &+ x\ln(1-x)\left[4k_1^2k_1\cdot k_2x^3 - x^4(k_1^2)^2 + k_1^2k_2^2\left(3x^3-9x^2+6x-2\right) - 4(k_1\cdot k_2)^2x^2\right] \\ &+ x^3\ln(x)\left[(k_1^2)^2\left(x^2-2\right) - 4k_1^2k_1\cdot k_2(x-2) - 4(k_1\cdot k_2)^2\right] \\ &+ x\ln(x)\left[k_2^2x\left(k_1^2\left(x^2+3x-6\right)+2k_1\cdot k_2\left(2x^2-7x+7\right)\right)+(k_2^2)^2(3x-4)\right] \\ &\left.+k_2^2(x-1)x\ln(x-1)(x(k_1^2(3x-2)-4k_1\cdot k_2x+2k_1\cdot k_2)+k_2^2(2x-1))\right]; \end{aligned} \tag{B.31}$$

$$
\begin{aligned}
T_{k_2k_2}(k_1,k_2,n) &= -\frac{4\ln(\delta)}{x}+\frac{x-6}{3x}\\
&\frac{1}{2x(x(k_1^2x-2k_1\cdot k_2)+k_2^2)^2}\left[k_1^2x\ln(x)\left[k_1^2\left(5x^2-x-2\right)+2k_1\cdot k_2(5-9x)\right]\right.\\
&-k_2^2\ln(x-1)\left[x\left(k_1^2\left(2x^3-6x^2+9x-3\right)-4k_1\cdot k_2\right)+k_2^2\right]\\
&+\ln(x)\left[k_1^2k_2^2\left(2x^3-2x^2+11x-7\right)+2x(k_2^2-2k_1\cdot k_2)^2\right]\\
&+k_1^2(x-1)\ln(1-x)(k_1^2x(x-2)-2k_1\cdot k_2(x-2)+k_2^2(2x-3))\\
&\left.-x^2\ln(x-1)\left[(k_1^2)^2x(2x-1)+k_1^2k_1\cdot k_2(2-6x)+4(k_1\cdot k_2)^2\right]\right];
\end{aligned}
\tag{B.32}
$$

$$
\begin{aligned}
T_g(k_1,k_2,n) &= \frac{2\ln(\delta)(x(k_1^2x+k_1^2-2k_1\cdot k_2)+k_2^2(x+1))}{x}\\
&+\frac{k_1^2x(9x+13)+k_2^2(13x+9)}{6x}\\
&+\frac{1}{2(x(k_1^2x-2k_1\cdot k_2)+k_2^2)}\left[k_2^2\ln(x)\left[2k_1\cdot k_2\left(x^2+2x-1\right)-2k_2^2x\right]\right.\\
&+k_1^2\ln(x)\left[k_1^2\left(x-x^3\right)+4k_1\cdot k_2x(x-1)+k_2^2\left(-2x^3+x^2-4x+3\right)\right]\\
&+k_1^2\ln(1-x)\left[x\left(x^2+1\right)(k_1^2x-2k_1\cdot k_2)-k_2^2\left(x^3-4x^2+3x-2\right)\right]\\
&\left.k_2^2\ln(x-1)\left[k_1^2x\left(2x^3-3x^2+4x-1\right)-2k_1\cdot k_2x\left(x^2+1\right)+k_2^2\left(x^2+1\right)\right]\right].
\end{aligned}
\tag{B.33}
$$

$$
\begin{aligned}
T_{k_1k_2}(k_1,k_2,n) &= 4\ln(\delta)+\frac{2x^2+x+2}{x}\\
&+\frac{1}{2(x(k_1^2x-2k_1\cdot k_2)+k_2^2)^2}\left[k_2^2x\ln(x)\left[2k_1\cdot k_2\left(6x^2-5x+1\right)+k_2^2(3-4x)\right]\right.\\
&+k_1^2x^2\ln(x)\left[k_1^2\left(-4x^4+6x^3-6x^2+x+2\right)+2k_1\cdot k_2\left(8x^3-12x^2+11x-5\right)\right]\\
&+x\ln(x)\left[k_1^2k_2^2\left(-8x^3+11x^2-12x+7\right)-4(k_1\cdot k_2)^2x\left(4x^2-6x+3\right)\right]\\
&+x^2\ln(1-x)\left[(k_1^2)^2x^2\left(2x^2-3x+2\right)-2k_1^2k_1\cdot k_2x\left(5x^2-9x+6\right)\right]\\
&+x^2\ln(1-x)\left[4(k_1\cdot k_2)^2\left(3x^2-6x+4\right)\right]-(k_2^2)^2\ln(1-x)\left[x^3-4x^2+6x-4\right]\\
&+k_2^2x\ln(1-x)\left[k_1^2x\left(-3x^3+12x^2-15x+8\right)+2k_1\cdot k_2\left(x^3-7x^2+12x-8\right)\right]\\
&+x^2\ln(x-1)\left[(k_1^2)^2x\left(4x^3-6x^2+4x-1\right)-2k_1^2k_1\cdot k_2\left(8x^3-12x^2+7x-1\right)\right]\\
&+k_2^2\ln(x-1)\left[x\left(k_1^2\left(8x^3-15x^2+12x-3\right)-2k_1\cdot k_2\left(6x^2-9x+5\right)\right)\right]\\
&\left.+4(k_1\cdot k_2)^2x^2\ln(x-1)\left(4x^2-6x+3\right)+(k_2^2)^2\ln(x-1)\left(2x^2-3x+2\right)\right];
\end{aligned}
\tag{B.34}
$$

$$
\begin{aligned}
T_{k_2k_1}(k_1,k_2,n) &= 4\ln(\delta)+\frac{1}{(x(k_1^2x-2k_1\cdot k_2)+k_2^2)^2}\left[k_1^2k_2^2(x-1)^3\left(x\ln(x-1)\right.\right.\\
&\left.-\ln(1-x)\right)-(x-1)\ln(x)\left[k_2^2x\left(k_1^2\left(x^2+3\right)-4k_1\cdot k_2\right)\right.\\
&\left.\left.+k_1^2x^2(k_1^2x+k_1^2-4k_1\cdot k_2)+(k_2^2)^2(x+1)\right]\right];
\end{aligned}
\tag{B.35}
$$

In all these coefficients we defined $x=\frac{k_2\cdot n}{k_1\cdot n}$. Here we omit the contributions from the tensorial structures that involve the gauge vector n. They are indeed very complicated and their explicit expression does not add much to the comprehension of the problem. As we can see, the result for this contribution is quite more complicated compared to the previous ones.

B.3 Total contribution to the effective vertex counterterm

In this section we report the final result for the counterterm of the effective vertex. To get this result we sum the result obtained in the previous sections. At this level we still made no assumption on the parametrization of the two momenta k_1 and k_2, we give the general expression with the two momenta off-shell. The final result can be written as

$$\begin{aligned}\mathrm{CT}^{\mu\nu}(k_1,k_2,n) = -\frac{\alpha_s c\, C_A \delta_{a,b}}{4\pi\,\epsilon}\,[&\mathrm{CT}_{k_1k_1}k_1^\mu k_1^\nu + \mathrm{CT}_{k_2k_2}k_2^\mu k_2^\nu + \mathrm{CT}_g g^{\mu\nu} + \mathrm{CT}_{k_1k2}k_1^\mu k_2^\nu \\ &+\mathrm{CT}_{k_2k1}k_2^\mu k_1^\nu + \mathrm{CT}_{k_1n}k_1^\mu n^\nu + \mathrm{CT}_{nk_1}n^\mu k_1^\nu + \mathrm{CT}_{k_2n}k_2^\mu n^\nu + \mathrm{CT}_{2\,nk_2}n^\mu k_2^\nu + \mathrm{CT}_{2\,nn}n^\mu n^\nu]\,,\end{aligned} \tag{B.36}$$

where the coefficients are

$$\begin{aligned}CT_{k_1k_1} = &-4x\ln(\delta) - 2x + \frac{x\ln(x)}{2(x(k_1^2x - 2k_1\cdot k_2) + k_2^2)^2}\left(x^2k_1^3\left(x^2-2\right)\right.\\
&+x^2k_1^2\left(-4k_1^2k_1\cdot k_2(x-2) - 4k_1\cdot k_2^2\right)\\
&\left.+k_2^2x\left(k_1^2\left(x^2+3x-6\right) + 2k_1\cdot k_2\left(2x^2-7x+7\right)\right) + (k_2^2)^2(3x-4)\right)\\
&+\frac{x\ln(1-x)}{2(x(k_1^2x - 2k_1\cdot k_2) + k_2^2)^2}\left(4k_1^2k_1\cdot k_2x^3 + k_1^2k_2^2\left(3x^3-9x^2+6x-2\right)\right.\\
&\left.-(k_1^2)^2x^4 - 4k_1\cdot k_2^2x^2 - 2k_1\cdot k_2k_2^2(x-3)x + (k_2^2)^2(x-2)\right)\\
&+\frac{k_2^2(x-1)x\ln(x-1)(x(k_1^2(3x-2) - 4k_1\cdot k_2x + 2k_1\cdot k_2) + k_2^2(2x-1))}{2(x(k_1^2x - 2k_1\cdot k_2) + k_2^2)^2};\end{aligned} \tag{B.37}$$

$$\begin{aligned}CT_{k_2k_2} = &-\frac{4\ln(\delta)}{x} - \frac{2}{x} + \frac{k_1^2(x-1)\ln(1-x)(k_1^2x(x-2) - 2k_1\cdot k_2(x-2) + k_2^2(2x-3))}{2(x(k_1^2x - 2k_1\cdot k_2) + k_2^2)^2}\\
&+\frac{\ln(x)}{2(x(k_1^2x - 2k_1\cdot k_2) + k_2^2)^2}\left[(k_1^2)^2x\left(5x^2-x-2\right) + 2k_1^2k_1\cdot k_2x(5-9x)\right.\\
&\left.+k_1^2k_2^2\left(2x^3-2x^2+11x-7\right) + 2x(k_2^2 - 2k_1\cdot k_2)^2\right]\\
&-\frac{\ln(x-1)}{2x(x(k_1^2x - 2k_1\cdot k_2) + k_2^2)^2}\left[x^2\left((k_1^2)^2x(2x-1) + k_1^2k_1\cdot k_2(2-6x) + 4k_1\cdot k_2^2\right)\right.\\
&\left.+k_2^2x\left(k_1^2\left(2x^3-6x^2+9x-3\right) - 4k_1\cdot k_2\right) + (k_2^2)^2\right];\end{aligned} \tag{B.38}$$

$$
\begin{aligned}
CT_{k_1k_2} &= 4\ln(\delta) + \frac{2x^2+x+2}{x} \\
&+ \frac{x\ln(x)}{2(x(k_1^2x-2k_1\cdot k_2)+k_2^2)^2}\left[(k_1^2)^2x\left(-4x^4+6x^3-6x^2+x+2\right)\right. \\
&+ 2k_1^2k_1\cdot k_2x\left(8x^3-12x^2+11x-5\right)+k_1^2k_2^2\left(-8x^3+11x^2-12x+7\right) \\
&\left.-4k_1\cdot k_2^2x\left(4x^2-6x+3\right)+2k_1\cdot k_2k_2^2\left(6x^2-5x+1\right)+(k_2^2)^2(3-4x)\right] \\
&\frac{\ln(1-x)}{2x^2(x(k_1^2x-2k_1\cdot k_2)+k_2^2)^2}\left[x^3k_1^2\left(k_1^2x\left(2x^2-3x+2\right)-2k_1\cdot k_2\left(5x^2-9x+6\right)\right)\right. \\
&+ 4x^2(k_1\cdot k_2)^2\left(3x^2-6x+4\right)+x^2k_1^2k_2^2\left(-3x^3+12x^2-15x+8\right) \\
&\left.+2xk_1\cdot k_2k_2^2\left(x^3-7x^2+12x-8\right)-(k_2^2)^2\left(x^3-4x^2+6x-4\right)\right] \\
&+ \frac{\ln(x-1)}{2(x(k_1^2x-2k_1\cdot k_2)+k_2^2)^2}\left[x^3(k_1^2)^2\left(4x^3-6x^2+4x-1\right)\right. \\
&+ x^2k_1\cdot k_2\left(-2k_1^2\left(8x^3-12x^2+7x-1\right)+4k_1\cdot k_2\left(4x^2-6x+3\right)\right) \\
&\left.+k_2^2x\left(k_1^2\left(8x^3-15x^2+12x-3\right)-2k_1\cdot k_2\left(6x^2-9x+5\right)\right)+(k_2^2)^2\left(2x^2-3x+2\right)\right];
\end{aligned}
\tag{B.39}
$$

$$
\begin{aligned}
CT_{k_2k_1} &= 4\ln(\delta) - \frac{k_1^2k_2^2(x-1)^3\ln(1-x)}{(x(k_1^2x-2k_1\cdot k_2)+k_2^2)^2} + \frac{k_1^2k_2^2(x-1)^3x\ln(x-1)}{(x(k_1^2x-2k_1\cdot k_2)+k_2^2)^2} \\
&- \frac{(x-1)\ln(x)\left(k_2^2x\left(k_1^2\left(x^2+3\right)-4k_1\cdot k_2\right)+k_1^2x^2(k_1^2x+k_1^2-4k_1\cdot k_2)+(k_2^2)^2(x+1)\right)}{(x(k_1^2x-2k_1\cdot k_2)+k_2^2)^2};
\end{aligned}
\tag{B.40}
$$

$$
\begin{aligned}
CT_g &= -4k_1\cdot k_2\ln(\delta) \\
&+ \frac{k_1^2\ln(1-x)\left(x\left(x^2+1\right)\left(k_1^2x-2k_1\cdot k_2\right)-k_2^2\left(x^3-4x^2+3x-2\right)\right)}{2x(x(k_1^2x-2k_1\cdot k_2)+k_2^2)} \\
&+ \frac{k_2^2\ln(x-1)\left(k_1^2x\left(2x^3-3x^2+4x-1\right)-2k_1\cdot k_2x\left(x^2+1\right)+k_2^2\left(x^2+1\right)\right)}{2x(x(k_1^2x-2k_1\cdot k_2)+k_2^2)} \\
&+ \frac{\ln(x)}{2(x(k_1^2x-2k_1\cdot k_2)+k_2^2)}\left[(k_1^2)^2\left(x-x^3\right)+4k_1^2k_1\cdot k_2(x-1)x\right. \\
&\left.+k_1^2k_2^2\left(-2x^3+x^2-4x+3\right)+2k_1\cdot k_2k_2^2\left(x^2+2x-1\right)-2(k_2^2)^2x\right].
\end{aligned}
\tag{B.41}
$$

As in the previous section, we do not report the coefficients of the tensorial structures involving the gauge vector n due to their complicated expression. We notice that every coefficient still depends on the PV regulator δ. This counterterm will be used in Appendix C to cancel the UV singularities of the one-loop correction to the effective vertex.

Appendix C

One-loop virtual correction to the HDIS computed with PV prescription

In this appendix, we report the results of the one-loop virtual correction to the off-shell amplitude of the Higgs-induced DIS. We can compare these results with the ones presented in Chapter 5 computed with the ML prescription. The following results are reported diagram by diagram. Here we report the contribution to the amplitude only from the 2GI diagrams defined in Chapter 4. These diagrams are the ones in Fig.(5.11), Fig.(5.10), and Fig.(5.9). In Section C.4, we report the final result obtained by summing the contribution of all the diagrams. In this last section, the cancellation of the UV singularities has been performed using the counterterms reported in Appendix B.

In the following results, we use the following notation:

$$\begin{aligned} \xi &= \frac{\mathbf{k}_1^2}{Q^2} \\ \rho &= \frac{Q^2}{2k\cdot n} = \frac{Q^2}{S} \\ \tau &= \frac{Q^2}{2k_1\cdot q}, \end{aligned} \tag{C.1}$$

To write the coefficients in a more compact way, we also use the phase space Dirac delta that sets

$$\tau = \frac{1}{1+\xi}, \tag{C.2}$$

as we already did in Chapter 5.

C.1 Diagram A

We start reporting the contribution of the diagram shown in figure (5.11). This diagram, as we saw in Chapter 5, has no UV singularities, but only a finite part. The calculations are the same as the ones described in Section 5.4.1 of Chapter 5. The

result of this diagram is

$$D^{\mu\rho} = -\frac{\alpha_s}{8\pi} c^2 C_A \delta_{a,b} Q^2 \left[\frac{\xi+1}{\xi} k_2^\mu k_2^\rho - \frac{1}{2}(k_1^\mu k_2^\rho + k_2^\mu k_1^\rho) - \frac{Q^2}{2}(\xi-1) g^{\mu\rho} + \dots \right], \quad \text{(C.3)}$$

where we dropped the tensorial structures depending on the gauge vector n, as we did in Chapter 5. We can notice that the contribution from this diagram is quite simple and does not depend on the regulator for the spurious gauge singularities.

C.2 Diagram B

In this section, we report the contribution of the diagram shown in Fig.(5.10). The calculations to get this contribution are the same as the ones described in Section 5.4.2 of Chapter 5. The only difference is that here we regularise the spurious gauge singularities with the PV prescription and we compute them using the method reported in Appendix A, Section A.2. Since this result is more complicated than the previous one, we can write it as

$$\begin{aligned} B^{\mu\rho}(k_1,k_2,n) = -\frac{\alpha_s}{4\,\pi} c^2 C_A Q^2 \delta_{a,b} \Big[& B_{k_1 k_1} k_1^\mu k_1^\rho + B_{k_2 k_2} k_2^\mu k_2^\rho + \frac{1}{2} B_{k_1 k_2} (k_1^\mu k_2^\rho + k_2^\mu k_1^\rho) \\ & + B_g Q^2 g^{\mu\rho} + \dots \Big], \end{aligned} \quad \text{(C.4)}$$

where the coefficients of the tensorial structures are

$$\begin{aligned} B_{k_1\,k_1} = & \frac{\xi-1}{12(\xi+1)} \frac{1}{\epsilon} \left[3\xi(8\ln(\delta) - 2\ln(\xi) + \ln(\xi+1)) + 10\xi - 2 \right] - \frac{(\xi-1)\xi}{\xi+1} \ln^2(\delta) \\ & - \frac{(\xi-1)\xi}{4(\xi+1)} \ln(\xi+1)\ln(\delta) + \frac{\xi-1}{72(\xi+1)} \left[-20 + 42\pi^2\xi^3 + 84\pi^2\xi^2 + 108\xi^3 \ln^2(\xi) \right. \\ & + 216\xi^2 \ln^2(\xi) - 72\xi^3 \ln(\xi-1)\ln(\xi) - 72\xi^3 \ln(\xi)\ln(\xi+1) - 144\xi^2 \ln(\xi-1)\ln(\xi) \\ & + 72\xi^2 \ln(\xi) - 144\xi^2 \ln(\xi)\ln(\xi+1) - 72\xi^2 \ln(\xi+1) + 18\pi^2\xi + 124\xi + 144\xi \ln^2(\xi) \\ & \left. + 9\xi \ln^2(\xi+1) - 36\xi \ln(\xi-1)\ln(\xi) - 90\xi \ln(\xi)\ln(\xi+1) - 36\xi \ln(\xi+1) \right] \\ & - \frac{(\xi-1)\xi}{2(\xi+1)} \left[\left(2\xi^2+4\xi+1\right) \mathrm{Li}_2\left(\frac{1}{\xi+1}\right) - \mathrm{Li}_2\left(\xi^2\right) - \mathrm{Li}_2(1-\xi) \right]; \end{aligned} \quad \text{(C.5)}$$

$$\begin{aligned} B_{k_2\,k_2} = & \frac{1}{6\xi\epsilon} \left[3\left(4\xi^2+2\xi+1\right)\ln(\xi+1) - 6\xi^2\ln(\xi) - 12\xi\ln(\delta) - \xi(22\xi+13) \right] \\ & - \ln^2(\delta) + \frac{(2\xi^2+2\xi+1)}{2\xi} \ln(\xi+1)\ln(\delta) + \frac{1}{36\xi} \left[21\pi^2\xi^4 + 42\pi^2\xi^3 \right. \\ & + 72\pi^2\xi^2 + 45\pi^2\xi - 196\xi + 15\pi^2 - 18 - 268\xi^2 + 9\left(4\xi^2+2\xi+1\right)\ln^2(\xi+1) \\ & + 18\left(3\xi^2+6\xi+5\right)\xi^2\ln^2(\xi) - 18\left(2\xi^3+\xi^2-2\xi-1\right)\ln(\xi+1) \\ & - 18\ln(\xi)\left[-2\xi\left(\xi^2-1\right) + 2\left(\xi^4+2\xi^3+6\xi^2+4\xi+2\right)\ln(\xi-1) \right. \\ & \left. \left. + \left(2\xi^4+4\xi^3+6\xi^2+2\xi+1\right)\ln(\xi+1) \right] \right] - \frac{1}{\xi} \left[(\xi+2)\xi^3 \mathrm{Li}_2\left(\frac{1}{\xi+1}\right) \right. \\ & \left. + \left(2\xi^2+2\xi+1\right)\mathrm{Li}_2(1-\xi) + \left(2\xi^2+2\xi+1\right)\mathrm{Li}_2\left(\xi^2\right) \right]; \end{aligned} \quad \text{(C.6)}$$

$$
\begin{aligned}
B_{k_1\,k_2} &= \frac{1}{12\xi(\xi+1)}\frac{1}{\epsilon}\left[24\xi\left(-\xi^2+\xi+1\right)\ln(\delta)+2\xi(\xi(17\xi+14)-5)+2\right.\\
&\left.+3\xi(\xi+1)(6(\xi-1)\ln(\xi)+(5-9\xi)\ln(\xi+1))\right]+\frac{(-\xi^2+\xi+1)}{\xi+1}\ln^2(\delta)\\
&-\frac{1}{4}(3\xi+1)\ln(\xi+1)\ln(\delta)-\frac{1}{72\xi(\xi+1)}\left[84\pi^2\xi^5+168\pi^2\xi^4+2\left(60\pi^2-206\right)\xi^3\right.\\
&+2\left(3\pi^2-206\right)\xi^2+2\left(44-30\pi^2\right)\xi-20+216\xi\left(\xi^4+2\xi^3+\xi^2-\xi-1\right)\ln^2(\xi)\\
&+9\xi\left(9\xi^2+4\xi-5\right)\ln^2(\xi+1)-18\xi(\xi+1)\ln(\xi)\left[2\left(4\xi^3+4\xi^2+7\xi-3\right)\ln(\xi-1)\right.\\
&\left.\left.+\left(8\xi^3+8\xi^2+5\xi-9\right)\ln(\xi+1)-8(\xi-1)\xi\right]-72\xi\left(2\xi^3+\xi^2-2\xi-1\right)\ln(\xi+1)\right]\\
&+\frac{1}{2}\left[(3\xi+1)\mathrm{Li}_2\left(\xi^2\right)+\left(4\xi^3+4\xi^2-5\xi+1\right)\mathrm{Li}_2\left(\frac{1}{\xi+1}\right)+(3\xi+1)\mathrm{Li}_2(1-\xi)\right];
\end{aligned}
\tag{C.7}
$$

$$
\begin{aligned}
B_g &= \frac{1}{12(\xi+1)}\frac{1}{\epsilon}\left[12\left(\xi^3-1\right)\ln(\delta)-3\left(2\xi^3-3\xi+1\right)\ln(\xi+1)-6(\xi-1)\ln(\xi)\right.\\
&\left.+\xi(\xi-1)(22\xi+13)\right]-\frac{(\xi^3-1)}{2(\xi+1)}\ln^2(\delta)+\frac{(-2\xi^3+\xi+1)}{4(\xi+1)}\ln(\xi+1)\ln(\delta)\\
&-\frac{(\xi-1)}{72(\xi+1)}\left[24\pi^2\xi^2-268\xi^2-18\left(3\xi^2+6\xi+5\right)\ln^2(\xi)+9\left(2\xi^2+2\xi-1\right)\ln^2(\xi+1)\right.\\
&+3\pi^2\xi-196\xi-12\pi^2-18+36(2\xi+1)\ln(\xi+1)-18\ln(\xi)\left[-(2\xi+3)\ln(\xi+1)\right.\\
&\left.\left.+4\xi+2(3\xi+2)\xi\ln(\xi-1)\right]\right]+\frac{(\xi-1)}{2(\xi+1)}\left[\left(2\xi^2+2\xi+1\right)\mathrm{Li}_2(1-\xi)\right.\\
&\left.+\left(2\xi^2+2\xi+1\right)\mathrm{Li}_2\left(\xi^2\right)-\xi(\xi+2)\mathrm{Li}_2\left(\frac{1}{\xi+1}\right)\right].
\end{aligned}
\tag{C.8}
$$

This result is quite complicated but we can make some observations. First of all, we see that each coefficient depends on the regulator of the spurious gauge singularities. This is the main difference between this result and the one obtained with the ML prescription reported in Eq.(5.77).

C.3 Diagram C

The last contribution to the 2GI part of the amplitude is the diagram shown in Fig.(5.9). The calculations are the same as the ones performed in Section 5.4.3 of Chapter 5. We can write this result as

$$
\begin{aligned}
C^{\mu\rho}(k_1,k_2,n) = -\frac{\alpha_s}{4\,\pi}c^2C_A\delta_{a,b}Q^2\left[C_{k_1k_1}k_1^\mu k_1^\rho+C_{k_2k_2}k_2^\mu k_2^\rho+\frac{1}{2}C_{k_1k_2}(k_1^\mu k_2^\rho+k_2^\mu k_1^\rho)\right.\\
\left.+C_gQ^2g^{\mu\rho}+\ldots\right],
\end{aligned}
\tag{C.9}
$$

where the coefficients are

$$
B_{1\,k_1k_1} = \frac{(\xi-1)}{3\epsilon}+\frac{5}{9}(\xi-1);
\tag{C.10}
$$

$$
\begin{aligned}
B_{1\,k_2k_2} = &\frac{1}{3\epsilon}\left[12(2\xi+1)\ln(\delta)+22\xi+13\right]-2Q^2(2\xi+1)\ln^2(\delta)\\
&-\frac{1}{18}\left[15\pi^2(2\xi+1)-2(134\xi+89)\right];
\end{aligned}
\tag{C.11}
$$

$$
\begin{aligned}
B_{1\,k_1k_2} = &-\frac{1}{3\xi(\xi+1)\epsilon}\left[12(2\xi+1)\xi^2\ln(\delta)+23\xi^3+14\xi^2+\xi+1\right]\\
&+2\xi\left(\frac{\xi}{\xi+1}+1\right)\ln^2(\delta)+\frac{\left[(30\pi^2-278)\,\xi^3+(15\pi^2-188)\,\xi^2-10\xi-10\right]}{18\xi(\xi+1)};
\end{aligned}
\tag{C.12}
$$

$$
\begin{aligned}
B_{1\,g} = &-\frac{(\xi-1)\xi}{6(\xi+1)\epsilon}\left[12(2\xi+1)\ln(\delta)+22\xi+13\right]+\frac{(\xi-1)\xi(2\xi+1)}{\xi+1}\ln^2(\delta)\\
&+\frac{(\xi-1)\xi}{36(\xi+1)}\left[15\pi^2(2\xi+1)-2(134\xi+89)\right].
\end{aligned}
\tag{C.13}
$$

We notice that also these coefficients depend on the regulator δ as we expect from results computed using PV prescription.

C.4 Renormalised result

In this section, we will report the final result for the 2GI amplitude of the Higgs-induced DIS computed with the PV prescription. This result is obtained by summing all the results in the previous sections with the counterterms computed in Appendix B. We can write it as

$$
\begin{aligned}
\mathcal{A}^{\mu\rho}_{2\mathrm{GI}}(k_1,k_2,n) = -\frac{\alpha_s}{4\,\pi}c^2C_A\delta_{a,b}Q^2\Big[&\mathcal{A}_{k_1k_1}k_1^\mu k_1^\rho+\mathcal{A}_{k_2k_2}k_2^\mu k_2^\rho+\frac{1}{2}\mathcal{A}_{k_1k_2}(k_1^\mu k_2^\rho+k_2^\mu k_1^\rho)\\
&+\mathcal{A}_gQ^2g^{\mu\rho}+\ldots\Big],
\end{aligned}
\tag{C.14}
$$

where the coefficients are

$$
\begin{aligned}
\mathcal{A}_{k_1\,k_1} = &-\frac{1}{\epsilon}\frac{(\xi-1)\xi(2\xi(\xi+2)+3)}{4(\xi+1)}\ln\left(\frac{\xi}{\xi+1}\right)-\frac{(\xi-1)\xi}{\xi+1}\ln^2(\delta)\\
&-\frac{(\xi-1)\xi}{4(\xi+1)}\ln(\xi+1)\ln(\delta)+\frac{(\xi-1)\left(42\pi^2\xi^3+84\pi^2\xi^2+36\,(3\xi^2+6\xi+4)\,\xi\ln^2(\xi)\right)}{72(\xi+1)}\\
&+\frac{(\xi-1)Q^2\left(-18\xi\ln(\xi)\left((4\xi^2+8\xi+2)\ln(\xi-1)+(4\xi^2+8\xi+5)\ln(\xi+1)-4\xi\right)\right)}{72(\xi+1)}\\
&+\frac{(\xi-1)\left((52+9\pi^2)\,\xi+9\xi\ln^2(\xi+1)-36(2\xi+1)\xi\ln(\xi+1)-40\right)}{72(\xi+1)}\\
&-\frac{(\xi-1)\xi\left(-\mathrm{Li}_2\left(\xi^2\right)+(2\xi^2+4\xi+1)\,\mathrm{Li}_2\left(\frac{1}{\xi+1}\right)-\mathrm{Li}_2(1-\xi)\right)}{2(\xi+1)}.
\end{aligned}
\tag{C.15}
$$

$$
\begin{aligned}
\mathcal{A}_{k_2\,k_2} &= -\frac{\xi(\xi(\xi+2)+2)}{2\epsilon}\ln\left(\frac{\xi}{\xi+1}\right) - 2(\xi+1)\ln^2(\delta) \\
&+ \frac{(2\xi(\xi+1)+1)}{2\xi}\ln(\xi+1)\ln(\delta) - \frac{(\pi^2\,(7\xi^4+14\xi^3+14\xi^2-10\xi-5))}{12\xi} \\
&- \frac{\left(-6\,(16\xi^4+32\xi^3+21\xi^2-10\xi-5)\ln^2(\xi)\right) - 12\xi\,(\xi^2-1)\ln(\xi)}{12\xi} \\
&- \frac{-3\,(32\xi^4+64\xi^3+28\xi^2-38\xi-19)\ln^2(\xi+1)}{12\xi} \\
&- \frac{6\,(26\xi^4+52\xi^3+22\xi^2-30\xi-15)\ln(\xi+1)}{12\xi} \\
&- \frac{24(\xi-1)(\xi+1)^3\ln(\xi-1)\ln(\xi)}{12\xi} \\
&- \frac{-6\,(\xi^2-1)\,(-2\xi+4(\xi+1)^2\ln(\xi-1)-1)\ln(\xi+1)}{12\xi} \\
&- \frac{1}{\xi}\left[\left(-3\xi^4-6\xi^3-4\xi^2+4\xi+2\right)\mathrm{Li}_2\left(\frac{1}{\xi+1}\right) + 3(\xi-1)(\xi+1)^3\mathrm{Li}_2\left(\frac{\xi-1}{\xi}\right)\right].
\end{aligned}
\tag{C.16}
$$

$$
\begin{aligned}
\mathcal{A}_{k_1\,k_2} &= \frac{\xi(2\xi+1)^2-5}{4\epsilon}\ln\left(\frac{\xi}{\xi+1}\right) + (\xi+1)\ln^2(\delta) \\
&- \frac{1}{4}(3\xi+1)\ln(\xi+1)\ln(\delta) + \frac{28\pi^2\xi^4+56\pi^2\xi^3+50\pi^2\xi^2-48\xi^2}{24(\xi+1)} \\
&+ \frac{(32\xi^4+64\xi^3+31\xi^2-42\xi-41)\ln^2(\xi)}{2(\xi+1)} + \frac{(-48\pi^2\xi-50\pi^2-48)}{24(\xi+1)} \\
&+ \frac{(-384\xi^4-768\xi^3-327\xi^2+612\xi+555)\ln^2(\xi+1)}{24(\xi+1)} \\
&+ \frac{-24\,(\xi^2-1)\,((4\xi^2+8\xi+6)\ln(\xi-1)-2\xi-1)\ln(\xi+1)}{24(\xi+1)} \\
&+ \frac{2(\xi+1)\ln(\xi)\ln(\xi-1)\,(2\xi^3+2\xi^2-\xi-3)}{(\xi+1)} \\
&+ \frac{6(\xi+1)\ln(\xi)\,((104\xi^3+104\xi^2-19\xi-145)\ln(\xi+1)-8(\xi-1)\xi)}{24(\xi+1)} \\
&+ \frac{1}{2}\left[6\left(2\xi^3+2\xi^2-\xi-3\right)\mathrm{Li}_2\left(\frac{\xi-1}{\xi}\right) - \left(12\xi^3+12\xi^2+3\xi-23\right)\mathrm{Li}_2\left(\frac{1}{\xi+1}\right)\right]
\end{aligned}
\tag{C.17}
$$

$$
\begin{aligned}
\mathcal{A}_g = & -\frac{\xi^3+\xi^2-2}{4(\xi+1)\epsilon}\ln\left(\frac{\xi}{\xi+1}\right)+\frac{1}{2}(\xi-1)^2 \\
& -\frac{(2\xi^3-\xi-1)\ln(\xi+1)}{4(\xi+1)}\ln(\delta)-\frac{(\xi-1)\left(4\pi^2\left(\xi^2+2\xi+2\right)\right)}{8(\xi+1)} \\
& -\frac{(\xi-1)\left(-4\left(13\xi^2+21\xi+18\right)\ln^2(\xi)\right)}{8(\xi+1)} \\
& -\frac{(1-\xi)\left(\left(70\xi^2+102\xi+85\right)\ln^2(\xi+1)-8\left(3\xi^2+4\xi+3\right)\ln(\xi-1)\ln(\xi)\right)}{8(\xi+1)} \\
& -\frac{(\xi-1)\left(\left(56\xi^2+82\xi+67\right)\ln(\xi+1)-4\xi\right)\ln(\xi)}{4(\xi+1)} \\
& +\frac{(\xi-1)\left(4\left(\left(6\xi^2+8\xi+6\right)\ln(\xi-1)+2\xi+1\right)\ln(\xi+1)\right)}{8(\xi+1)} \\
& -\frac{(\xi-1)}{2(\xi+1)}\left[3\left(3\xi^2+4\xi+3\right)\mathrm{Li}_2\left(\frac{\xi-1}{\xi}\right)-\left(7\xi^2+10\xi+10\right)\mathrm{Li}_2\left(\frac{1}{\xi+1}\right)\right].
\end{aligned}
\tag{C.18}
$$

We observe that, once we cancel the UV singularities the coefficient of the remaining IR poles does not depend on the regulator of the spurious gauge singularities δ. The finite part, however, still depends on δ. This means that the 2GI virtual contribution to the off-shell amplitude is not gauge invariant and so the PV prescription can not be used to regularise the singularities.

Appendix D

Coefficients of the contribution from the diagram B to the off-shell virtual amplitude

In this appendix, we list the finite part of the coefficients of the tensorial structures contributing to the diagram B computed in Chapter 5, Section 5.4.2. We did not report this finite part in the main part of the thesis because they are quite complicated. We use the following definitions:

$$\begin{aligned} \xi &= \frac{\mathbf{k}_1^2}{Q^2} \\ \rho &= \frac{Q^2}{2k\cdot n} = \frac{Q^2}{S} \\ \tau &= \frac{Q^2}{2k_1\cdot q}, \end{aligned} \tag{D.1}$$

To write the coefficients in a more compact way, we also use the phase-space delta that sets

$$\tau = \frac{1}{1+\xi}. \tag{D.2}$$

The contribution to the amplitude from the diagram B can be written as

$$\begin{aligned} B^{\mu\rho}(k_1,k_2,n) = -\frac{\alpha_s}{4\,\pi}c^2 C_A Q^2 \delta_{a,b}\Big[& B_{k_1k_1}k_1^\mu k_1^\rho + B_{k_2k_2}k_2^\mu k_2^\rho + \frac{1}{2}B_{k_1k_2}(k_1^\mu k_2^\rho + k_2^\mu k_1^\rho) \\ & + B_g g^{\mu\rho} + \ldots\Big], \end{aligned} \tag{D.3}$$

where we omitted the tensorial structures depending on the gauge-vector n because, as we discussed in Chapter 3, they vanish once contracted with the projector that selects the dominant part pd the amplitude in the high-energy region. The coefficients of the

tensorial structures in Eq.(D.3) are:

$$
\begin{aligned}
B_{k_1k_1} = &-\frac{(\xi-1)}{288(\xi+1)}\left[24\pi^2\xi^6+12\pi^2\xi^5-192\pi^2\xi^4-84\pi^2\xi^3-6\pi^2\xi^2+216\xi^2\right.\\
&-144\xi^6\ln^2(\xi+1)-72\xi^5\ln^2(\xi+1)-216\xi^4\ln^2(\xi+1)-180\xi^3\ln^2(\xi+1)\\
&+360\xi^2\ln^2(\xi+1)+18\left(24\xi^5+12\xi^4+16\xi^3+20\xi^2+6\xi+3\right)\xi\ln^2(\xi)+576\xi^6\ln(\xi+1)\\
&+288\xi^5\ln(\xi+1)-432\xi^4\ln(\xi+1)-648\xi^3\ln(\xi+1)-684\xi^2\ln(\xi+1)-180\xi\ln(\xi+1)\\
&-12\ln(\xi)\left(24\xi^6+12\xi^5+54\xi^4+45\xi^3-39\xi^2-53\xi+4\right)-81\pi^2\xi-568\xi+72\xi\ln^2(\xi+1)\\
&\left.-72\left(4\xi^5+2\xi^4-2\xi^3+\xi^2+2\xi-2\right)\xi\ln(\xi+1)+108\left(4\xi^3+6\xi^2+\xi-1\right)\xi\ln(z)-208\right]\\
&+\frac{\xi\left(2\xi^2-\xi-1\right)\mathrm{Li}_2(1-\xi)}{2(\xi+1)}+\frac{3\xi\left(-2\xi^2+\xi+1\right)\mathrm{Li}_2(-\xi)}{4(\xi+1)}\\
&+\frac{1}{4}\xi\left(4\xi^5-6\xi^4+6\xi^3-5\xi^2+1\right)\mathrm{Li}_2\left(\frac{1}{\xi+1}\right);
\end{aligned}
\tag{D.4}
$$

$$
\begin{aligned}
B_{k_2k_2} = &\frac{1}{144\xi^3}\left[120\pi^2\xi^7+60\pi^2\xi^6+120\pi^2\xi^5+360\xi^5+168\pi^2\xi^4+368\xi^4\right.\\
&+96\pi^2\xi^3+152\xi^3+24\pi^2\xi^2+360\xi^2+72\xi^5\ln^2(\xi+1)+288\xi^4\ln^2(\xi+1)-72\xi^7\ln(\xi+1)\\
&+72\left(\xi^2-\xi+1\right)\xi^3\ln^2(\xi)+792\xi^3\ln^2(\xi+1)+180\xi^2\ln^2(\xi+1)+180\xi^6\ln(\xi+1)\\
&+504\xi^5\ln(\xi+1)+288\xi^4\ln(\xi+1)+234\xi^3\ln(\xi+1)+207\xi^2\ln(\xi+1)\\
&-3\ln(\xi)\left(-264\xi^7-204\xi^6+216\xi^5-80\xi^4-290\xi^3-123\xi^2+6\xi+3\right)+18\xi\ln(\xi+1)\\
&-72\left(2\xi^5+\xi^4+4\xi^3+2\xi^2+6\xi+1\right)\xi^2\ln(\xi)\ln(\xi+1)+9\ln(\xi+1)\\
&\left.-36\left(6\xi^5+9\xi^4+2\xi^3+2\xi^2+11\xi+8\right)\xi^2\ln(z)\right]-\frac{\left(2\xi^2+4\xi+1\right)\mathrm{Li}_2(1-\xi)}{\xi}\\
&-\frac{\left(2\xi^5+\xi^4+2\xi^3-4\xi-1\right)\mathrm{Li}_2\left(\frac{1}{\xi+1}\right)}{2\xi}+\frac{3\left(2\xi^2+4\xi+1\right)\mathrm{Li}_2(-\xi)}{2\xi};
\end{aligned}
\tag{D.5}
$$

$$
\begin{aligned}
B_{k_1k_2} = &\frac{1}{288\xi(\xi+1)}\left[-480\pi^2\xi^6-240\pi^2\xi^5-96\pi^2\xi^4-504\xi^4-495\pi^2\xi^3-1016\xi^3\right.\\
&+84\pi^2\xi^2+568\xi^2+216\xi^5\ln^2(\xi+1)+972\xi^4\ln^2(\xi+1)+504\xi^3\ln^2(\xi+1)\\
&-216\xi^2\ln^2(\xi+1)+18\left(4\xi^4+14\xi^3+39\xi^2+28\xi-1\right)\xi\ln^2(\xi)+288\xi^6\ln(\xi+1)\\
&-720\xi^5\ln(\xi+1)-2124\xi^4\ln(\xi+1)-612\xi^3\ln(\xi+1)+972\xi^2\ln(\xi+1)\\
&+12\left(-264\xi^6-204\xi^5+303\xi^4+121\xi^3-191\xi^2-25\xi+8\right)+243\pi^2\xi+440\xi\\
&+72\left(8\xi^5+2\xi^4-7\xi^3-11\xi^2-14\xi-4\right)\xi\ln(\xi)\ln(\xi+1)+36\xi\ln^2(\xi+1)+368\\
&\left.+612\xi\ln(\xi+1)+144\ln(\xi+1)+36(\xi+1)^2\left(24\xi^4-12\xi^3-5\xi^2+7\xi-4\right)\ln(z)\right]\\
&\frac{1}{2}\left(-2\xi^3-5\xi^2+5\xi+1\right)\mathrm{Li}_2(1-\xi)+\frac{1}{4}\left(8\xi^4-2\xi^3+11\xi^2-6\xi-6\right)\mathrm{Li}_2\left(\frac{1}{\xi+1}\right)\\
&\frac{1}{4}\xi\left(4\xi^2+12\xi-13\right)\mathrm{Li}_2(-\xi);
\end{aligned}
\tag{D.6}
$$

$$
\begin{aligned}
B_g = \frac{(\xi-1)}{72(\xi+1)} \big[& 30\pi^2\xi^3 - 108\xi^3 + 3\pi^2\xi^2 + 6\pi^2\xi + 70\xi^2 - 18 - 54\xi^2 \ln^2(\xi+1) \\
& + 18\left(2\xi^2-1\right)\ln^2(\xi) - 90\xi^3\ln(\xi+1) - 27\xi^2\ln(\xi+1) + 70\xi - 180\xi\ln^2(\xi+1) \\
& - 3\ln(\xi)\left(-114\xi^3 - 19\xi^2 + 6\left(2\xi^3+3\xi^2-2\xi-1\right)\ln(\xi+1) + 77\xi + 24\right) \\
& -63\ln^2(\xi+1) + 135\xi\ln(\xi+1) + 72\ln(\xi+1) - 9\left(6\xi^2+5\xi-1\right)\xi\ln(z) + 24\pi^2\big] \\
& + \frac{(2\xi^3+2\xi^2-3\xi-1)\,\mathrm{Li}_2(1-\xi)}{2(\xi+1)} - \frac{(2\xi^4+\xi^3+3\xi^2-3\xi-3)\,\mathrm{Li}_2\left(\frac{1}{\xi+1}\right)}{4(\xi+1)} \\
& + \frac{3\,(-2\xi^3-2\xi^2+3\xi+1)\,\mathrm{Li}_2(-\xi)}{4(\xi+1)}.
\end{aligned}
\tag{D.7}
$$

Appendix E

Coefficients of the one-loop off-shell virtual correction to the HDIS

In this appendix, we list the finite part of the coefficients of the tensorial structures that enter in the one-loop virtual contribution to Higgs-induced DIS. The divergent part of these coefficients is reported in Chapter 5, Section 5.4.6. We did not report this finite part in the main text of the thesis because they are quite complicated.

The expression for the one-loop virtual contribution to the HDIS can be written as

$$\mathcal{M}^{\mu\nu}(k_1,k_2,n) = \frac{\alpha_s}{4\,\pi} c^2 C_A Q^2 \delta_{a,b} \Big[\mathcal{M}_g Q^2 g^{\mu\nu} + \mathcal{M}_{k_1\,k_1} k_1^\mu k_1^\nu + \mathcal{M}_{k_2\,k_2} k_2^\mu k_2^\nu + \frac{1}{2}\mathcal{M}_{k_1\,k_2}\left(k_1^\mu k_2^\nu + k_1^\nu k_2^\mu\right) + \ldots\Big], \tag{E.1}$$

where we omitted the tensorial structures depending on the gauge-vector n because, as we discussed in Chapter 3, they vanish once contracted with the projector that selects the dominant part pd the amplitude in the high-energy region.

The coefficients of the tensorial structures in Eq.(E.1) are:

$$\begin{aligned}
\mathcal{M}_g = &-\frac{(\xi-1)}{288(\xi+1)}\Big[12\pi^2\xi^5 + 6\pi^2\xi^4 - 90\pi^2\xi^3 + 432\xi^3 + 9\pi^2\xi^2 - 816\xi^2 - 72\xi^5\ln^2(\xi+1)\\
&-36\xi^4\ln^2(\xi+1) - 144\xi^3\ln^2(\xi+1) + 108\xi^2\ln^2(\xi+1) + 576\xi^5\ln(\xi+1) - 180\xi^2\ln(\xi+1)\\
&+18\left(12\xi^5 + 6\xi^4 + 14\xi^3 + 5\xi^2 + 2\xi + 6\right)\ln^2(\xi) + 288\xi^4\ln(\xi+1) - 216\xi^3\ln(\xi+1)\\
&-12\ln(\xi)\left(42\xi^5 + 21\xi^4 + 36\xi^3 - 51\xi^2 + 6\left(2\xi^5 + \xi^4 - \xi^2 + 2\xi + 1\right)\ln(\xi+1) - 91\xi - 46\right)\\
&-6\pi^2\xi - 488\xi + 648\xi\ln^2(\xi+1) + 180\ln^2(\xi+1) - 540\xi\ln(\xi+1)\\
&-288\ln(\xi+1) + 36\left(6\xi^2 + 5\xi - 1\right)\xi\ln(z) - 78\pi^2 - 392\Big]\\
&+\frac{\left(2\xi^3 + 2\xi^2 - 3\xi - 1\right)\mathrm{Li}_2(1-\xi)}{2(\xi+1)} + \frac{1}{4}(\xi-1)^2\left(2\xi^3 + \xi^2 + 4\xi + 1\right)\mathrm{Li}_2\left(\frac{1}{\xi+1}\right)\\
&+\frac{3\left(-2\xi^3 - 2\xi^2 + 3\xi + 1\right)\mathrm{Li}_2(-\xi)}{4(\xi+1)};
\end{aligned} \tag{E.2}$$

$$\mathcal{M}_{k_1k_1} = -\frac{(\xi-1)}{288(\xi+1)}\left[24\pi^2\xi^6+12\pi^2\xi^5-192\pi^2\xi^4-84\pi^2\xi^3-6\pi^2\xi^2+216\xi^2\right.$$
$$-81\pi^2\xi-144\xi^6\ln^2(\xi+1)-72\xi^5\ln^2(\xi+1)-216\xi^4\ln^2(\xi+1)-180\xi^3\ln^2(\xi+1)$$
$$+360\xi^2\ln^2(\xi+1)+18\left(24\xi^5+12\xi^4+16\xi^3+20\xi^2+6\xi+3\right)\xi\ln^2(\xi)+576\xi^6\ln(\xi+1)$$
$$+288\xi^5\ln(\xi+1)-432\xi^4\ln(\xi+1)-648\xi^3\ln(\xi+1)-684\xi^2\ln(\xi+1)-1640\xi$$
$$-12\ln(\xi)\left(24\xi^6+12\xi^5+54\xi^4+45\xi^3-39\xi^2-97\xi-16\right)+72\xi\ln^2(\xi+1)$$
$$-72\left(4\xi^5+2\xi^4-2\xi^3+\xi^2+2\xi-2\right)\xi\ln(\xi)\ln(\xi+1)-180\xi\ln(\xi+1)-704$$
$$\left.+108\left(4\xi^3+6\xi^2+\xi-1\right)\xi\ln(z)\right]+\frac{\xi\left(2\xi^2-\xi-1\right)\mathrm{Li}_2(1-\xi)}{2(\xi+1)}$$
$$\frac{1}{4}\xi\left(4\xi^5-6\xi^4+6\xi^3-5\xi^2+1\right)\mathrm{Li}_2\left(\frac{1}{\xi+1}\right)+\frac{3\xi\left(-2\xi^2+\xi+1\right)\mathrm{Li}_2(-\xi)}{4(\xi+1)};\tag{E.3}$$

$$\mathcal{M}_{k_2k_2} = \frac{1}{144\xi^3}\left[120\pi^2\xi^7+504i\pi\xi^7+60\pi^2\xi^6+120\pi^2\xi^5+360\xi^5+144\pi^2\xi^4+368\xi^4\right.$$
$$+120\pi^2\xi^3-272\xi^3+24\pi^2\xi^2+216\xi^2+72\xi^5\ln^2(\xi+1)+288\xi^4\ln^2(\xi+1)-72\xi^7\ln(\xi+1)$$
$$+72\left(\xi^2-\xi+1\right)\xi^3\ln^2(\xi)+792\xi^3\ln^2(\xi+1)+180\xi^2\ln^2(\xi+1)+180\xi^6\ln(\xi+1)$$
$$+504\xi^5\ln(\xi+1)+288\xi^4\ln(\xi+1)+234\xi^3\ln(\xi+1)+207\xi^2\ln(\xi+1)$$
$$-3\ln(\xi)\left(-264\xi^7-204\xi^6+216\xi^5-80\xi^4-346\xi^3-123\xi^2+6\xi+3\right)+18\xi\ln(\xi+1)$$
$$-72\left(2\xi^5+\xi^4+4\xi^3+2\xi^2+6\xi+1\right)\xi^2\ln(\xi)\ln(\xi+1)+9\ln(\xi+1)$$
$$\left.-36\left(6\xi^5+9\xi^4+2\xi^3+2\xi^2+11\xi+8\right)\xi^2\ln(z)\right]-\frac{\left(2\xi^2+4\xi+1\right)\mathrm{Li}_2(1-\xi)}{\xi}$$
$$-\frac{\left(2\xi^5+\xi^4+2\xi^3-4\xi-1\right)\mathrm{Li}_2\left(\frac{1}{\xi+1}\right)}{2\xi}+\frac{3\left(2\xi^2+4\xi+1\right)\mathrm{Li}_2(-\xi)}{2\xi};\tag{E.4}$$

$$\mathcal{M}_{k_1k_2} = \frac{1}{144\xi(\xi+1)}\left[24\pi^2\xi^8+12\pi^2\xi^7-198\pi^2\xi^6-87\pi^2\xi^5-57\pi^2\xi^4-252\xi^4-264\pi^2\xi^3\right.$$
$$-1044\xi^3+3\pi^2\xi^2+460\xi^2-144\xi^8\ln^2(\xi+1)-72\xi^7\ln^2(\xi+1)-180\xi^6\ln^2(\xi+1)$$
$$-54\xi^5\ln^2(\xi+1)+558\xi^4\ln^2(\xi+1)+252\xi^3\ln^2(\xi+1)+576\xi^8\ln(\xi+1)+288\xi^7\ln(\xi+1)$$
$$+18\left(24\xi^7+12\xi^6+10\xi^5+19\xi^4-10\xi^3+7\xi^2+11\xi-3\right)\xi\ln^2(\xi)-1008\xi^6\ln(\xi+1)$$
$$-936\xi^5\ln(\xi+1)-486\xi^4\ln(\xi+1)-18\xi^3\ln(\xi+1)+486\xi^2\ln(\xi+1)+99\pi^2\xi+1044\xi$$
$$-6\ln(\xi)\left(48\xi^8+24\xi^7+6\xi^6+39\xi^5-129\xi^4-60\xi^3+199\xi^2+69\xi-28\right)+72\ln(\xi+1)$$
$$-36\left(8\xi^7+4\xi^6-6\xi^5+3\xi^4+\xi^3+6\xi^2+14\xi+4\right)\xi\ln(\xi)\ln(\xi+1)+108\xi\ln^2(\xi+1)$$
$$\left.+306\xi\ln(\xi+1)+18(\xi+1)^2\left(24\xi^4-12\xi^3-5\xi^2+7\xi-4\right)\ln(z)-12\pi^2+80\right]$$
$$+\frac{1}{2}\left(-2\xi^3-5\xi^2+5\xi+1\right)\mathrm{Li}_2(1-\xi)+\frac{1}{4}\xi\left(4\xi^2+12\xi-13\right)\mathrm{Q2Li}_2(-\xi)$$
$$-\frac{1}{4}\left(8\xi^6-4\xi^5+6\xi^4-3\xi^3-10\xi^2+5\xi+1\right)\mathrm{Li}_2\left(\frac{1}{\xi+1}\right).\tag{E.5}$$

Bibliography

[1] L. N. Lipatov, "Reggeization of the Vector Meson and the Vacuum Singularity in Nonabelian Gauge Theories," *Sov. J. Nucl. Phys.*, vol. 23, pp. 338–345, 1976.

[2] V. S. Fadin, E. A. Kuraev, and L. N. Lipatov, "On the Pomeranchuk Singularity in Asymptotically Free Theories," *Phys. Lett. B*, vol. 60, pp. 50–52, 1975.

[3] E. A. Kuraev, L. N. Lipatov, and V. S. Fadin, "Multi - Reggeon Processes in the Yang-Mills Theory," *Sov. Phys. JETP*, vol. 44, pp. 443–450, 1976.

[4] E. A. Kuraev, L. N. Lipatov, and V. S. Fadin, "The Pomeranchuk Singularity in Nonabelian Gauge Theories," *Sov. Phys. JETP*, vol. 45, pp. 199–204, 1977.

[5] I. I. Balitsky and L. N. Lipatov, "The Pomeranchuk Singularity in Quantum Chromodynamics," *Sov. J. Nucl. Phys.*, vol. 28, pp. 822–829, 1978.

[6] V. S. Fadin and L. N. Lipatov, "BFKL pomeron in the next-to-leading approximation," *Phys. Lett. B*, vol. 429, pp. 127–134, 1998.

[7] G. P. Salam, "A Resummation of large subleading corrections at small x," *JHEP*, vol. 07, p. 019, 1998.

[8] M. Ciafaloni, D. Colferai, and G. P. Salam, "Renormalization group improved small x equation," *Phys. Rev. D*, vol. 60, p. 114036, 1999.

[9] M. Ciafaloni, D. Colferai, G. P. Salam, and A. M. Stasto, "Renormalization group improved small x Green's function," *Phys. Rev. D*, vol. 68, p. 114003, 2003.

[10] M. Ciafaloni, D. Colferai, G. P. Salam, and A. M. Stasto, "A Matrix formulation for small-x singlet evolution," *JHEP*, vol. 08, p. 046, 2007.

[11] R. D. Ball and S. Forte, "Summation of leading logarithms at small x," *Phys. Lett. B*, vol. 351, pp. 313–324, 1995.

[12] R. D. Ball and S. Forte, "Asymptotically free partons at high-energy," *Phys. Lett. B*, vol. 405, pp. 317–326, 1997.

[13] G. Altarelli, R. D. Ball, and S. Forte, "Factorization and resummation of small x scaling violations with running coupling," *Nucl. Phys. B*, vol. 621, pp. 359–387, 2002.

[14] G. Altarelli, R. D. Ball, and S. Forte, "An Anomalous dimension for small x evolution," *Nucl. Phys. B*, vol. 674, pp. 459–483, 2003.

[15] G. Altarelli, R. D. Ball, and S. Forte, "Perturbatively stable resummed small x evolution kernels," *Nucl. Phys. B*, vol. 742, pp. 1–40, 2006.

[16] G. Altarelli, R. D. Ball, and S. Forte, "Small x Resummation with Quarks: Deep-Inelastic Scattering," *Nucl. Phys. B*, vol. 799, pp. 199–240, 2008.

[17] S. Catani, M. Ciafaloni, and F. Hautmann, "GLUON CONTRIBUTIONS TO SMALL x HEAVY FLAVOR PRODUCTION," *Phys. Lett. B*, vol. 242, pp. 97–102, 1990.

[18] S. Catani, M. Ciafaloni, and F. Hautmann, "High-energy factorization and small-x heavy flavor production," *Nucl. Phys. B*, vol. 366, pp. 135–188, 1991.

[19] J. C. Collins and R. K. Ellis, "Heavy quark production in very high-energy hadron collisions," *Nucl. Phys. B*, vol. 360, pp. 3–30, 1991.

[20] S. Catani, M. Ciafaloni, and F. Hautmann, "High-energy factorization in QCD and minimal subtraction scheme," *Phys. Lett. B*, vol. 307, pp. 147–153, 1993.

[21] S. Catani and F. Hautmann, "Quark anomalous dimensions at small x," *Phys. Lett. B*, vol. 315, pp. 157–163, 1993.

[22] S. Catani and F. Hautmann, "High-energy factorization and small-x deep inelastic scattering beyond leading order," *Nucl. Phys. B*, vol. 427, pp. 475–524, 1994.

[23] R. D. Ball, "Resummation of Hadroproduction Cross-sections at High Energy," *Nucl. Phys. B*, vol. 796, pp. 137–183, 2008.

[24] F. Caola, S. Forte, and S. Marzani, "Small x resummation of rapidity distributions: The Case of Higgs production," *Nucl. Phys. B*, vol. 846, pp. 167–211, 2011.

[25] S. Marzani, R. D. Ball, V. Del Duca, S. Forte, and A. Vicini, "Higgs production via gluon-gluon fusion with finite top mass beyond next-to-leading order," *Nucl. Phys. B*, vol. 800, pp. 127–145, 2008.

[26] S. Marzani and R. D. Ball, "High Energy Resummation of Drell-Yan Processes," *Nucl. Phys. B*, vol. 814, pp. 246–264, 2009.

[27] C. Muselli, M. Bonvini, S. Forte, S. Marzani, and G. Ridolfi, "Top Quark Pair Production beyond NNLO," *JHEP*, vol. 08, p. 076, 2015.

[28] S. Forte and C. Muselli, "High energy resummation of transverse momentum distributions: Higgs in gluon fusion," *JHEP*, vol. 03, p. 122, 2016.

[29] S. Marzani, "Combining Q_T and small-x resummations," *Phys. Rev. D*, vol. 93, no. 5, p. 054047, 2016.

[30] S. Zoia and C. Muselli, "High Energy Resummation of Jet Observables," *JHEP*, vol. 12, p. 097, 2017.

[31] F. Silvetti and M. Bonvini, "Differential heavy quark pair production at small x," *Eur. Phys. J. C*, vol. 83, no. 4, p. 267, 2023.

[32] M. Bonvini, S. Marzani, and T. Peraro, "Small-x resummation from HELL," *Eur. Phys. J. C*, vol. 76, no. 11, p. 597, 2016.

[33] M. Bonvini, S. Marzani, and C. Muselli, "Towards parton distribution functions with small-x resummation: HELL 2.0," *JHEP*, vol. 12, p. 117, 2017.

[34] M. Bonvini, "Small-x phenomenology at the LHC and beyond: HELL 3.0 and the case of the Higgs cross section," *Eur. Phys. J. C*, vol. 78, no. 10, p. 834, 2018.

[35] R. D. Ball, V. Bertone, M. Bonvini, S. Marzani, J. Rojo, and L. Rottoli, "Parton distributions with small-x resummation: evidence for BFKL dynamics in HERA data," *Eur. Phys. J. C*, vol. 78, no. 4, p. 321, 2018.

[36] H. Abdolmaleki *et al.*, "Impact of low-x resummation on QCD analysis of HERA data," *Eur. Phys. J. C*, vol. 78, no. 8, p. 621, 2018.

[37] R. K. Ellis, W. J. Stirling, and B. R. Webber, *QCD and Collider Physics*. Cambridge Monographs on Particle Physics, Nuclear Physics and Cosmology, Cambridge University Press, 1996.

[38] J. Collins, *Foundations of perturbative QCD*. Cambridge University Press, 2011.

[39] J. Campbell, J. Huston, and F. Krauss, *The Black Book of Quantum Chromodynamics : a Primer for the LHC Era*. Oxford University Press, 2018.

[40] M. E. Peskin, *An introduction to quantum field theory*. CRC press, 2018.

[41] S. Weinberg, *The quantum theory of fields*, vol. 2. Cambridge university press, 1995.

[42] M. Srednicki, *Quantum field theory*. Cambridge University Press, 1 2007.

[43] M. D. Schwartz, *Quantum Field Theory and the Standard Model*. Cambridge University Press, 3 2014.

[44] S. Marzani, R. D. Ball, V. Del Duca, S. Forte, and A. Vicini, "Higgs production via gluon–gluon fusion with finite top mass beyond next-to-leading order," *Nuclear physics B*, vol. 800, no. 1-2, pp. 127–145, 2008.

[45] M. Bonvini, "Resummation of soft and hard gluon radiation in perturbative qcd," 2012.

[46] F. Silvetti, *Resummation phenomenology and PDF determination for precision QCD at the LHC*. Phd thesis, Sapienza, Universitiy of Rome, 9 2023. Available at: `https://hdl.handle.net/11573/1707274`.

[47] M. Beneke, "Renormalons," *Phys. Rept.*, vol. 317, pp. 1–142, 1999.

[48] F. Herzog, B. Ruijl, T. Ueda, J. Vermaseren, and A. Vogt, "The five-loop beta function of yang-mills theory with fermions," *Journal of High Energy Physics*, vol. 2017, no. 2, pp. 1–18, 2017.

[49] T. Luthe, A. Maier, P. Marquard, and Y. Schröder, "The five-loop beta function for a general gauge group and anomalous dimensions beyond feynman gauge," *Journal of High Energy Physics*, vol. 2017, no. 10, pp. 1–19, 2017.

[50] S. Coleman and D. J. Gross, "Price of asymptotic freedom," *Physical Review Letters*, vol. 31, no. 13, p. 851, 1973.

[51] A. J. Buras, "Asymptotic freedom in deep inelastic processes in the leading order and beyond," *Reviews of Modern Physics*, vol. 52, no. 1, p. 199, 1980.

[52] J. C. Collins and D. E. Soper, "The theorems of perturbative qcd," *Annual Review of Nuclear and Particle Science*, vol. 37, no. 1, pp. 383–409, 1987.

[53] Y. L. Dokshitzer, "Calculation of the structure functions for deep inelastic scattering and e+e- annihilation by perturbation theory in quantum chromodynamics," *Zh. Eksp. Teor. Fiz*, vol. 73, p. 1216, 1977.

[54] V. N. Gribov and L. N. Lipatov, "Deep inelastic ep-scattering in a perturbation theory.," tech. rep., Inst. of Nuclear Physics, Leningrad, 1972.

[55] G. Altarelli and G. Parisi, "Asymptotic freedom in parton language," *Nuclear Physics B*, vol. 126, no. 2, pp. 298–318, 1977.

[56] V. S. Fadin, E. Kuraev, and L. Lipatov, "On the pomeranchuk singularity in asymptotically free theories," *Physics Letters B*, vol. 60, no. 1, pp. 50–52, 1975.

[57] L. Lipatov, "Reggeization of the vector meson and the vacuum singularity in nonabelian gauge theories," *Yad. Fiz.;(USSR)*, vol. 23, no. 3, 1976.

[58] E. A. Kuraev, L. Lipatov, and V. S. Fadin, "Multireggeon processes in the yang-mills theory," *Zhurnal Ehksperimental'noj i Teoreticheskoj Fiziki*, vol. 71, no. 9, pp. 840–855, 1976.

[59] E. A. Kuraev, L. Lipatov, and V. S. Fadin, "Pomeranchuk singularity in nonabelian gauge theories," *Sov. Phys.-JETP (Engl. Transl.);(United States)*, vol. 45, no. 2, 1977.

[60] J. R. Forshaw and D. A. Ross, *Quantum chromodynamics and the pomeron*. No. 9, Cambridge University Press, 1997.

[61] M. Ciafaloni, D. Colferai, G. Salam, and A. Staśto, "Renormalization group improved small-x green's function," *Physical Review D*, vol. 68, no. 11, p. 114003, 2003.

[62] R. S. Thorne, "Explicit calculation of the running coupling BFKL anomalous dimension," *Phys. Lett. B*, vol. 474, pp. 372–384, 2000.

[63] R. S. Thorne, "NLO BFKL equation, running coupling and renormalization scales," *Phys. Rev. D*, vol. 60, p. 054031, 1999.

[64] R. S. Thorne, "The Running coupling BFKL anomalous dimensions and splitting functions," *Phys. Rev. D*, vol. 64, p. 074005, 2001.

[65] C. D. White and R. S. Thorne, "A Global Fit to Scattering Data with NLL BFKL Resummations," *Phys. Rev. D*, vol. 75, p. 034005, 2007.

[66] M. Bonvini and S. Marzani, "Four-loop splitting functions at small x," *JHEP*, vol. 06, p. 145, 2018.

[67] A. H. Mueller and H. Navelet, "An Inclusive Minijet Cross-Section and the Bare Pomeron in QCD," *Nucl. Phys. B*, vol. 282, pp. 727–744, 1987.

[68] D. Y. Ivanov and A. Papa, "Electroproduction of two light vector mesons in the next-to-leading approximation," *Nucl. Phys. B*, vol. 732, pp. 183–199, 2006.

[69] D. Y. Ivanov and A. Papa, "Electroproduction of two light vector mesons in next-to-leading BFKL: Study of systematic effects," *Eur. Phys. J. C*, vol. 49, pp. 947–955, 2007.

[70] F. Caporale, F. G. Celiberto, G. Chachamis, D. Gordo Gómez, and A. Sabio Vera, "BFKL Azimuthal Imprints in Inclusive Three-jet Production at 7 and 13 TeV," *Nucl. Phys. B*, vol. 910, pp. 374–386, 2016.

[71] F. Caporale, F. G. Celiberto, G. Chachamis, D. G. Gomez, and A. Sabio Vera, "Stability of Azimuthal-angle Observables under Higher Order Corrections in Inclusive Three-jet Production," *Phys. Rev. D*, vol. 95, no. 7, p. 074007, 2017.

[72] F. G. Celiberto, *High-energy resummation in semi-hard processes at the LHC*. PhD thesis, Calabria U., 2017.

[73] R. Boussarie, B. Ducloué, L. Szymanowski, and S. Wallon, "Forward J/ψ and very backward jet inclusive production at the LHC," *Phys. Rev. D*, vol. 97, no. 1, p. 014008, 2018.

[74] K. Golec-Biernat, L. Motyka, and T. Stebel, "Forward Drell-Yan and backward jet production as a probe of the BFKL dynamics," *JHEP*, vol. 12, p. 091, 2018.

[75] A. D. Bolognino, F. G. Celiberto, M. Fucilla, D. Y. Ivanov, and A. Papa, "Inclusive production of a heavy-light dijet system in hybrid high-energy and collinear factorization," *Phys. Rev. D*, vol. 103, no. 9, p. 094004, 2021.

[76] A. D. Bolognino, F. G. Celiberto, M. Fucilla, D. Y. Ivanov, and A. Papa, "High-energy resummation in heavy-quark pair hadroproduction," *Eur. Phys. J. C*, vol. 79, no. 11, p. 939, 2019.

[77] F. G. Celiberto, D. Y. Ivanov, B. Murdaca, and A. Papa, "High-energy resummation in heavy-quark pair photoproduction," *Phys. Lett. B*, vol. 777, pp. 141–150, 2018.

[78] F. G. Celiberto, M. Fucilla, D. Y. Ivanov, M. M. A. Mohammed, and A. Papa, "The next-to-leading order Higgs impact factor in the infinite top-mass limit," *JHEP*, vol. 08, p. 092, 2022.

[79] S. Catani, M. Ciafaloni, and F. Hautmann, "Gluon contributions to small χ heavy flavour production," *Physics Letters B*, vol. 242, no. 1, pp. 97–102, 1990.

[80] M. Ciafaloni, "Coherence Effects in Initial Jets at Small q**2 / s," *Nucl. Phys. B*, vol. 296, pp. 49–74, 1988.

[81] G. Curci, W. Furmanski, and R. Petronzio, "Evolution of Parton Densities Beyond Leading Order: The Nonsinglet Case," *Nucl. Phys. B*, vol. 175, pp. 27–92, 1980.

[82] S. Marzani, "High energy resummation in quantum chromo–dynamics," 2008.

[83] G. Soar, S. Moch, J. Vermaseren, and A. Vogt, "On higgs-exchange dis, physical evolution kernels and fourth-order splitting functions at large x," *Nuclear Physics B*, vol. 832, no. 1-2, pp. 152–227, 2010.

[84] F. Hautmann, "Heavy top limit and double logarithmic contributions to Higgs production at m(H)**2 / s much less than 1," *Phys. Lett. B*, vol. 535, pp. 159–162, 2002.

[85] W. Konetschny and W. Kummer, "Ghost Free Nonabelian Gauge Theory: Renormalization and Gauge-Invariance," *Nucl. Phys. B*, vol. 100, pp. 106–124, 1975.

[86] S. Mandelstam, "Light-cone superspace and the ultraviolet finiteness of the N= 4 model," *Nuclear Physics B*, vol. 213, no. 1, pp. 149–168, 1983.

[87] G. Leibbrandt, "Light-cone gauge in yang-mills theory," *Physical Review D*, vol. 29, no. 8, p. 1699, 1984.

[88] A. Bassetto, G. Nardelli, and R. Soldati, *Yang-Mills theories in algebraic non-covariant gauges: canonical quantization and renormalization*. World Scientific, 1991.

[89] D. J. Pritchard and W. J. Stirling, "QCD Calculations in the Light Cone Gauge. 1," *Nucl. Phys. B*, vol. 165, pp. 237–268, 1980.

[90] C. Becchi, A. Rouet, and R. Stora, "Renormalization of the Abelian Higgs-Kibble Model," *Commun. Math. Phys.*, vol. 42, pp. 127–162, 1975.

[91] C. Becchi, A. Rouet, and R. Stora, "The Abelian Higgs-Kibble Model. Unitarity of the S Operator," *Phys. Lett. B*, vol. 52, pp. 344–346, 1974.

[92] C. Becchi, A. Rouet, and R. Stora, "Renormalization of Gauge Theories," *Annals Phys.*, vol. 98, pp. 287–321, 1976.

[93] I. V. Tyutin, "Gauge Invariance in Field Theory and Statistical Physics in Operator Formalism," 1975.

[94] S. Dawson, "Radiative corrections to higgs boson production," *Nuclear Physics B*, vol. 359, no. 2-3, pp. 283–300, 1991.

[95] A. Daleo, G.-D. Ridder, T. Gehrmann, G. Luisoni, *et al.*, "Antenna subtraction at nnlo with hadronic initial states: initial-final configurations," *Journal of High Energy Physics*, vol. 2010, no. 1, pp. 1–84, 2010.